REACTIVITY MEASUREMENT USING DETERMINISTIC AND NOISE METHODS IN BRAHMMA SUBCRITICAL SYSTEM

By

NIRMAL KUMAR RAY

Enrolment No: PHYS01201604021

Bhabha Atomic Research Centre, Mumbai

A thesis submitted to the

Board of Studies in Physical Sciences

In partial fulfillment of requirements

for the Degree of

DOCTOR OF PHILOSOPHY

of

HOMI BHABHA NATIONAL INSTITUTE

March, 2021

Homi Bhabha National Institute

Recommendations of the Viva Voce Committee

As members of the Viva Voce Committee, we certify that we have read the dissertation prepared by **Nirmal Kumar Ray** entitled **"Reactivity Measurement Using Deterministic and Noise Methods in BRAHMMA Subcritical System"** and recommend that it may be accepted as fulfilling the thesis requirement for the award of Degree of Doctor of Philosophy.

Umasankari Kannan ---------- Date: 03/03/2021
Chairman- Dr. Umasankari K.

---------- Date: 03 March 2021
Guide/ Convener - Dr. L.M. Pant

Amar Sinha ---------- Date: 3.3.21
Co-guide- Dr. Amar Sinha

---------- Date:
Examiner- Prof. S. Mukherjee SMukherjee

---------- Date: 18/3/2021
Member 1- Dr. K. P. Singh K.P.S. 03/03/2021

Vishwajeet Jha. ---------- Date: 03.03.2021
Member 2- Dr. Vishwajeet Jha

Palit ---------- Date: 3/3/21
Member 3- Dr. Rudrajyoti Palit

Tushar Roy ---------- Date: 03/03/2021
Technical advisor- Dr. Tushar Roy

Final approval and acceptance of this thesis is contingent upon the candidate's submission of the final copies of the thesis to HBNI.

We hereby certify that we have read this thesis prepared under our direction and recommend that it may be accepted as fulfilling the thesis requirement.

Date: 03 March 2021
Place: Mumbai.

Amar Sinha
Dr. Amar Sinha
(Co-guide)

Dr. L.M. Pant
(Guide)

STATEMENT BY AUTHOR

This dissertation has been submitted in partial fulfillment of requirements for an advanced degree at Homi Bhabha National Institute (HBNI) and is deposited in the Library to be made available to borrowers under rules of the HBNI.

Brief quotations from this dissertation are allowable without special permission, provided that accurate acknowledgement of source is made. Requests for permission for extended quotation from or reproduction of this manuscript in whole or in part may be granted by the Competent Authority of HBNI when in his or her judgment the proposed use of the material is in the interests of scholarship. In all other instances, however, permission must be obtained from the author.

Nirmal Kumar Ray
03/03/2021

Nirmal Kumar Ray

DECLARATION

I, hereby declare that the investigation presented in the thesis has been carried out by me. The work is original and has not been submitted earlier as a whole or in part for a degree / diploma at this or any other Institution / University.

Nirmal Kumar Ray
03/03/2021

Nirmal Kumar Ray

List of Publications arising from the thesis

Journal

1. "Pulse shape measurement and experimental validation of noise theory developed under consideration of finite pulse width in D-T neutron generator driven subcritical system", **Nirmal Kumar Ray**, Tarun Patel, Rajeev Kumar, P. S. Sarkar, L. M. Pant, ***Progress in Nuclear Energy***, **2020**, *120*, 103191.
2. "Experimental validation of noise theory developed by considering the source as an exponentially correlated process in DT neutron generator driven subcritical system", **Nirmal Kumar Ray**, L. M. Pant, T. Patel, R. Kumar, T. Roy, P. S. Sarkar, ... & S. C. Gadkari, ***Progress in Nuclear Energy***, **2019**, *117*, 103087.
3. "Reactivity Measurement Using the Area-Ratio Method in the BRAHMMA Subcritical System", **Nirmal Kumar Ray**, T. Roy, S. Bajpai, T. Patel, Y. Kashyap, M. Shukla, & A. Sinha, ***Nuclear Technology***, **2017**, *197*, 110-115.
4. "Pulsed Neutron Source Measurements in the BRAHMMA Accelerator-Driven Subcritical System", T. Roy, **Nirmal Ray,** S. Bajpai, T. Patel, M. Shukla, Y. Kashyap, ... & S. C. Gadkari, ***Nuclear Science and Engineering***, **2016**, *184*, 584-590.

International Conference

1. "Noise Experiments in BRAHMMA Subcritical System using Isotopic Poisson Source and Accelerator based Neutron Source", **Nirmal Kumar Ray**, Rajeev Kumar, Tarun Patel, P. S. Sarkar, L. M. Pant, Oral presentation, ***19th International conference on Emerging Nuclear Energy Systems***, **2019**, Indonesia.
2. "Source correlation factor measurement using DT neutron generator", **Nirmal Kumar Ray,** R. Kumar, L. M. Pant, T. Patel, P. S. Sarkar, ***DAE Symp. Nucl. Phys.***, **2018**, *63*, 1066-1067.

Nirmal Kumar Ray
03/03/2021
Nirmal Kumar Ray

DEDICATIONS

To my Mother

ACKNOWLEDGEMENTS

This thesis is the result of direct and indirect effort of many persons in my life. I am thankful to Bhabha Atomic Research Centre and Homi Bhabha National Institute for the approval to conduct the study.

My heartiest gratitude to my guide Dr. L. M. Pant for his support, guidance and motivation in carrying out the study. I am deeply indebted to my co-guide Dr. Amar Sinha who introduced me to the field of Accelerator Driven Subcritical system. He was responsible for conceptualisation and realisation of the BRAHMMA system. He has also encouraged me to explore this field. I sincerely thank Dr. Umasankari K. for her constant motivation to carry out the study. I thank Dr. K. P. Singh, Dr. Vishwajeet Jha, Dr. Rudrajyoti Palit and Dr. Tushar Roy for their suggestions during all the technical discussion to make the research productive.

I am thankful to Dr. P. S. Sarkar for his constructive support and motivation through the entire journey. I am thankful to Mr. Tarun Patel and Mr. P. S. Adhikari for their technical support to conduct this study. I am also thankful to Dr. Rajeev Kumar for his support to conduct noise experiments. I deeply acknowledge Dr. Degweker and Dr. Rana for their suggestions and help as part of my research is based on their theory. I would like to express my gratitude to Dr. Saroj, Mrs. Jilju, Mr. Shaleen and Mr. Manoj for all of their support.

Furthermore, I am thankful to my wife Chandra for dealing my all those emotional swings at home during this journey and for always being supportive. Moreover, as always, my two families remained the bedrock on which I exist. Lastly, I thank you God, for being my constant guiding force and for all the countless blessings in everyday life that made me who I am.

LIST OF ABBREVIATION

ADS	Accelerator Driven Subcritical system
BRAHMMA	Beryllium oxide Reflected And HDPe Moderated Multiplying Assembly
EA	Energy Amplifier
PNS	Pulsed Neutron Source
HDPe	High Density Polyethylene
EC	Experimental Channel
LC	Lattice Channel
PNG	Purnima Neutron Generator
ACCT	AC Current Transformer
V/M	Variance to Mean ratio
V/M-1	Feynman-alpha
ACF	Auto Correlation Function
ACV	Auto Covariance
PSD	Power Spectral Density
APSD	Auto Power Spectral Density
CPS	Counts Per Second
DAQ	Data Acquisition system

CONTENTS

LIST OF FIGURES

LIST OF TABLES

CHAPTER SEVEN

CONCLUSION

Accelerator Driven Subcritical (ADS) system has been conceptualised towards solving problems related to transmutation and safe power production using accelerator-based neutron source coupled to a subcritical reactor. Research work in this direction is being carried out in India for power production based on vast reserves of Thorium. In such a system, the energy gain can be maximised for a certain accelerator beam power by reducing the subcriticality. Though, the reactor core will be subcritical, still there may be a chance of criticality due to accumulation of ^{233}U on account of breeding. Moreover, in case of any transient, the changes in the neutron source may mask the changes in reactivity and the situation will be more susceptible in case of operation of ADS with highest possible value of reactivity. Thus, reactivity measurement is essential from commercial, control and safety point of view. The present study has focused on the development of robust method for reactivity measurement using BRAHMMA subcritical system and PNG.

In the context of reactivity measurement using deterministic methods, Area-ratio, Slope-fit and Source-jerk method have been studied in BRAHMMA subcritical system. It has been observed that the measured reactivity using Area-ratio and Source-jerk methods have dependency on the detector's location, which is due to the prompt and delayed neutron harmonics. Bell-Glasstone correction factor has been incorporated to estimate the correct reactivity. In Area-ratio and Source-jerk methods, k_{eff} of BRAHMMA subcritical system has been estimated using the corrected reactivity along with the theoretical value of β_{eff}. In case of Slope-fit method, the rising edge of histogram and the initial part of the decay have been masked to eliminate the higher harmonics. Rest of the histogram has been used to estimate the prompt neutron decay constant of BRAHMMA subcritical system. The Prompt neutron decay constant along with β_{eff} and Λ have been used to estimate the k_{eff}. It has been observed that the measured k_{eff} using Slope-fit method is close to the theoretical estimate, whereas, in Area-ratio and Source-jerk method the measured k_{eff} has deviation from the theoretical estimate. But, Area-ratio and Source-jerk methods can be used for reactivity measurement (in $) without prior estimation of β_{eff}.

However, deterministic methods have limitations due to thermal recycle of core and power fluctuation. Furthermore, the high energy particle accelerators, which will be coupled with ADS, will be operated in RF range. As a result, the decay of prompt neutrons between the beam pulses will be very small and the source will be similar to the continuous beam current. So, the applicability of deterministic methods using RF accelerator will be a serious technical issue. Thus, it is essential to develop robust method for reactivity measurement in ADS operating under such condition. Another important technique which can overcome the limitations of deterministic methods is based on neutron noise.

Noise method based on neutron correlation may be useful for reactivity measurement during continuous operation of ADS. The present work has studied noise methods for reactivity measurement in a deep subcritical system. Noise methods have already been studied in different subcritical systems using accelerator-based neutron source under the assumption of Poisson source characteristics. However, the assumption of non-Poisson behaviour for accelerator-based neutron source can be traced back to 1985 (Srinivasan, 1985). Later, Degweker and Rana (2007) have postulated a noise theory for ADS under assumption of external neutron source as exponentially correlated Gaussian character. Authors have also postulated various noise descriptors for different pulse width, for example, Dirac-delta pulse and finite pulse width (Gaussian and Rectangular shape). However, very little experimental work has been reported to address the non-Poisson character of the accelerator-based neutron source and experimental validation of the noise theory.

During the present study, investigation has been carried out for evaluating the characteristics of accelerator-based D-T neutron source (PNG). This has been carried out using a ^{3}He detector and time stamp data acquisition system. It has been observed that PNG has fluctuation ~2-2.5% and measured *V/M*-1 has an asymptotic value of 0.1. Thus, the above stated facts validate the basic assumptions of Degweker and Rana (2007). Furthermore, time stamped data have been analysed using *ACV* method and the exponential decay of *ACV* has been used to estimate the source correlation time. This particular new approach has been implemented to understand the characteristics of accelerator-based neutron source. The measured source correlation factor (for example, 50.44±10.76 ms^{-1} at accelerator frequency 10 kHz), which appears due to the periodic nature of ion beam current, is large compared to the accelerator frequency and the prompt neutron decay constant of BRAHMMA. Furthermore, it has been observed that the source correlation time is comparable to the finite pulse width at lower accelerator frequencies. Therefore, the variation of the source correlation time with accelerator pulse width has been studied and it has been observed that the finite pulse width has significant contribution to the source correlation time. Moreover, pulse shape characterisation is essential for validation experiment of the noise theory. For this purpose, an ACCT has been introduced in D^+ beam path of PNG and the measured pulse shape was found to be rectangular.

In the next step, first ever experimental validation of the above-mentioned noise theory has been carried out using BRAHMMA and PNG. During noise experiments, eight ^{3}He detectors have been placed at designated locations based on the system modal analysis (Kumar et al., 2017). This symmetric arrangement of detectors cancels out the first symmetric modes and all anti-symmetric modes in the measured reactivity (Rana et al., 2013). In noise experiment, time stamped data have been analysed using *V/M*, *ACV* and *APSD* method. It has been observed that the measured prompt neutron decay constant using various noise descriptors are in good agreement with the theoretical estimate. Furthermore, a modest approach has been made for analysis of prompt neutron decay constant with the exact noise descriptor as proposed by Degweker and Rana (2007). However, it has been observed that the noise descriptors used in the present study are more appropriate according to the accelerator parameters. The present study also provides qualitative discussion of the space dependent noise theory for the first time in measured *V/M* as discussed theoretically by several authors.

This work has also validated the noise theory postulated by Degweker and Rana (2007) considering finite and rectangular pulse width using PNG and BRAHMMA subcritical system. In this context, authors have postulated different cases for source correlation time, accelerator pulse width and frequency. In the present study, based on the observed variation of source correlation time with accelerator pulse width, validation experiments have been carried out for source correlation time smaller compared to the pulse width along with rectangular pulse shape.

During noise analysis, it has been observed that the correlated amplitude in *V/M* method decreases and uncorrelated oscillation increases with lower accelerator frequency. The variation of correlated and uncorrelated amplitude in *V/M* method suggests that accelerator frequency which is smaller compared to the prompt neutron decay constant (α) is responsible for such behaviour. In case of *V/M* and *ACV* method, the oscillation of uncorrelated part makes the fitting of the experimental data difficult and the number of higher order term increases with smaller accelerator frequency. On the other hand, in case of *APSD*, the measurement of α is much easier compared to *V/M* and *ACV* method as the integer multiple of source frequency appears as delta function. However, it has also been observed that the prompt neutron decay constant measured using different noise methods developed under consideration of rectangular and finite pulse width are in good agreement with the reference value other than measured using *ACV* at 4 kHz. This deviation may be attributed to the change of correlation of neutrons for accelerator frequency close to prompt neutron decay constant for the particular system in consideration. Hence, based on this observed variation of *V/M* and *ACV* with accelerator parameters, the ADS community will be benefited in deciding the accelerator frequency and other beam parameters for reactivity measurement in ADS.

The time stamp data acquisition system (Kumar et al., 2015), which has been used during the present study, has limitations of number of samples, trigger with PNG. Thus, an advanced time stamp data acquisition system has been developed for further noise experiments. The development has been carried out using NI6602 time stamp system, LabVIEW student edition 32 bit and NI-DAQ driver package (National Instruments, 2019). The newly developed time stamp data acquisition system has additional features, for example, no limitation of sample length, synchronous or asynchronous mode, real time visualisation of source stability and two-timing inputs. The time stamp data acquisition system has been validated with isotopic neuron source (Am-Be) and it performed satisfactorily.

To conclude, the outcome of the present study are as follows:

- The research work has studied the reactivity measurement using deterministic methods in a deep subcritical system.
- A methodology has been developed to characterise the accelerator-based neutron source for noise experiments.
- First ever experimental validation of the noise theory developed by Degweker and Rana (2007) under assumption of exponentially correlated Gaussian source characteristics has been carried out for Dirac-delta pulse as well as finite pulse width.
- The study has discussed the variations of noise descriptors with accelerator frequency.
- It has been attempted to develop a robust method for reactivity measurement in ADS. Reactivity measurement using *APSD* is much easier compared to *V/M* and *ACV*.
- The study has also developed an advanced time stamp data acquisition system for further noise experiments.

Future Scope

The present work can be further extended to noise experiment in synchronous mode with PNG using newly developed data acquisition system. Furthermore, the study has discussed, qualitatively, the space dependency of the correlated amplitude in *V/M*. However, there is a further scope of quantitative research on the space dependency of correlated amplitude. Moreover, the variation of the source correlation time with the accelerator pulse width needs to be studied with exact theoretical model.

Summary

Nuclear energy plays a vital role in energy security of a country for its rapid economic growth without disturbing the environmental balance. It requires addressing two important issues, optimum use of available nuclear fuel resource in the country, and simultaneously solve the problem of nuclear waste which would come as a by-product. Accelerator Driven Subcritical (ADS) system can address both the issues. Such system can provide a solution to sustain the supply of fuel for Indian nuclear power programme, by utilizing vast Thorium reserves of India with an external neutron source to first breed Thorium to fissile element ^{233}U and use for power production. Furthermore, the long-lived transuranic elements can be burnt in the fast spectrum of ADS easing the burden on waste management. However, fast ADS has a problem during the burning of actinides. The delayed neutron fraction of such a system with minor actinide as fuel is low, leading to its control issues. Therefore, reactivity, which is the most important parameter of any reactor system, needs to be monitored continuously for power production, control and safety of ADS. This requires the development of robust method for reactivity measurement. As a part of ADS programme in India, a thermal subcritical system has been commissioned for basic research on reactivity measurement.

The study has focused on reactivity measurement in a deep subcritical system namely, **B**eO **R**eflected **A**nd **H**DPe **M**oderated **M**ultiplying **A**ssembly (BRAHMMA), commissioned in Bhabha Atomic Research Centre, India. Initially, reactivity measurement experiments have been carried out using deterministic methods, for example, Area-ratio, Slope-fit and Source-jerk based on the perturbation of external D-T neutron source. But deterministic methods are not suitable for reactivity measurement during continuous operation of ADS due to thermal recycle of the core and power fluctuations. On the other hand, noise method based on correlation technique may be useful for reactivity measurement during continuous operation of ADS. In this context, a noise theory assuming the accelerator-based neutron source as

exponentially correlated Gaussian character had been developed by Degweker and Rana (2007) for reactivity measurement in ADS. First-ever experimental validation of this noise theory has been carried out using D-T neutron generator and BRAHMMA subcritical system. As a part of validation experiments, a methodology has been developed to study the statistical properties of accelerator-based neutron source for noise experiments. Then validation experiments have been carried out for different pulse shape using various noise descriptors, for example, Feynman-alpha, Auto Covariance and Auto Power Spectral Density. Furthermore, variations of noise descriptors with accelerator parameter(s) have also been studied for a fixed subcriticality.

Time stamp data acquisition system is essential to conduct noise experiments as noise descriptors are based on the time signature of neutron detection. The time stamp data acquisition system used in noise experiments in the present study had some limitations, such as single input for time stamp, maximum sample of 10 million and asynchronous mode only. Hence, an advanced time stamp data acquisition system has been developed with incorporation of more features, such as three input channels, trigger input, data archiving for high sample length and real-time visualisation of source stability for further noise experiments.

To conclude, reactivity measurement using deterministic and noise methods have been studied in a deep subcritical system BRAHMMA. During noise experiments, a methodology has been developed to study the statistical property of accelerator-based neutron source. Furthermore, first-ever experimental validation of the noise theory developed by Degweker and Rana (2007) has been carried out using BRAHMMA subcritical system and D-T neutron generator. Based on the research output, the ADS community will certainly be benefited in carrying out reactivity measurement using noise method along with accelerator-based non-Poisson neutron source. Moreover, an advanced time stamp data acquisition system has also been developed for further noise experiments.

CHAPTER ONE

INTRODUCTION

1.1 Nuclear Energy Scenario

The rapid growth in the technology sector with increasing power demand has increased the consumption of fossil fuel which in turn is responsible for surge in carbon emission. The carbon emission is a matter of concern as it is directly related to global warming and climate change (BP Statistical Review of World Energy, 2019). Therefore, the policy and decision-makers have put forth a framework, the Paris Agreement (United Nations Climate Change, 2019), to control global warming by rapidly reducing the dependency on fossil fuel in different areas, including power generation. To meet the specificities, developed as well as developing countries should revise their energy policies to reduce the dependency on fossil fuel and promote clean and green energy sources such as solar, hydro and nuclear power.

Among the clean and green energy sources, nuclear energy is more suitable in terms of resource use, installed capacity and land requirement. According to International Atomic Energy Agency (IAEA) report, by 31st December 2019, globally, 450 commercial nuclear power plants are operating with total 398.9 GWe capacities (IAEA, Preliminary Nuclear Power Facts and Figures for 2019). In addition, as of 1st January 2017, the power generation capacity and Uranium requirement were approximately 391 GWe and 62825 tonnes respectively. In this context, IAEA has predicted that by 2035, the global installed nuclear power generation capacity might be in between 331 GWe (low scenario) to 568 GWe (higher scenario) (Grancea & Hanly, 2018). Whereas, as per Nuclear Energy Agency of the Organisation for Economic Co-operation and Development (OECD/NEA), it will be within the range of 580 GWe (lower scenario) to 1400 GWe (higher scenario) by 2050 (Nuclear Energy Outlook, 2008). Moreover, modest growth of nuclear power generation can be seen mainly in the region of Asia, Africa, Central and South America by 2035 (Grancea & Hanly, 2018).

Presently, throughout the world, nuclear power is dependent on Uranium sources on the Earth, and the currently defined resource is more than adequate to meet the maximum Uranium demand by 2035 (Grancea & Hanly, 2018). Apart from Uranium, other vital factors, which may affect the future nuclear industry, include projected electricity demand, economic competitiveness of nuclear power plants, funding for nuclear power installations, production cost for other electricity generation technologies, waste management strategies and public acceptance of nuclear energy.

In India, as of 1st January 2020, the total installed nuclear power capacity is 6780 MWe, which comprises of 2 Boiling Water Reactors (BWRs), 18 Pressurised Heavy Water Reactors (PHWRs) and 2 Water Water Energy Reactors (VVERs) (Nuclear Power Corporation of India (NPCIL), 2020). Additionally, 4x700 MWe PHWRs, 2x1000 MWe VVERs (NPCIL, 2020) and 1x500 MWe Prototype Fast Breeder Reactor (PFBR) (Bharatiya Nabhikiya Vidyut Nigam Limited (BHAVINI), 2020) are under construction which will increase the installed capacity to about 12080 MWe.

In 2015, annual Uranium requirement in India amounted to about 1300 tonnes. The Uranium requirements for PHWRs in India are being met with a combination of internal and external sources (Grancea & Hanly, 2018). The identified internal Uranium resources are enough to support 10-15 GWe installed capacity of PHWR operating at lifetime capacity factor of 80% for 40 years. But, the other two types of nuclear reactors such as BWRs and VVERs are entirely fuelled by imported Uranium (Grancea & Hanly, 2018).

The issue of using Uranium as nuclear fuel is the permanent disposal of discharged fuel from Light Water Reactors (LWRs) as well as PHWRs due to the presence of long-lived radioactive wastes. The discharged fuel contains approximately 0.4 wt% long-lived fission products, for example, Caesium, Strontium, Technetium, and Iodine. Moreover, the presence of approximately 1 wt% of minor actinides (namely, Neptunium, Americium, Curium and

Californium) and Plutonium in spent fuel make nuclear fuel management more complicated because of their long half-lives (Status of Minor Actinides Fuel Development, 2009). These transuranic nuclei, heavier than Uranium, are produced by neutron capture in reactor and after a few hundred years, the radioactivity of transuranic elements will be higher than the fission products. Therefore, permanent disposal of these long-lived transuranic elements is always a matter of concern. In order to lower the environmental impact and further growth of nuclear power, robust nuclear waste management plan is being developed by several nations (Status of Minor Actinides Fuel Development, 2009). Several reprocessing plants for spent fuel have already been developed in France, United Kingdom (UK), Russia, Japan and India (Country Nuclear Fuel Cycle Profiles, 2005). The separation of these long-lived transuranic elements and incineration in a dedicated reactor can reduce the half-life by few orders. Incineration occurs due to fission of actinide isotope which depends on the fission cross-section. However, fissile isotopes, such as ^{239}Pu, ^{241}Pu have high fission cross-section, but fertile isotopes, such as ^{240}Pu, ^{242}Pu have very low fission cross-section for thermal neutron. On the other hand, all actinides have significant fission cross-section for fast neutron. Also, the incineration of transuranic elements in critical reactor may deteriorate the neutronic characteristics of the core, in particular, the coolant void temperature coefficient, the Doppler coefficient and delayed neutron fraction (Status of Minor Actinides Fuel Development, 2009). Based on the above-mentioned facts, it can be said that fast spectrum along with subcritical system driven by an external neutron source which can be switched 'ON' and 'OFF', will be more suitable for incineration of actinides in large quantity.

In the context of nuclear fuel, Thorium is more abundant than Uranium on the Earth crust. During 1960s, Thorium has been recognised as alternate of Uranium as nuclear fuel, and till date, several concepts have been proposed for Thorium based reactor. Several studies have also demonstrated the advantages of Thorium as nuclear fuel, for example, superior physical and nuclear properties, reduced Plutonium and minor actinide production. Among the disadvantages, Thorium is a fertile element, Thorium oxide is chemically inert and the intermediate production of Protoactinium-233, which is neutron absorber (Humphrey & Khandaker, 2018). Therefore, Thorium needs conversion or breeding to ^{233}U upon neutron irradiation, which is fissile material and can be used for fission. The estimated Thorium resources in Earth crust are around 6 million tonnes, and India has the highest inventory (846000 t) of Thorium (World Thorium Occurrences Deposits and Resources, 2019). Thorium can be used for power production in a planned way, for example, the 'Three-stage nuclear power programme', which is being pursued by India (Grover & Chandra, 2006). Moreover, with an aim to burn the surplus weapon grade Plutonium and minor actinides using Thorium-Plutonium fuel initially and subsequently with Th-^{233}U self-sustain fuel cycle, Rubbia et al. (1995) proposed fast Energy Amplifier (EA). The EA module consists of a 1500 MWe_{th} subcritical unit driven by a high energy proton accelerator (1 GeV and 12.5 mA). The core heat removal is passive and through natural convection. A large quantity of minor actinides can be transmutated safely because of subcriticality of the core. According to Rubbia et al. (1995), EA system has the potential to become the future energy solution with closed fuel cycle. An approach has been adopted for suitable use of Thorium in Indian nuclear power programme by using EA, which is also known as Accelerator Driven Subcritical (ADS) system.

The history of accelerator-based breeding and ADS has further been discussed in section 1.2. The ADS system consists of a subcritical core and a high energy particle accelerator along with beam target as an external neutron source. External neutrons will be produced by interaction of high energy particles with beam target through cascade chain reaction, which is also known as spallation reaction as discussed in section 1.3. The concept of ADS for energy production and waste transmutation has investigated by several researchers around the world as discussed in section 1.4. There are various technical and physics issues related to ADS as discussed in section 1.5. Among the physics issues, measurement of reactivity, which is defined as relative departure from criticality is essential from commercial, control and safety point of view. The reactivity of subcritical system can be measured by either deterministic methods or noise methods. Deterministic methods, for example, Pulsed Neutron Source techniques and Source-jerk have been developed by perturbation of external neutron source. These deterministic methods may be suitable for reactivity measurement during core loading but not suitable for reactivity measurement during continuous operation of ADS, because of thermal recycle of the core along with power fluctuation. On the other hand, noise methods based on correlation of fission neutrons can infer reactivity during continuous operation of ADS. Therefore, researches have been carried out for noise theory development and experiments under assumption of Poisson characteristics (events are random and uncorrelated) of external neutron source. However, the statistical property of source neutrons, which will be produced by spallation reaction, will play an important role in reactivity measurement in ADS. In case of accelerator-based neutron source, there will be statistical fluctuation in the number of neutrons produced per pulse and the spallation neutrons are also correlated because of the cascade chain reaction. Additionally, the periodically chopped beam cannot be considered as random event. From the above stated facts, it can be said that accelerator-based neutron source cannot be assumed as Poisson character. Therefore, researchers have also developed noise theory for ADS assuming the non-Poisson source characteristics. In this context, Degweker and Rana (2007) have developed a more general noise theory for ADS assuming the external neutron source as exponentially correlated Gaussian character. Though, theoretical work has been carried out to address the non-Poisson character of accelerator-based neutron source, very little experimental work has been reported to characterise an accelerator-based neutron source and validate this noise theory. Therefore, the aim or the novelty of the present research is to characterise an accelerator-based neutron source along with validate the noise theory developed under consideration of exponentially correlated Gaussian source characteristics. However, the detail research histories on reactivity measurement in subcritical system and rationale of the present study have been discussed in section 1.6 and 1.7 respectively.

1.2 History of Breeding and Accelerator Driven Subcritical (ADS) System

The accelerator-based breeding of fissile material was demonstrated by Glenn Seaborg around 1940. The initial attempts to build accelerator-based neutron sources were made during 1940s by E.O. Lawrence in the United States of America (USA) and W.N. Semenov in the former Soviet Union (Kadi & Revol, 2003). The discovery of the spallation process (Goeckermann & Perlman, 1948) opened the possibility of breeding using intense neutron source. During 1950s, MTA (Materials Testing Accelerator) programme at Lawrence Livermore, the accelerator-based breeding was investigated in detail. At the same time, Lewis initiated spallation neutron yield measurements with the McGill cyclotron. In 1960, Lawrence et al. patented fissile material production using accelerator on Uranium and Thorium target. The concept of accelerator-based breeding was also studied on depleted Uranium in Soviet Union. More recently, Bowman et al. (1992) proposed the energy generation and waste transmutation using accelerator-based intense thermal neutron source. Rubbia et al. (1995, 1997) proposed the fast energy amplifier based on Th-Pu along with Th-^{233}U fuel cycle. Soon after the proposal of fast energy amplifier, a group of scientists carried out feasibility studies of Fast Energy Amplifier Test (FEAT) (Andriamonje et al., 1995) and Transmutation by Adiabatic Resonance Crossing (TARC) (Arnould et al., 1999) project at CERN laboratory.

1.3 General Description of Accelerator Driven Subcritical (ADS) System

At present, nuclear power is being generated from critical reactors. In a critical system, there is a self-sustaining chain reaction. Whereas, in case of subcritical system, the self-sustain chain reaction does not exist. As a result, the neutron population will die away with time and to sustain the chain reaction, an external neutron source is needed. Due to this fact, ADS as the name suggests consists of a subcritical core driven by an external neutron source.

In ADS, initially the subcritical core will be loaded with Thorium and fissile material (^{239}Pu), which acts as fuel and produces power by fission reaction. Therefore, long lived minor actinides and Pu can be transmuted into short live fission products in ADS system. Some of the fast neutrons will interact with Thorium and causes conversion of ^{232}Th to ^{233}U with some intermediate stages, which is named as breeding process. As a result, after few life cycles the Pu can be replaced by ^{233}U. According to several studies, the self-sustain Thorium cycle is possible in ADS due to higher burnup (Rubbia et al., 1995; Bowman, 2000; Kadi & Adonai, 2006).

External neutrons, which will play an important role in ADS, can be produced from several nuclear reactions, for example, photo neutron, fusions and spallation. In photo neutron source, high energy photons interact with low-Z target material to produce neutrons. In case of fusion reaction, two light nuclei (D-D/D-T) are fused, which emits neutrons (2.45 MeV or 14.1 MeV). In case of spallation, a high energy particle (around 1 GeV), such as proton or deuteron will interact with some high Z-target material such as Lead, Uranium, Lead-Bismuth eutectic. For particle energy comparable to its rest mass energy, the De-Broglie wavelength of the projectile will be very small, and it may be considered as a classical particle. The projectile will interact with the nucleons, which in turn interact with other nucleons. As a result, there will be an intra-nuclear cascade, and some nucleons will be emitted from the nucleus. Subsequently, the emitted high energy nucleons will interact further with another nucleus in target material, and this is defined as inter-nuclear cascade. Finally, the residual nucleus will be de-excited by evaporation of nucleons and fission. The spallation neutrons have a spectrum similar to fission with a peak around 3-4 MeV and high energy tail (Kadi & Revol, 2003). The total number of neutrons produced per incident particle will depend on the projectile mass, energy and the target material. However, in the case of Pb target and 1 GeV proton, approximately 25 neutrons will be produced per incident proton. The spallation has the highest yield for incident particle energy of 1-2 GeV. At higher energy, the projectile will lose its energy by neutral Pion production. Among the target materials, Lead Bismuth eutectic is more suitable, because of its low melting point. The nominal beam current and power for spallation source are 12.5 mA and 12.5 MW respectively (Rubbia et al., 1995) and the corresponding neutron yield is approximately 10^{16} n/s. The spallation has the highest efficiency compared to other reactions and will play an important role for the external neutron source in ADS (Kadi & Revol, 2003).

1.4 The Existing High-intensity Particle Accelerators and Subcritical Systems

Soon after the proposal of ADS by Rubbia et al. (1995), the experimental research has been initiated by several researchers around the globe. The plan of energy amplification has been demonstrated in the CERN lab in Europe using FEAT subcritical assembly (Andriamonje et al., 1995). The power, flux, temperature distribution and energy gain have been studied using 3.5 tonnes metallic natural Uranium, CERN-PS proton beam with Lead and Uranium as beam target. The maximum gain was observed at 1 GeV. In the next step, the TARC experiment has been carried out to study the adiabatic resonance crossing for ^{99}Tc and ^{129}I in Lead matrix. It has been demonstrated that the adiabatic resonance crossing is a powerful technique for burning long-life fission fragments showing resonance (Arnould et al., 1999).

Transmutation and energy production are possible in ADS using high energy (~1 GeV) and high current (~10 mA) particle accelerator. At present, several countries have high-energy particle accelerators, for example, PSI in Switzerland with proton beam current of 1.4 mA and energy 590 MeV, ISIS in UK having proton energy 800 MeV, LANSCE with proton beam current of 1.5 mA and energy 800 MeV and ORNL with beam energy 800-1000 MeV in USA. India is also developing a high energy high current proton accelerator for ADS programme (Degweker et al., 2017).

However, before using high power accelerator, it is essential to study the physics of subcritical system using an alternate neutron source as discussed in the previous section. At present, the physics research on subcritical system has been pursued in several countries, either using isotopic source or D-D/D-T neutron generator. For example, subcriticality measurement using Pulsed Neutron Source (PNS) and noise methods at neutron multiplication factor (k_{eff}) of 0.96 to 0.99 have been studied using MASURCA in France (Soule et al., 2004; Plaschy et al., 2005; Lebrat et al., 2008). Flux measurement, PNS and noise experiments at thermal (k_{eff}=0.92 to 0.95) and booster (k_{eff}=0.99) core have been studied on YALINA subcritical systems in Belarus (Persson et al., 2005, 2008; Gohar et al., 2009; Tesinsky et al., 2011). Research on the spectrum of fast ADS along with reactivity measurement using PNS and noise methods at k_{eff} of 0.95 to 0.99 have been carried out in GUINEVERE project in Belgium (Mercatali et al., 2010; Uyttenhove et al., 2011). Similarly, KUCA in Japan is having k_{eff} of 0.992 and has been used to study reaction rate distribution, source multiplication factor measurement, reactivity measurement using PNS and noise methods (Pyeon et al., 2007, 2008).

In India, a road map has been prepared (Kapoor, 2002) for physics studies of subcritical system, high energy proton accelerator and beam target development. As a part of physics research on subcritical core, a zero-power subcritical system namely, **B**eryllium-Oxide

Reflected **A**nd **H**DPe **M**oderated **M**ultiplying **A**ssembly (BRAHMMA) (Sinha et al., 2015) has been designed and commissioned in Bhabha Atomic Research Centre (BARC), India.

However, the existing facilities are for advanced research on subcritical system and accelerator technology. The demonstration of ADS by coupling the different components (accelerator, spallation target and subcritical core) at the power level of 100 MWe is under advanced stage of development by SCK-CEN, MYRRAHA (Abderrahim et al., 2012; Bruyn et al., 2015).

1.5 Challenges in ADS

ADS is being studied worldwide because of its potential use in energy production and transmutation of long-lived higher actinides. It has superior safety characteristics compared to critical reactor as discussed in section 1.1. Apart from these factors, the vast resource of Thorium and its utilisation has thrust ADS related studies. On the other hand, several issues exist in designing and operation of ADS system which are related to high end critical technology and physics. Among the technical aspects, the crux is the development of high energy and high current particle accelerator. Other technical issues are related to beam target design, the cooling of the beam target and the beam window design.

In addition, major physics issues related to subcritical core is the development of code and nuclear data, which is an integral part of designing an ADS system. At present, simulations of ADS are divided into two steps; the first step involves the interaction of high energy particle with target and the next involves low energy neutronic calculation of the subcritical core. The first step involves the calculation related to the number of spallation neutrons per incident particle, the energy spectrum of neutrons, the heat deposition and the distribution of spallation products. Several computer codes such as FLUCA, LAHET, and CASCADE (Prael & Madland, 2000; Ferrari & Sala, 1996; Kumawat & Barashenkov, 2005) are used for simulation of spallation source. In the next step, the deterministic and Monte-Carlo based codes are used for neutronic studies, for example, neutron multiplication, reactivity parameters, neutron flux distribution, burnup calculation and transient studies. The accurate modelling of the subcritical core requires the cross-section files for higher energy neutrons. There are also several experimental facilities such as CERN Time of Flight facility for high energy cross-section measurement (Abbondanno et al., 2002).

Furthermore, another physics issue is that the neutron multiplication factor at the centre and boundary will not be the same. This fact leads to the concept of source multiplication factor (k_s), which is defined by the ratio of the total fission neutron produced to the total fission and source neutron. Whereas, neutron multiplication factor (k_{eff}) is defined by the ratio of the rate of neutron production and the rate of absorption along with leakage. Moreover, in ADS, the average importance of source neutron to the fission neutron is defined by source importance factor (Ψ^*), which depends on the source location and energy. The k_{eff} and k_s are correlated with Ψ^*, which is related to the power produced in subcritical system (Shahbunder et al., 2010) as shown in equation 1.1. Thus, there is a need to study k_s and Ψ^* before designing such a system.

$$P = \frac{\varepsilon k_{eff} S_0 \Psi^*}{\bar{\nu}(1-k_{eff})} \tag{1.1}$$

where, ε and $\bar{\nu}$ are the mean energy and average number of neutrons per fission, S_0 is the source strength.

Reactivity is an important parameter in reactor design along with operation and is defined as fractional departure from criticality as shown in equation 1.2.

$$\rho = \frac{k_{eff} - 1}{k_{eff}} \tag{1.2}$$

In ADS, the power is inversely proportional to reactivity or subcriticality of core and proportional to the source strength (S_0) as shown in equation 1.1. Thus, for fixed source strength, the power can be increased by reducing the subcriticality. But, in a slightly subcritical system, there is a chance of having k_{eff} =1 due to the addition of reactivity, which results from Xenon decay (in thermal system) and accumulation of ^{233}U due to ^{232}Th breeding. Thus, safety margin should be taken into account during design of ADS to avoid any accidental scenario. During operation, the safety margin can only be ensured by periodic measurement of the reactivity. Therefore, accurate measurement of reactivity in subcritical system is important from commercial, control and safety point of view. Hence, the development of suitable and robust method for reactivity measurement is essential for ADS system.

1.6 Empirical Research on Reactivity Measurement in ADS

In a critical system, measurement of reactivity is necessary during fuel loading, calibration of safety and control rods, continuous operation and shutdown process. The subcriticality in power reactor during fuel loading is monitored by the neutron flux level of Start-up and Intermediate Range Monitor (SIRM). In case of neutron flux higher than a specified limit, SIRM shutdown or scram the reactor. Furthermore, the effect of any transient during operation is studied by asymptotic period method and the shutdown margin needs to be calibrated by suitable method.

However, the above mentioned SIRM is not good enough in case of prompt criticality during fuel loading or any operational transient in case of subcritical core. So, suitable reactivity measurement technique should be used as an extra precaution in addition to SIRM. Since, the power in ADS is inversely proportional to the reactivity, the energy gain can be maximised by reducing the subcriticality for a specific beam power. Thus, in case of any transient, the changes in neutron source may mask the changes in reactivity. The situation will be more susceptible in case of slightly subcritical system. Therefore, the above-mentioned facts necessitate the development of robust method for reactivity measurement in ADS.

The research on reactivity measurement in multiplying system started way back in 1950s using pulse neutron source and was developed by Sjöstrand and Gozani (Sjöstrand, 1956; Gozani 1962), presently known as Area-ratio method. They used the detector response along with pulsed neutron source to measure the subcriticality. Other researchers used the slope of the decay of neutron population following the neutron pulse to infer the reactivity, which is termed as Slope-fit method (Simmons & King, 1958). Later, a new method of reactivity measurement in a subcritical system named as Source-jerk method was also developed, which is similar to the Rod-drop method in case of critical system (Ryves & Scott, 1962). The Area-ratio, Slope-fit and Source-jerk methods are also known as deterministic method. Further development of deterministic methods using pulsed neutron source has been carried out in different subcritical systems (Christopher & Cady, 1967; Preskitt et al., 1967; Dragt, 1973; Rosselet et al., 1998; Perdu et al., 2003; Soule et al., 2004; Jammes et al., 2005, 2006; Persson et al., 2005, 2008; Billebaud et al., 2007; Gabrielli et al., 2008; Talamo et al., 2009; Taninaka et al, 2011; Gajda et al., 2013; Bécares et al., 2013; Talamo et al., 2017; Pyeon et al., 2017). These methods are based on the simple point kinetic approach. However, the presence of the localised neutron source in subcritical system leads to spatial variation of power and simple point kinetic approach becomes invalid (Kulik and Lee, 2006). In this context, it has also been demonstrated that measured reactivity depends on the detector location (Kulik and Lee, 2006) and this spatial effect is induced by the prompt and delayed neutron harmonics (Cao and Lee, 2010). Theoretical development has also been carried out to get rid of detector and source dependency of the measured reactivity (Kulik & Lee, 2006; Cao & Lee, 2010; Talamo et al., 2012a, 2012b; Gajda et al., 2013; Uyttenhove et al., 2014). Janczyszyn (2013) has presented the Sjöstrand method using transport equations and concluded that the information for the reactivity calculation should come from the entire system by placing multiple detectors. Author further stated that the calculation of reactivity should be made by weighted average from these detectors or by placing a single detector at the location that is equivalent to the entire system. Another theoretical development related to reactivity measurement is Source Modulation method, which infers the reactivity by monitoring the neutron flux along with periodic modulation of the external neutron source (Carta & D'Angelo, 1999; Rineiski & Maschek, 2005; Wright & Pázsit, 2006). More recently, Marie et al., (2019) demonstrated the Current to Flux method for reactivity measurement in VENUS-F subcritical system.

Though, the above-mentioned methods are useful for reactivity measurement, they also have some drawbacks. For example, in Pulsed Neutron Source and Source-jerk method, the beam should be 'OFF' for a time length which depends on the prompt neutron decay time of subcritical system. Since, the prompt neutron decay time in fast ADS is in microsecond and generated jerking for such a short time will give neutronic response but no thermal response. Thus, these methods might be suitable for fast ADS. In case of thermal ADS, such as heavy water system, generated jerking time scale must be higher than the prompt neutron decay time (~ millisecond). As a result, thermal cycle and power fluctuation will take place for this time duration which is non-desirable. Furthermore, high energy particle accelerator operates at Radio Frequency (RF) (Seidel et al., 2010) and the corresponding pulse period is in few tens of nano-second. Thus, the applicability of deterministic methods using RF accelerator will be a serious technical issue. Source Modulation requires periodic modulation of beam power and very little experimental work has been reported. In addition, the Current to Flux method requires periodic calibration for accelerator beam current, reactor flux and reactivity using other method. All these drawbacks of deterministic methods initiated the development of robust method for reactivity measurement in ADS using neutron noise.

Noise methods can play an important role to infer reactivity during continuous operation of ADS. Development of noise method for measurement of reactivity as well as reactor kinetic parameters can be traced back to 1960s based on neutron correlation techniques

(Williams, 1974). The popular noise methods, namely Feynman-alpha or Variance to Mean ratio minus one (*V/M-1*), Auto Covariance (*ACV*), Cross Covariance, Rossi-alpha and Power Spectral Density (*PSD*) have been developed for noise analysis in time and frequency domain. Later, we can find that the research using noise method gained renewed interest with the proposal of ADS by Rubbia et al. (1995). Theoretical development of various noise descriptors was advanced with continuous and pulsed neutron source assuming Poisson source characteristics (Pázsit & Yamane, 1998b; Kuang & Pázsit, 2000; Muñoz-Cobo et al., 2001; Kostić, 2002; Kitamura et al., 2005). Various noise descriptors have been redefined for synchronous and asynchronous detection techniques. The reactivity measurement using neutron correlation techniques have been conducted in several zero power subcritical system using D-D/D-T neutron source (Rugama et al., 2004; Kloosterman & Rugama, 2005; Pázsit et al., 2005; Ballester et al., 2005; Kitamura et al., 2006a, 2006b; Berglöf et al., 2011; Sakon et al., 2013).

The above-mentioned researches have been carried out under assumption of external neutron source follows Poisson distribution. In this regard, Srinivasan (1985) has discussed the feasibility of correlation technique to study the multiplication of 14 MeV neutron in Beryllium assembly. Author has also assumed the non-Poisson character of the accelerator-based neutron source and mentioned that the correlation property of such source needs to be studied. The reasons for the non-Poisson character of the accelerator-based neutron source have already been discussed in section 1.1. Later, various eminent researchers have considered the non-Poisson characteristics of accelerator-based neutron source in noise theory development (Pázsit & Yamane, 1998a; Degweker, 2000, 2003; Ballester & Muñoz-Cobo, 2005, 2006; Muñoz-Cobo et al., 2008). In this regard, Degweker and Rana (2007) had carried out extensive theoretical work by considering the external neutron source as pulsed and exponentially correlated Gaussian character.

In the context of experimental research, measurement of reactivity in subcritical system is always challenging due to the presence of higher harmonics of prompt and delayed neutrons. The higher harmonics have major contribution towards neutron population in deep subcritical system. Therefore, the measured reactivity will be contaminated by higher harmonics. Theoretical studies have also been carried out to discuss the modal influence on the measured reactivity in ADS (Rugama et al., 2002; Muñoz-Cobo et al., 2011; Singh et al., 2009, 2011; Yamamoto, 2013, 2014). Rana et al. (2013) proposed the mode cancellation theory using multiple detectors at designated locations based on system modal analysis. Furthermore, Szieberth et al. (2015) demonstrated the space dependency of the measured reactivity due to source and detector location in DELPHI subcritical system (k_{eff}=0.92). Based on the theoretical postulate of mode cancellation (Rana et al., 2013), Kumar et al. (2017) have discussed the fundamental and higher symmetric modes in BRAHMMA subcritical system using in-house developed diffusion theory-based code KINFIN (Singh et al., 2009). Authors also validated the mode cancellation theory as proposed by Rana et al. (2013) using isotopic neutron source (Am-Be) having Poisson characteristics. Pyeon et al., 2017 also conducted noise experiments using spallation neutrons under the consideration of Poisson source characteristics. To conduct the noise experiments, authors have coupled a 100 MeV proton accelerator (20 Hz beam repetition) with Kyoto University Critical Assembly (KUCA).

1.7 Rationale of the Study

According to the above-stated literatures, it has been observed that the research on deterministic methods has been carried out in thermal and fast cores at different subcritical levels from k_{eff}=0.92 to 0.99. These deterministic methods can be used for reactivity measurement in subcritical system and critical system during fuel loading. However, the reactivity measurement using deterministic methods in a deep subcritical system (subcriticality more than 10,000 pcm) needs to be studied. Despite the importance of deterministic method for reactivity measurement in subcritical system, very little research has been carried out on the applicability of deterministic methods in a deep subcritical system.

In spite of the usefulness of deterministic methods, from the above-stated literatures it can be said that these methods mainly Pulsed Neutron Source, Source-jerk and Current to Flux method have some disadvantages. On the other hand, noise methods are absolute and can infer reactivity during continuous operation of ADS. Thus, noise methods can take care of all these disadvantages to infer the reactivity in a subcritical system.

From the existing literatures, it has been observed that noise experiments have been conducted only under the consideration of external neutron source following Poisson distribution. But in principle, external neutron sources based on particle accelerators cannot be assumed as Poisson characteristics whether in stationary or pulsed mode of operation. The non-Poisson character of the accelerator-based neutron source is important because of the internal fluctuations of the beam current and accelerating voltage. Furthermore, periodically chopped beam cannot be considered as Poisson character (Srinivasan, 1985). Based on the non-Poisson characteristics of the accelerator-based neutron source, Degweker (2003) has developed a noise theory for ADS. Degweker and Rana (2007) have also redefined the noise descriptors by considering the external neutron source as pulsed and exponentially correlated Gaussian character. The Gaussian character refers to the fact that number of neutrons in a pulse follows Gaussian statistics rather than Poisson statistics, whereas, exponential correlation means that neutrons in a pulse are dependent on the subsequent pulses. In the latter case, the source is correlated and the correlation is assumed to decay exponentially with time between pulses which is related to the fluctuation of the accelerator ion current (Degweker & Rana, 2007). The decay constant of correlated pulsed neutron source is termed as source correlation factor. Authors have also postulated about the circumstances under which the derived formulae will be same for uncorrelated Gaussian source characteristics. Although theoretical work has been developed to address the non-Poisson character of the external source, it is very hard to find any experimental work in this area which necessitates to validate the noise theory developed under consideration of exponentially correlated Gaussian source characteristics and Dirac-delta pulse.

On the other hand, there could be situation when the pulse width is finite and comparable with prompt neutron decay time ($1/\alpha$). In this perspective, Degweker and Rana (2007) have postulated noise descriptors for different pulse shape (Rectangular and Gaussian) with finite width. They also considered different cases for source correlation time, accelerator pulse width and frequency. Furthermore, in case of accelerator frequency less than the prompt neutron decay constant (α), the fission chain induced by external neutron source will die away between consecutive pulses. Thus, the correlation of fission neutrons from one pulse to the next pulse will be very small and will be reflected in the behaviour of various noise descriptors. However, very little experimental works in this direction have been reported to describe how the noise descriptors behave for a wide range of accelerator frequencies with fixed subcriticality and source strength. Therefore, there is a need to validate the noise theory developed under consideration of exponentially correlated Gaussian source characteristics along with finite pulse width and to study the behaviour of the noise descriptors for a wide range of accelerator frequency.

Finally, considering the above-mentioned facts, it can be stated that there is a need to study the reactivity measurement using both deterministic and noise methods in a same subcritical system to examine their suitability.

Time stamp data acquisition system is indispensable to conduct noise experiments as these are based on the time signature of neutron detection. Kumar et al. (2015) have developed a time stamp data acquisition system for noise experiments. Authors stated that, in their system, data could be stored for the arrival time of each detected neutrons using 80 MHz internal clock frequency. The data acquisition system has a maximum sample length of 10 million and works in asynchronous mode only. However, there is a need to enhance the capacity of existing data acquisition system for incorporation of advanced features such as, higher sample length, online stability assessment of the external neutron source and synchronous as well as asynchronous mode of data acquisition with pulse neutron source for further noise studies in ADS. The above-mentioned facts pave the way to develop an advanced time stamp data acquisition system for further noise experiments.

1.8 Objective of the Study

Based on the above-mentioned rationale, objectives of the present study are as follows:

- Reactivity measurement in a deep-subcritical system using deterministic methods.
- Experimental validation of noise theory developed under consideration of exponentially correlated Gaussian source characteristics and Dirac-delta pulse.
- Pulse shape measurement and experimental validation of noise theory developed under consideration of finite pulse width.
- Comparative study of reactivity measurement using deterministic and noise methods.
- Development of an advanced time stamp data acquisition system for further noise experiments.

CHAPTER TWO

DESCRIPTION OF SUBCRITICAL SYSTEM AND REACTIVITY MEASUREMENT METHODS

2.1 Introduction

In ADS power is related with the subcriticality of core and the energy gain can be maximised for a certain beam power by reducing the subcriticality. However, in case of any transient, the changes in neutron source may mask the changes in reactivity. This situation will be more susceptible in case of operation of ADS with highest possible value of reactivity, in order to minimise the accelerator power requirement. Therefore, to avoid any unpleasant situation, it is necessary to monitor the reactivity in ADS.

The reactivity measurement in subcritical system can be carried out using deterministic methods, for example, Pulsed Neutron Source technique (PNS), Source-Jerk, Current to Flux monitoring and Source Modulation. PNS and Source-Jerk method may be useful during core loading in critical and subcritical system but not suitable during continuous operation of ADS due to the thermal recycle of the core. On the other hand, noise method based on correlation of fission chain may be suitable for reactivity measurement during continuous operation of ADS as discussed in section 1.6. Therefore, the study has been conducted with an aim to develop robust method for reactivity measurement in ADS.

A detailed description of the different resources to conduct the present research work, different reactivity measurement techniques, data acquisition systems and data analysis procedures have been discussed in this chapter.

2.2 Systems Description

The study has been carried out using a deep subcritical system BRAHMMA, D-T neutron generator and data acquisition systems which have been discussed here.

2.2.1 BRAHMMA Subcritical System

The study has been conducted on a zero-power subcritical system namely, BRAHMMA which has been commissioned to conduct basic research on subcritical system and reactivity measurement (Sinha et al., 2015). It consists of metallic natural Uranium as fuel, high density polyethylene (HDPe) as moderator and Beryllium Oxide (BeO) as reflector. The fuel pins are inserted in 13X13 square lattices with pitch of 4.8 cm as shown in Figure 2.1. One of the unique properties of the core is its compactness because of HDPe and use of BeO as reflector. BeO has excellent property as neutron reflector and has diffusion length approximately 21 cm for thermal neutron. The core is surrounded in radial direction by 20 cm thick BeO reflector. Finally, the core is encapsulated by 5 cm thick Borated polyethylene (1 wt% ^{10}B) followed by 0.15 cm Cadmium to stop thermal neutrons leaving the assembly as well as those entering it from outside. The front half of the central 3X3 lattices acts as central cavity for external neutron source and the rear half is filled with lead and BeO as shown in Figure 2.2. Lead is used to slow down the fast neutrons and BeO will multiply the source neutrons by (n, 2n) reaction.

The system has total 160 fuel pins made from 3.2 t natural Uranium. The fuel pins have active length and diameter of 100 cm and 3.454 cm respectively. The system is modular due to use of HDPe blocks as moderator. The final k_{eff} (theoretical) of the system is 0.890±0.001, which can be increased by using enriched fuel only. Details of the BRAHMMA subcritical system have been presented in Table 2.1.

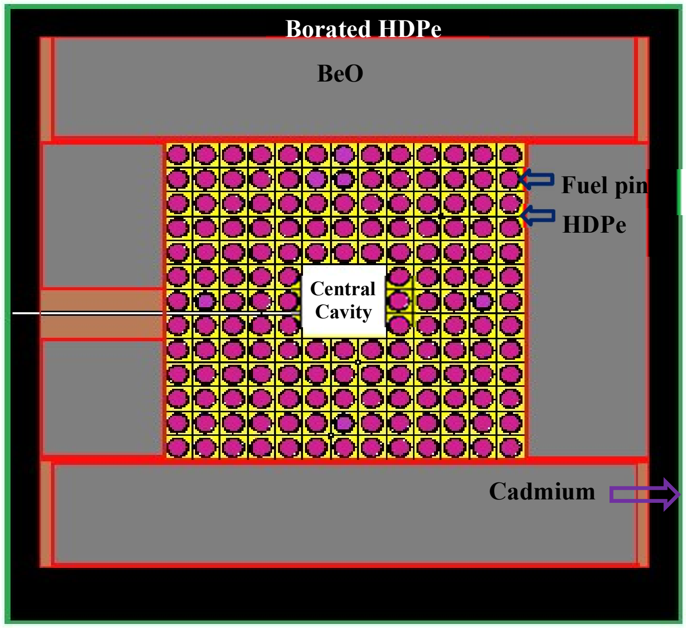

Figure 2.1. Schematic representation of BRAHMMA subcritical system along radial direction.

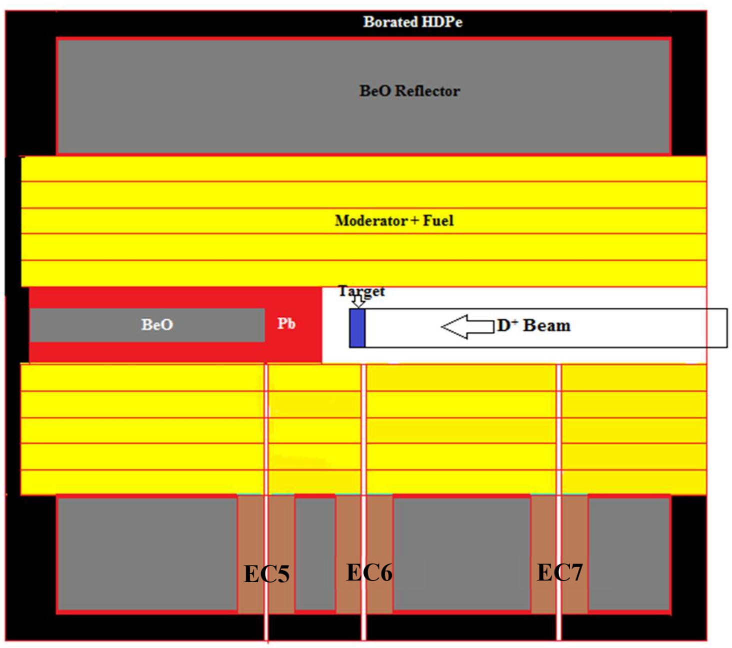

Figure 2.2. Schematic representation of BRAHMMA subcritical system along axial direction.

Table 2.1. *Details of BRAHMMA subcritical system.*

Fuel	Material	Natural Uranium
	No. of fuel pin	160
	Total length	120 cm
	Total diameter	3.656 cm
	Active length	100 cm
	Active diameter	3.454 cm
	Cladding material	Aluminium
	End cap	Aluminium
Central cavity	Radial dimension	14.4 cm X 14.4 cm
	Front half	60 cm
	Material	Hollow
	Rear half	60 cm
	Material	Lead and Beryllium Oxide
Moderator	Material	High density polyethylene
	Pitch	4.8 cm
Reflector	Material	Beryllium Oxide
	Thickness	20 cm
Shielding	Material	Borated polyethylene, Cadmium
	Thickness	5 cm,0.15 cm

2.2.1.1 Experimental Channels in BRAHMMA Subcritical System

BRAHMMA has several experimental channels along axial and radial direction for different experiments, for example, flux profile mapping and reactivity measurement. Details of the experimental channels are as follows:

1. Three experimental channels (EC1, EC2 and EC3) of diameter 10.0 mm are available along axial direction. EC1 is close to the external neutron source and EC3 is near to reflector as shown in Figure 2.3. The radial distance of axial channel (EC1, EC2 and EC3) are 12.2 cm, 23.8 cm and 26.5 cm respectively.
2. Four experimental channels (EC4, EC5, EC6 and EC7) of diameter 7.2 mm are available along the radial direction. EC5, EC6 and EC7 are in the mid-elevation plane and extended up to the central cavity only as shown in Figure 2.2. EC4 is located above the mid elevation plane as shown in Figure 2.4 and extended up to the inner surface of opposite reflector wall. Graphite plug of dimension 10 cm X 10 cm X 20 cm followed

by 5 cm Borated HDPe have been used to replace the BeO reflector along these radial channels. The channels are accessible through hole of 10 mm diameter in Graphite and Borated HDPe block. Details of the experimental channels have been presented in Table 2.2.

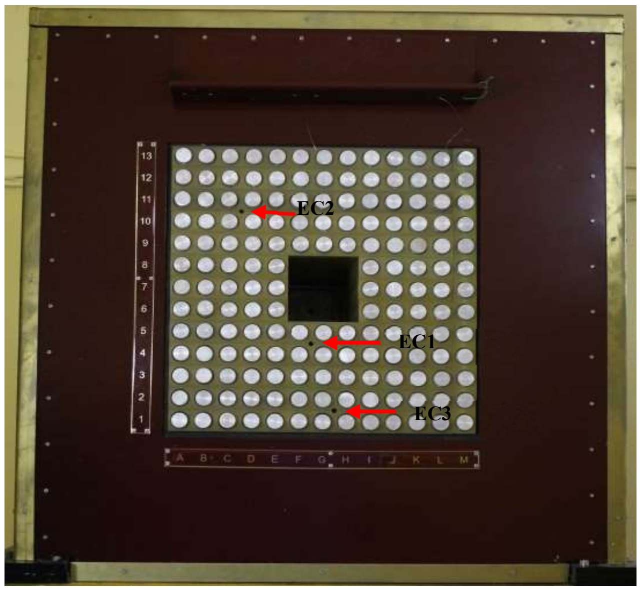

Figure 2.3. Experimental channels in BRAHMMA along axial direction.

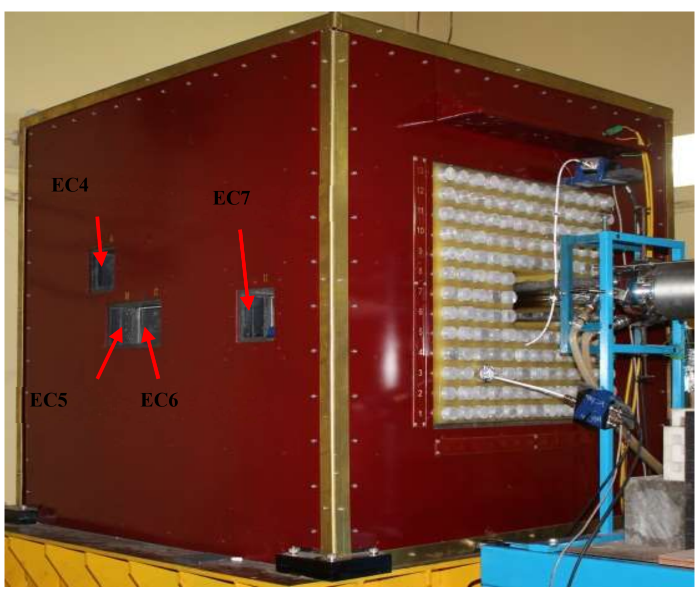

Figure 2.4. Experimental channels in BRAHMMA along radial direction.

Table 2.2. *Details of experimental channels.*

Axial channel	No. of channels	3
	Length	120 cm (EC1, EC2 and EC3)
	Diameter	1 cm
Radial channel	No. of channel	4
	Length	87.6 cm (EC4); 56.2 cm (EC5, EC6 and EC7)
	Diameter	0.72 cm

2.2.2 Purnima Neutron Generator

During the present research work, Purnima Neutron Generator (PNG) has been used as external neutron source. It is a 300 kV electrostatic DC accelerator-based neutron source. Radio Frequency (RF) ion source is being used to produce plasma in Deuterium gas. The D^+ ions are extracted from the plasma source to produce the Deuterium beam. The extracted beam is focused, accelerated and bombarded on Deuterium or Tritium target. In D-D and D-T mode, 2.45 MeV and 14.1 MeV neutrons are produced respectively. PNG has maximum yield of 5 X 10^{10} n/s in D-T mode.

PNG can be operated in continuous as well as pulsed mode. In pulsed mode, the frequency can be varied from 1 Hz to 10 kHz with variable pulse width and the minimum pulse width is 10 μs. Details of PNG have been presented in Table 2.3 and the pictorial representation of PNG along with its different beam components has been shown in Figure 2.5.

2.2.2.1 AC Current Transformer (ACCT)

During pulsed mode operation, an electrostatic voltage (2 kV) is used to chop the DC beam. The frequency and the width of the chopping voltage are according to the desired frequency and duty cycle of the PNG. Moreover, an ACCT has been introduced in the beam path as shown in Figure 2.5 to measure the pulse shape. ACCT is an evolution of the active transformer which has been proposed by Hereward (Unser, 1969, 1981). It has excellent features like low noise; reduction of DC offset and long-term stability (Bergoz Instrumentation). Finally, the ACCT output is fed into a high impedance device as shown in Figure 2.6 followed by an oscilloscope.

The ACCT has been used to measure the beam pulse shape and pulse width during noise experiments.

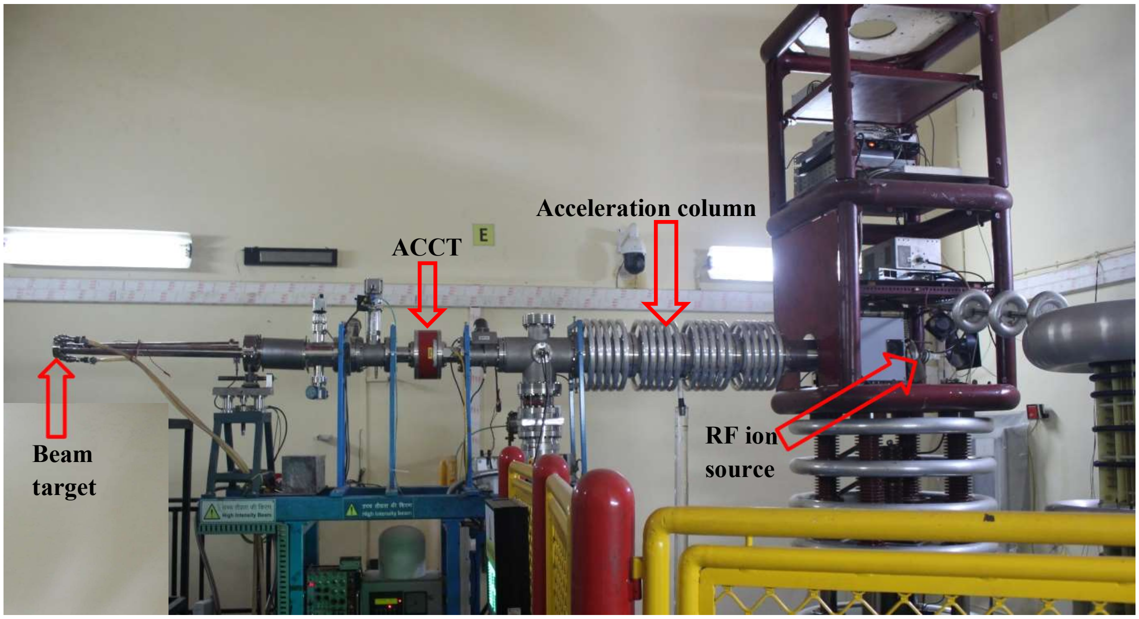

Figure 2.5. Purnima Neutron Generator (PNG).

Table 2.3. *Details of Purnima Neutron Generator.*

Sr. No.	Accelerator Type	DC electrostatic
1	Acceleration voltage	300 kV (max.)
2	Beam	Deuterium ion (D^+)
3	Beam current	3 mA (max.)
4	Ion source	Radio Frequency (RF)
5	RF frequency	13.5 MHz
6	Beam target	Deuterium/Tritium
7	Mode of operation	Continuous/Pulsed
8	Frequency range in pulsed mode	1 Hz to 10 kHz
9	Minimum pulse width	10 µs
10	Maximum yield	5 X 10^{10} n/s (D-T) 3 X 10^8 n/s (D-D)
11	Neutron energy	14.1 MeV (D-T) 2.45 MeV (D-D)

Figure 2.6. The ACCT (Bergoz Instrumentation) used to measure the beam pulse shape and width at different accelerator frequencies during noise experiments.

2.2.3 Detectors

Detectors are an indispensable part for reactivity measurement in subcritical system. The available experimental channels in BRAHMMA (EC1-EC7) have very small diameter (7.2 mm to 10.0 mm) as discussed in section 2.2.1.1 Therefore, miniature ^{3}He detectors have developed (Shukla et al., 2015) for flux profile mapping and reactivity measurement using deterministic method. The miniature detectors are filled with ^{3}He and Kr gas at different gas pressure and operate in proportional region. The thermal neutron will interact with the ^{3}He atom and produces Proton and Tritium. Kr has been used to reduce the mean free path of primary charge particles. The detectors have active length and diameter of 70 mm and 6.5 mm respectively and have different sensitivity in the range of 0.4-0.001 CPS/nv for different flux level inside BRAHMMA.

During noise experiments, multiple ^{3}He detectors (8 Nos.) have been used to cancel the higher order modes which will be discussed in detail in section 4.4. These detectors have active length and diameter of 10.0 cm and 2.438 cm respectively. The detectors have sensitivity of 18 CPS/nv. As the noise analysis is based on statistical method and the number of detected events for any gate width must be significant, detection efficiency must be high during noise experiments. Thus, high sensitivity detectors have been used for noise experiments in BRAHMMA along four fuel channels, which are based on the system modal analysis (Kumar et al., 2017). Details of the detectors used in deterministic and noise experiment have been shown in Table 2.4.

Table 2.4. *Details of detectors used in deterministic and noise experiments.*

Specifications	Detectors used in deterministic experiments	Detectors used in noise experiments
No. of detectors	4	8
Filling gas	^{3}He	^{3}He
Active length (cm)	7.0	10.0
Active diameter (cm)	0.65	2.438
Operating voltage (V)	850- 1100	900-1300
Thermal neutron sensitivity (CPS/nv)	0.4-0.001	18

2.2.4 Data Acquisition Systems

During the study, two different data acquisition systems have been used. The data acquisition system which has been used during reactivity measurement using deterministic method in BRAHMMA subcritical system consists of custom design charge sensitive preamplifier of fall time 10 μs and shaping amplifier of time constant 1 μs. The output from the shaping amplifier is fed into a Single Channel Analyser (SCA) with a particular threshold to discriminate the

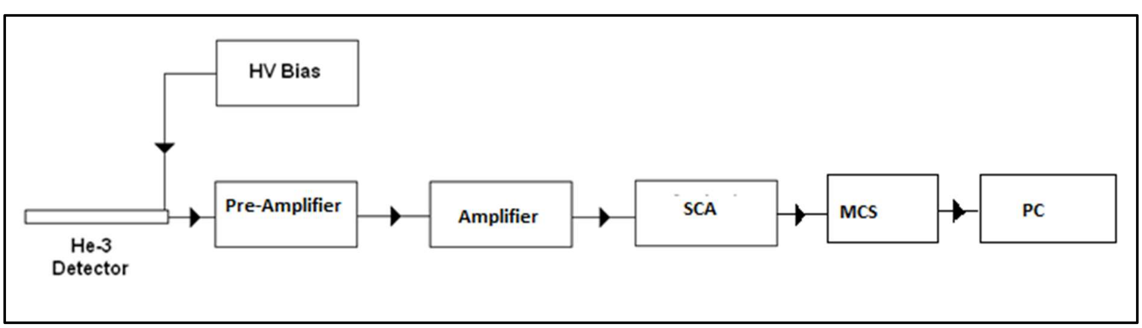

Figure 2.7. Schematic of data acquisition system used in PNS experiments.

signal from noise. Finally, the Transistor Transistor Logic (TTL) output from SCA is fed into a Multi-Channel Scalar (MCS) unit as shown in Figure 2.7. The MCS output is stored in a computer.

On the other hand, for noise experiments, the output from ^{3}He detectors has been fed into charge sensitive preamplifiers (Mesytek, MRS-2000). The advantage of MRS-2000 is that it can provide energy output and TTL output with adjustable threshold. Therefore, in case of multiple detectors the shaping amplifier and SCA are not required for data acquisition and it will minimise the resources. Further, the TTL output from charge sensitive preamplifiers were added in a TTL adder unit. Finally, the summed output from adder is fed into an in-house developed data acquisition system (Kumar et al., 2015). The main advantage of the data acquisition system is that the time history of each detected event is registered with an internal clock frequency of 80 MHz. The schematic of the data acquisition setup used during noise experiments has been shown in Figure 2.8. Finally, data are available in raw format and it permits noise analysis in time domain.

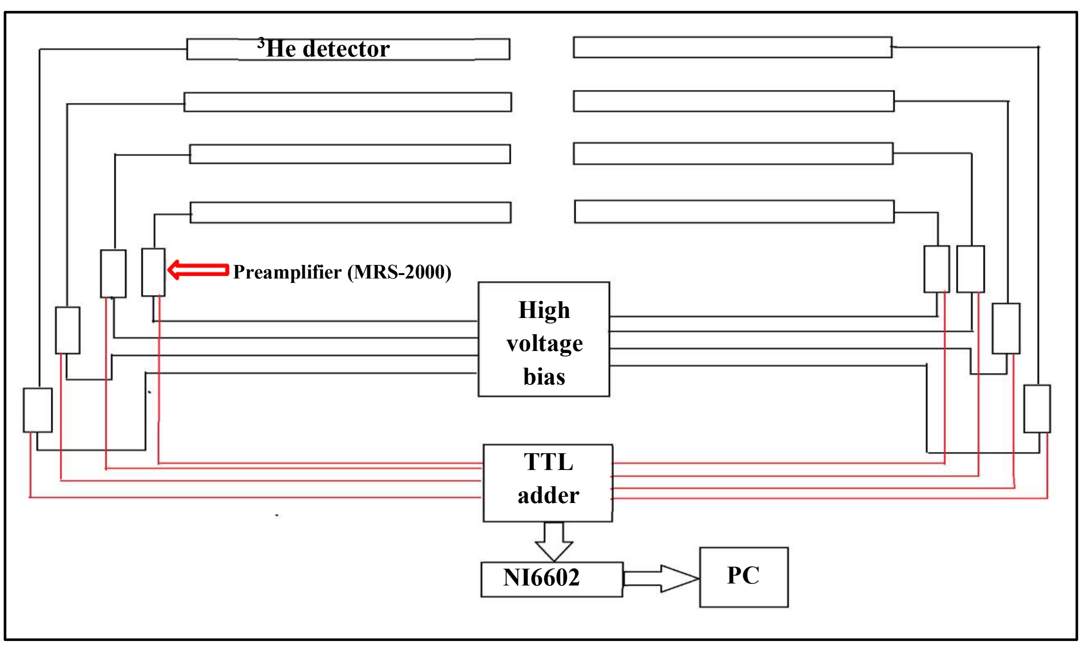

Figure 2.8. Schematic of data acquisition system used in noise experiments.

The BRAHMMA subcritical system coupled with Purnima Neutron Generator during the present research work has been shown in Figure 2.9

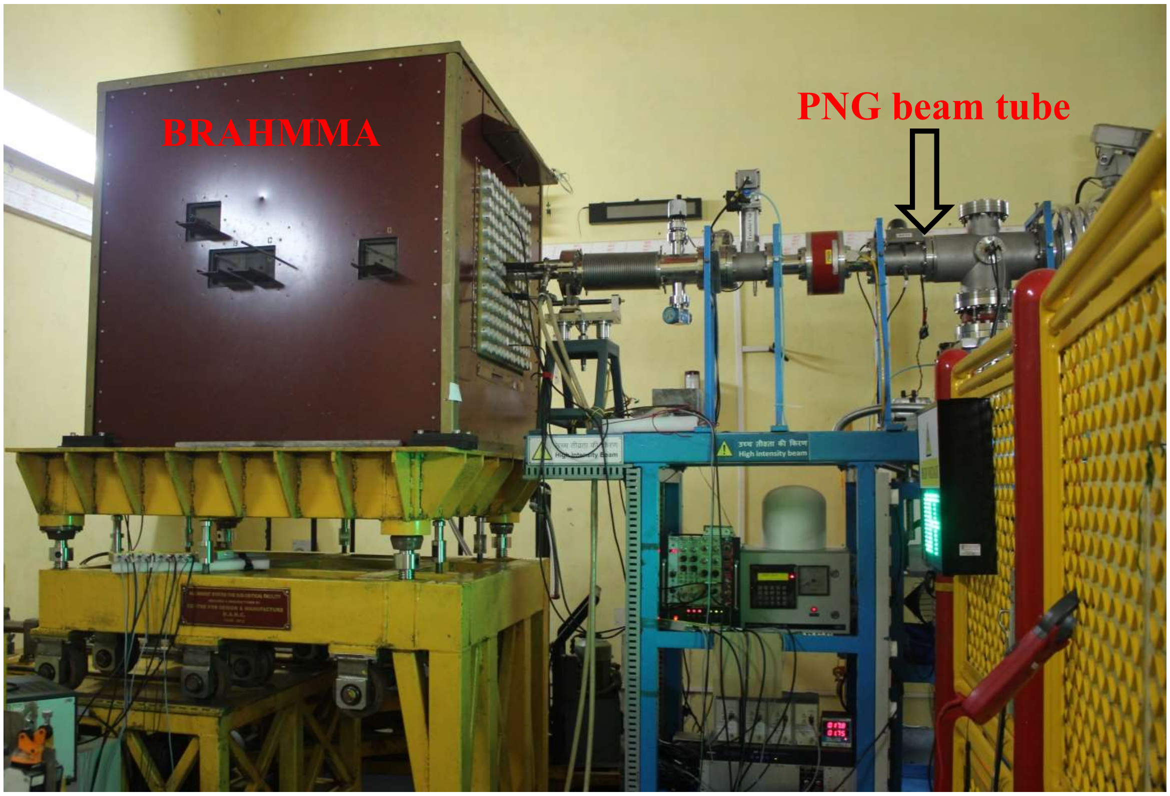

Figure 2.9. The BRAHMMA subcritical system coupled with PNG.

2.3 Different Reactivity Measurement Methods

The reactivity measurements in BRAHMMA subcritical system have been carried out using deterministic and noise method. The present section will discuss the various reactivity measurement methods in subcritical system which have been used during the present research work.

2.3.1 Deterministic Methods

The reactivity measurement in subcritical system has been conducted using deterministic methods such as Pulsed Neutron Source (PNS) technique and Source Jerk method. The details of these deterministic methods are as follows.

2.3.1.1 Pulsed Neutron Source Technique

The measurement of reactivity in subcritical system using Pulsed Neutron Source technique measures the detector response with short neutron pulses. The PNS measurement is based on the observation of detector response as a function of time following the injection of neutron pulse. Following the neutron pulse, the neutron population first rises to a peak and then dies away due to the subcritical nature of the system. After a short period of time, the detector response decay much slowly due to the emission of delayed neutrons. Therefore, the neutron density ($\phi(t)$) is composed of prompt neutron ($\phi_p(t)$) decay followed by slowly varying delayed neutron ($\phi_d(t)$) part. For pulse period (T) smaller compared with the delayed neutron precursors half live, $\phi_d(t)$ can be assumed to be constant during the pulse period. The area under the prompt neutron and delayed neutron are used to infer the reactivity using Area-ratio method as proposed by Sjöstrand. On the other hand, the slope of the prompt neutron decay is used to infer the reactivity in Slope-fit method.

2.3.1.1.1 Area-ratio Method

In Area-ratio method, the detector response is recorded following injection of a large number of neutron pulses into the system so that a constant delayed neutron background is achieved. Usually, the neutron pulse width ΔT is chosen to be small enough and the neutron pulse period T is required to be large so that the prompt neutrons die away between two consecutive pulses. Figure 2.10 shows the schematic of detector response using PNS technique in subcritical system. The pulse period (T) is also chosen to be relatively small compared to the shortest half-life of delayed neutron precursors. As a result, the change in the delayed neutron background is negligible within the neutron pulse period and the delayed neutron background can be considered as constant over the pulse period.

According to Area-ratio method (Sjöstrand), the reactivity (ρ) of the subcritical system in dollar is given by the negative ratio of the prompt-neutron area (A_p) and the delayed neutron area (A_d) measured by neutron detectors:

$$\frac{\rho}{\beta_{eff}} = \frac{-A_p}{A_d} \tag{2.1}$$

where, β_{eff} is the effective delayed neutron fraction. In practice, the delayed-neutron area (A_d) is given by the integration of the delayed neutron background over the pulse period. The prompt-neutron area (A_p) is obtained by integrating the total detector response subtracted by the delayed neutron area. Equation 2.1 can easily be obtained from the point kinetics equations:

$$\frac{d\phi(t)}{dt} = \frac{\rho - \beta_{eff}}{\Lambda}\phi(t) + \lambda C(t) + S(t) \tag{2.2}$$

$$\frac{dC(t)}{dt} = \frac{\beta_{eff}}{\Lambda}\phi(t) - \lambda C(t) \tag{2.3}$$

where, $\phi(t)$ is total neutron flux, $C(t)$ is delayed neutron precursors level, $S(t)$ is external pulsed neutron source, Λ is neutron generation time and λ is decay constant of delayed neutron precursor. The neutron flux ($\phi(t)$) of the point kinetic equation has prompt (ϕ_p) and delayed (ϕ_d) neutron part. Thus,

$$\phi(t) = \phi_p(t) + \phi_d(t) \tag{2.4}$$

Therefore, equations 2.2 and 2.3 can be rewritten as:

$$\frac{d\phi_p(t)}{dt} = \frac{\rho - \beta_{eff}}{\Lambda}\phi_p(t) + S_0\delta(t) \tag{2.5}$$

$$\frac{d\phi_d(t)}{dt} = \frac{\rho - \beta_{eff}}{\Lambda}\phi_d(t) + \lambda C(t) \tag{2.6}$$

$$\frac{dC(t)}{dt} = \frac{\beta_{eff}}{\Lambda}(\phi_p(t) + \phi_d(t)) - \lambda C(t) \tag{2.7}$$

where, $S(t)=S_0\delta(t)$ is the pulse neutron source. The prompt and delayed neutron area with initial conditions $\phi_p(0)=\phi_p(T)=0$, $\phi_d(0)=\phi_d(T)$ and $C(0)=C(T)$ is given by:

$$A_p=\frac{S_0\Lambda}{\beta_{eff}-\rho} \tag{2.8}$$

$$A_d=-\frac{S_0\Lambda\beta_{eff}}{\rho(\beta_{eff}-\rho)} \tag{2.9}$$

Thus, the reactivity is given by the ratio of prompt area and delayed area as follow:

$$\frac{\rho}{\beta_{eff}}=-\frac{A_p}{A_d} \tag{2.10}$$

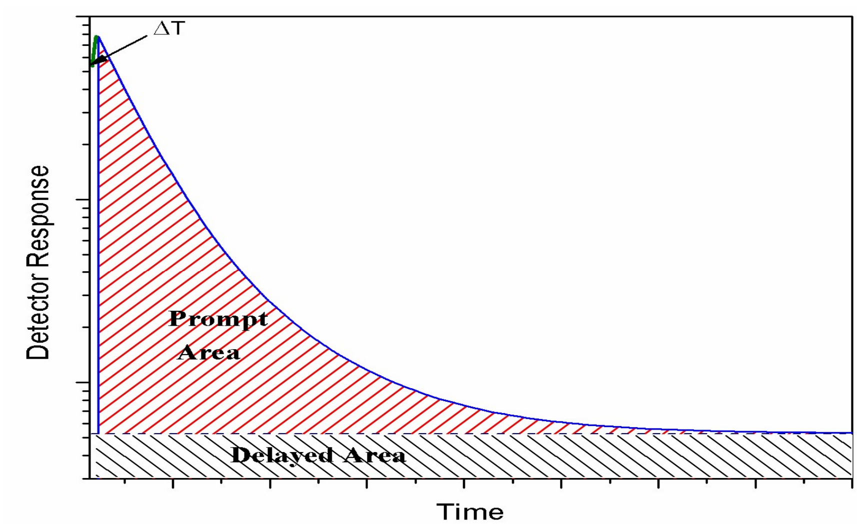

Figure 2.10. Schematic representation of detector response to neutron pulse in subcritical system.

2.3.1.1.2 Slope-fit Method

Assuming the source pulse as Dirac-delta function, the source neutron will be zero after the pulse. In such case, the equation 2.5 can be written as:

$$\frac{d\phi_p(t)}{dt}=\frac{\rho-\beta_{eff}}{\Lambda}\phi_p(t) \tag{2.11}$$

The prompt neutron flux is given by time integral of equation 2.11 as follow:

$$\phi_p(t) = \phi_{p_0} e^{-\alpha t} + \phi_0 \tag{2.12}$$

where, ϕ_0 is a constant, α is the prompt neutron decay constant and related with β_{eff}, ρ and Λ as:

$$\alpha = \frac{\beta_{eff} - \rho}{\Lambda} \tag{2.13}$$

Thus, the slope of the PNS histogram gives the prompt neutron decay constant of subcritical system. The prompt neutron decay constant can be estimated by exponential fitting to the detector response. However, single pulse is not sufficient to get the slope of the histogram. The detector response as function of time is recorded for large number of neutron pulse. The final histogram is given by the summation of response from all pulses. From the time histogram, the prompt neutron decay constant can be estimated by exponential fitting.

2.3.1.2 Source-jerk Method

The source jerk method of reactivity measurement involves continuous operation of subcritical system in steady state at a certain flux level (ϕ_0). If, the external neutron source is shut down suddenly, as a result, the system flux will make a prompt jump to a lower level (ϕ_1), followed by the decay of delayed neutron precursors. The reactivity of the system can be derived using equations 2.2 and 2.3 with boundary conditions. Finally, the reactivity in Source-jerk method is given by:

$$\frac{\rho}{\beta_{eff}} = -\frac{\phi_0 - \phi_1}{\phi_1} \tag{2.14}$$

2.3.2 Noise Methods

The reactivity measurement in subcritical system has also been conducted using noise methods, such as, Feynman-alpha or Variance to Mean ratio minus one (*V/M-1*), Auto Covariance (*ACV*) and Auto Power Spectral Density (*APSD*). Details of these noise methods are as follows.

2.3.2.1 Feynman-alpha

The neutron counts are registered along with the detection time for a long duration (τ). The time duration of the measurement (τ) should be higher compared to the characteristics time of the system. Also, the number of samples should be large for statistical analysis. The entire data have been divided into equal segment of time say, T. The number of counts in each segment ($Z(T)$) are used to calculate the variance to mean ratio using equation 2.15.

$$\frac{V(T)}{M(T)} = \frac{\langle Z(T)^2 \rangle - \langle Z(T) \rangle^2}{\langle Z(T) \rangle} = \frac{\frac{1}{N}\sum_{i=1}^{N} Z_i^2(T) - \left(\frac{1}{N}\sum_{i=1}^{N} Z_i(T)\right)^2}{\frac{1}{N}\sum_{i=1}^{N} Z_i(T)} \tag{2.15}$$

The process has been repeated for $2T$, $3T$ and so on to get the variance to mean ratio as a function of time (T). The variance to mean ratio minus one is also known by Feynman-alpha.

2.3.2.2 Auto Correlation and Auto Covariance

The Auto Correlation function ($ACF(T)$) of the neutron count is given by:

$$ACF(T) = \sum_{N_1}\sum_{N_2} N_1 N_2 P(N_1, N_2; t_1, t_2) = \lim_{\tau \to \infty} \frac{1}{2\tau} \int_{-\tau}^{\tau} N(t) N(t+T) dt \tag{2.16}$$

where, $P(N_1,N_2;t_1,t_2)$ is the joint probability of having N_1 and N_2 neutrons in the system at time t_1 and t_2 respectively. Furthermore, $N(t)$ and $N(t+T)$ are the number of counts at time t and $t+T$ respectively during time segment say, Δt. The left-hand side of equation 2.16 is ensemble average and the right-hand side is the time average. According to "Ergodic hypothesis" the ensemble average and the time average are same in a stationary random system (Williams, 1974).

To find the Auto Covariance function (ACV) of the detector response, the DC part ($\bar{N}$) is to be removed. So, by replacing $N(t)$ by $(N(t) - \bar{N})$ equation 2.16 is written as:

$$ACV(T) = \lim_{\tau \to \infty} \frac{1}{2\tau} \int_{-\tau}^{\tau} (N(t) - \bar{N})(N(t+T) - \bar{N}) dt = \frac{1}{M} \sum_{i=1}^{M} (N(i\Delta t) - \bar{N})(N(i\Delta t + T) - \bar{N}) \tag{2.17}$$

The discrete form of ACV as shown in equation 2.17 has been used for data analysis.

2.3.2.3 Auto Power Spectral Density

The Feynman-alpha and ACF as discussed in sections 2.3.2.1 and 2.3.2.2 respectively are based on the fluctuation of the neutron population in time domain. An alternative approach of noise analysis can be made through power spectral density. The power spectral density is defined by the Fourier transform of the ACF. Thus, the $APSD$ is given as:

$$\Phi(\omega) = \int_{-\infty}^{\infty} ACF(T) e^{-i\omega T} dT \tag{2.18}$$

The $APSD$ gives the frequency distribution of the reactor noise and a useful tool to measure the reactivity of subcritical system.

CHAPTER THREE

REACTIVITY MEASUREMENT USING DETERMINSTIC METHODS

3.1 Introduction

Energy gain in ADS is related to the source multiplication factor, which has been discussed in section 1.5. The energy gain can also be defined with the neutron multiplication factor and source importance factor. Source importance factor can be measured experimentally by reaction rate distribution inside the core (Shahbunder et al., 2010). Furthermore, the reaction rate and local power density depends on the flux level. Thus, the flux profile mapping in subcritical system is essential for source importance factor measurement and power distribution in ADS. Moreover, the measurement of reactivity using deterministic methods, such as, PNS and Current to Flux monitoring requires measurement of neutron population in subcritical system. However, the commercially available detectors are mainly fission reaction-based or gas-filled detectors. These detectors have preconfigured dimension, characteristics and sensitivity. On the other hand, the available experimental channels in BRAHMMA are very small in dimension (diameter). Furthermore, the experimental channels have different distance from the external neutron source. Thus, the flux level will be different along these experimental channels and a single detector of particular sensitivity is not enough for flux profile mapping and reactivity measurement at different experimental channels because of pulse pileup at higher flux level or less detection events at lower flux level. Thus, miniature ^{3}He detector of difference sensitivity has been designed according to different flux level inside BRAHMMA. Details of detectors and thermal flux profile measurement using miniature ^{3}He detectors have been discussed by Shukla et al. (2015). These detectors have also been used for reactivity measurement using deterministic methods.

3.2 Experimental Result Using Deterministic Methods

Reactivity measurements in BRAHMMA have been carried out using deterministic methods, namely PNS and Source-jerk. During reactivity measurement, the BRAHMMA subcritical system has been coupled with PNG in D-T mode. In PNS experiments, PNG has been operated in pulsed mode with pulse width of 10 μs and beam repetition frequency of 100 Hz. Miniature ^{3}He detectors have been used in axial and radial experimental channels, and a ^{3}He detector (Active length: 10 cm and diameter: 2.438 cm) has been used at specific lattice channels (LC-C3, LC-E5 and LC-E7) by replacing fuel pins as shown in Figure 3.1.

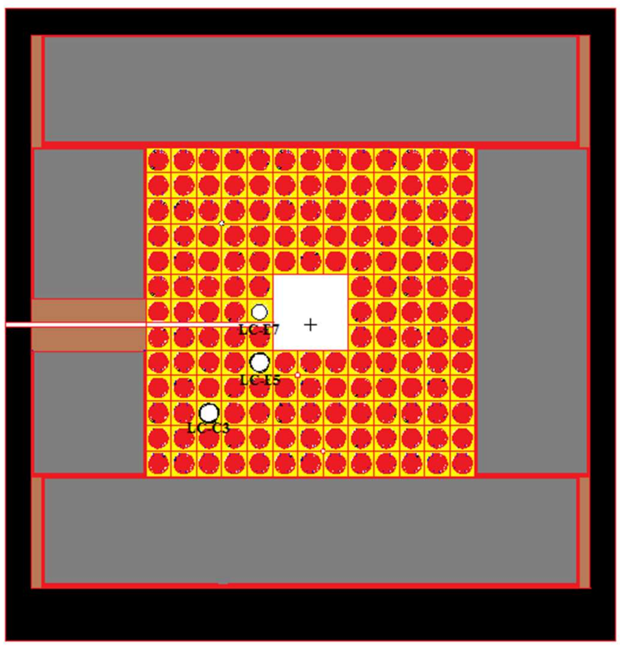

Figure 3.1. Schematic representation of detector locations at lattice channels at middle XY plane.

During reactivity measurement in axial channels, detectors of sensitivity 0.01, 0.1 and 0.4 cps/nv have been placed at the centre of EC1, EC2 and EC3 respectively. In case of radial direction, detector of sensitivity 0.4 cps/nv has been placed after the central cavity, at the end of the moderator and also in reflector as shown in Figure 3.2. The pulsed neutron response in subcritical system has been recorded using these detectors from repetitive neutron pulses (typically 50000), after reaching the constant delayed neutron background.

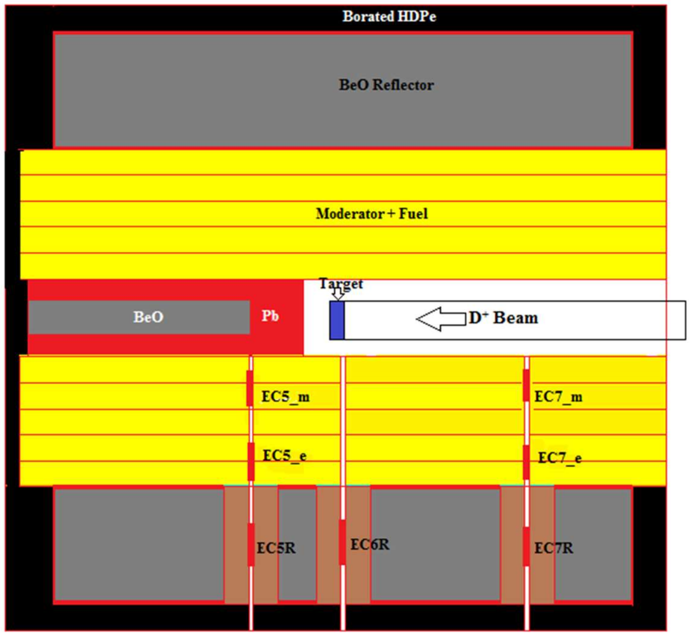

Figure 3.2. Schematic representation of detector locations along radial experimental channels.

3.2.1 Area-ratio Method

In Area-ratio method as proposed by Sjöstrand (1956), the subcriticality is given by the ratio of prompt neutron area and delayed neutron area. The measured detectors' response at middle of axial channels have been shown in Figure 3.3, whereas, Figures 3.4 and 3.5 show the detectors' response at different location along radial channels. Before estimating the prompt and delayed neutron area, the constant neutron background due to the spontaneous fission has to be removed. However, the constant neutron background measured using the miniature detectors are very small compared to the measured pulsed neutron histogram. Additionally, it has been observed that in case of low sensitivity detectors, the background has insignificant contribution to the measured reactivity.

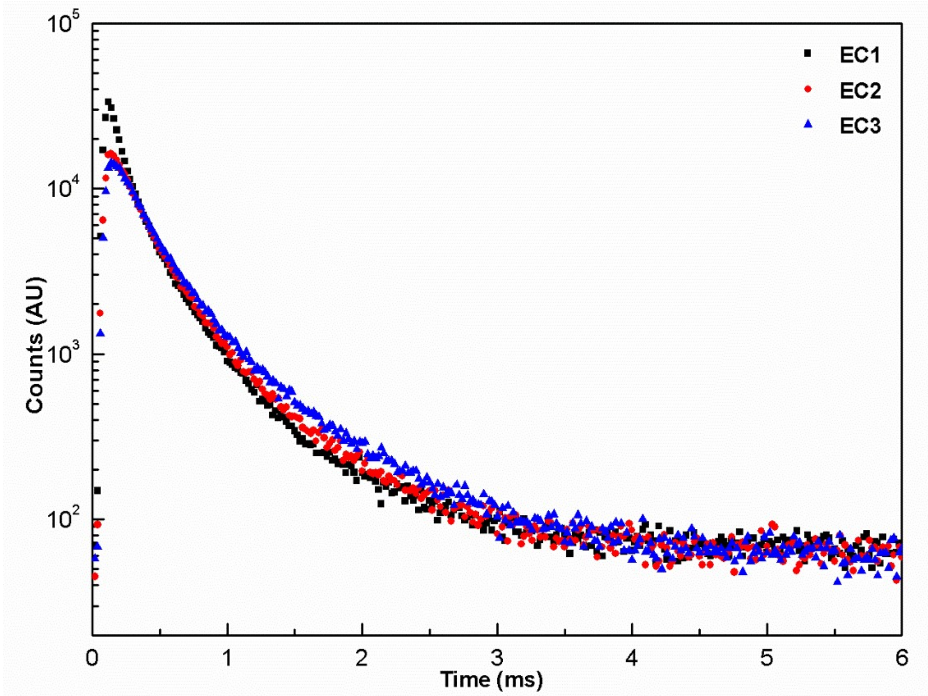

Figure 3.3. Time histogram for detectors located along axial channels.

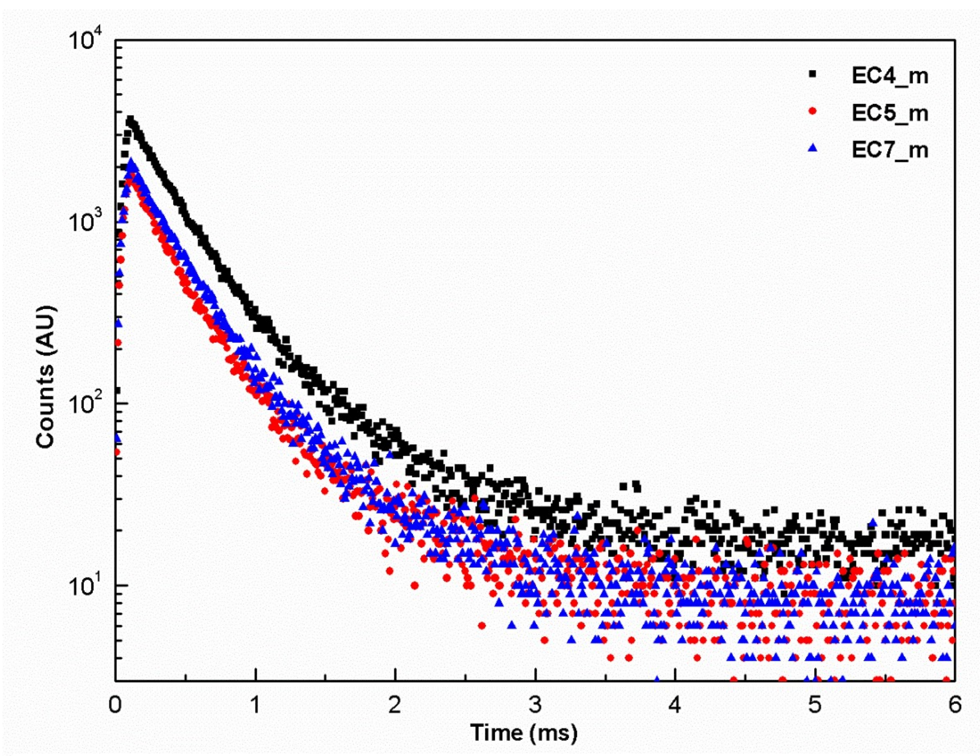

Figure 3.4. Time histogram for detectors located along radial channels.

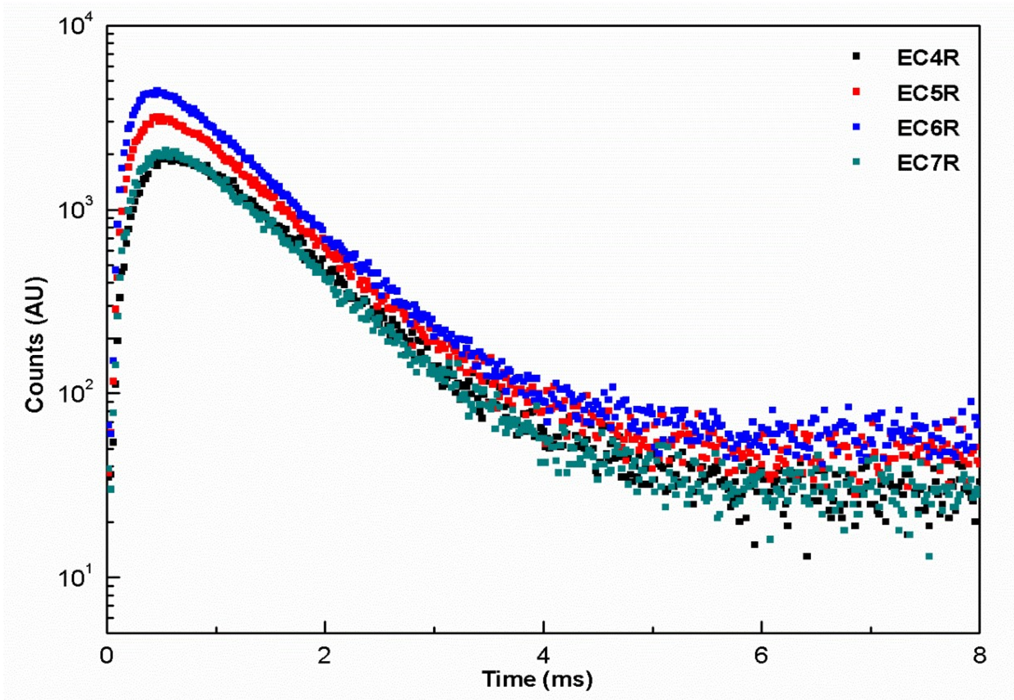

Figure 3.5. Time histogram for detectors located in reflector.

Whereas, in case of reactivity measurement using high sensitivity detector at lattice channels, the background has significant contribution towards the measured reactivity and the background has been subtracted from pulsed neutron response. Finally, the delayed neutron area has been estimated by integration over constant delayed neutron background during the pulse period. Whereas, the prompt neutron area has been obtained by numerically integrating the total detector response subtracted by the delayed neutron area. The measured reactivity using Area-ratio method has been tabulated in Table 3.1.

It has been observed that the measured reactivity using Area-ratio method as proposed by Sjöstrand, depends on the detector’s location. It occurs due to the deviation from point kinetic approximation. Moreover, the presence of higher harmonics in deep subcritical system results the spatial variation of the measured reactivity. Several researches have already been carried out to eliminate the spatial dependency of the measured reactivity, for example, system modal analysis and spatial correction factor as proposed by Bell and Glasstone (1970). During the present study, the Bell Glasstone correction factor has been used to correct the measured reactivity in Area-ratio method.

The calculation of the Bell Glasstone correction factor is a static simulation method, which has been implemented using Monte-Carlo technique. According to Bell and Glasstone (1970), correction factor is given by:

$$f=\left(\frac{\rho_{cri}}{\rho_{src}}\right)=-\left(\frac{A_d}{A_p}\right)\left(\frac{1}{\beta_{eff}}\right)\left(\frac{1-k_{eff}}{k_{eff}}\right) \tag{3.1}$$

where, A_p and A_d are the prompt and delayed neutron area respectively, ρ_{cri} and ρ_{src} are the reactivity in criticality mode and source mode during Monte-Carlo simulation. During simulation of ρ_{src} using static method (time-independent), two separate simulations have been carried out with external neutron for estimation of A_p and A_d. The reaction rate at detectors has been estimated during the pulse period in two steps, one with prompt neutrons and in the next step with prompt and delayed neutrons. The k_{eff} and β_{eff} have been estimated using Monte Carlo method. Finally, using the simulated A_p, A_d, k_{eff} and β_{eff}, the Bell Glasstone factor have been estimated using equation 3.1 and used to correct reactivity at specified detector location as presented in Table 3.1 (column 3). More details about the correction factor in BRAHMMA subcritical system have been discussed by Bajpai et al. (2015). However, Area-ratio method can be used to measure the reactivity (in unit of $) without prior knowledge of system β_{eff}.

Table 3.1. *The measured and corrected reactivity using Area-ratio method at different location in BRAHMMA.*

Experimental Channel	ρ (\$) (Measured)	Correction Factor		ρ (\$) (Corrected)	$\Delta\rho$ (\$)	k_{eff}	Δk_{eff}
		f	Δf				
EC1	-28.03	0.62	0.02	-17.38	0.56	0.886	0.003
EC2	-19.04	0.92	0.03	-17.52	0.57	0.885	0.003
EC3	-16.61	0.99	0.04	-16.44	0.66	0.896	0.004
EC4_m	-15.82	0.97	0.04	-15.35	0.63	0.902	0.004
EC5_m	-18.80	0.81	0.03	-15.23	0.56	0.903	0.003
EC7_m	-14.78	1.21	0.05	-17.88	0.74	0.888	0.004
EC4_e	-10.45	1.30	0.05	-13.58	0.52	0.913	0.003
EC5_e	-14.87	1.01	0.04	-15.02	0.59	0.904	0.004
EC7_e	-12.60	1.40	0.05	-17.64	0.63	0.890	0.004
EC4R	-12.10	1.28	0.05	-15.51	0.60	0.902	0.004
EC5R	-16.25	1.00	0.04	-16.25	0.65	0.897	0.004
EC6R	-14.99	1.11	0.04	-16.64	0.60	0.895	0.004
EC7R	-12.59	1.38	0.05	-17.37	0.63	0.891	0.004
LC-E7	-16.98	0.85	0.05	-14.43	0.65	0.908	0.004
LC-C3	-16.63	1.01	0.05	-16.80	0.61	0.894	0.004
LC-E5	-22.36	0.75	0.05	-16.77	0.63	0.894	0.004

3.2.2 Slope-fit Method

The PNS histogram as discussed in previous section has been used for estimation of prompt neutron decay constant (α) using Slope-fit method. The prompt neutron decay constant has been estimated from the slope of the histogram. The rising part of the histogram is due to build-up of neutron population which is followed by decay of prompt neutron harmonics. In subcritical system, the fundamental part has slower decay compared to higher harmonics. Therefore, during the analysis using Slope-fit method, the rising part of the histogram and initial decay has been masked and rest of the histogram has been used for fitting with exponential function. The measured prompt neutron decay constant (α) using Slope-fit method has been presented in Table 3.2.

Table 3.2. *Measured prompt neutron decay constant using Slope-fit method.*

Experimental channel	α (ms^{-1})	k_{eff}
EC1	2.246±0.112	0.887±0.005
EC2	2.318±0.116	0.884±0.005
EC3	2.346±0.117	0.883±0.005

3.2.3 Source-jerk Method

During reactivity measurement using Source-jerk method, PNG has been operated at frequency of 50 Hz with 50% duty cycle. As a result, the beam is 'ON' for 10 ms and 'OFF' for 10 ms. Neutron counts have been registered during the pulse period for gate width of 1 ms from repetitive neutron pulses (typically 50000), after achieving the constant delayed neutron background as discussed in Area-ratio method. The detectors' response in Source-jerk method at different location have been shown in Figures 3.6 and 3.7. Since the detector count is proportional to neutron flux, the neutron count obtained by linear fitting of detector response during beam 'ON' and 'OFF' have been used to estimate the reactivity using Source-jerk method. However, the measured reactivity using Source-jerk method depends on the detector's location, and the reason for this dependency has already been discussed in Area-ratio method. The Bell Glasstone factor has also been used to correct the measured reactivity using Source-jerk method. The measured reactivity along with corrected reactivity using Source-jerk method have been presented in Table 3.3. Thus, Source-jerk method can also be used to measure the reactivity (in unit of \$) without estimation of system β_{eff}.

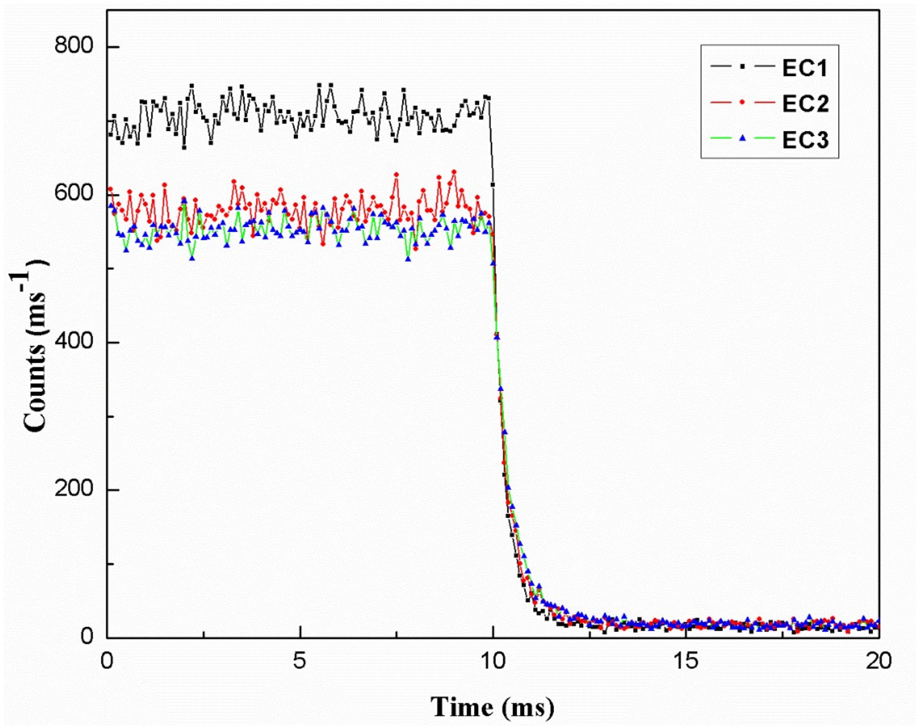

Figure 3.6. Detector response during Source-jerk experiment at axial channels.

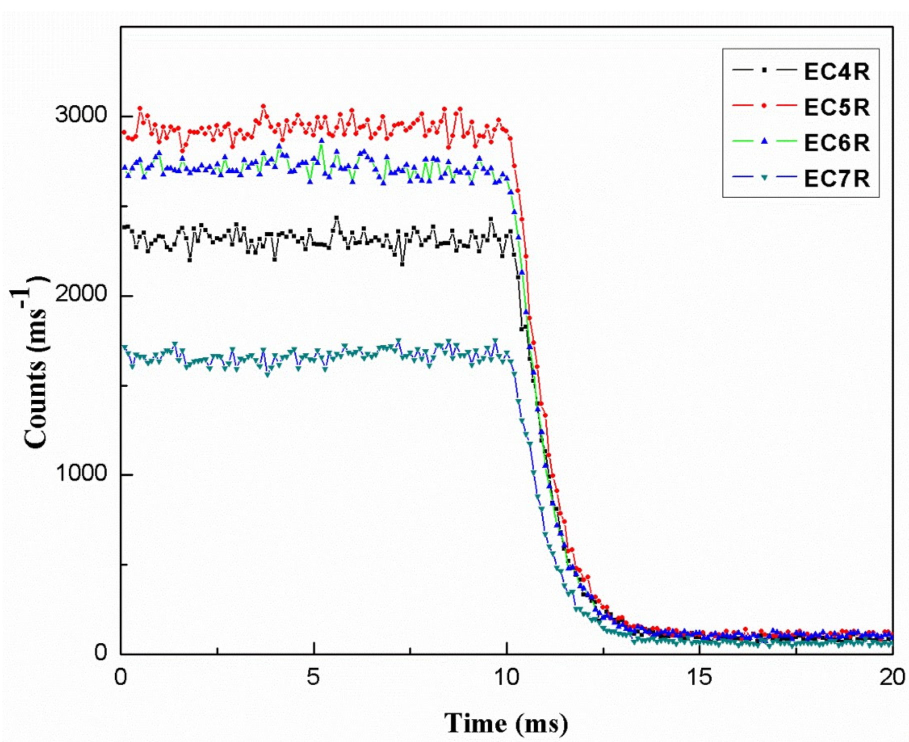

Figure 3.7. Detector response during Source-jerk experiment at radial channels.

Table 3.3. M*easured and corrected reactivity using Source-jerk method at different location in BRAHMMA.*

Experimental Channel	ρ (\$) (Measured)	Correction Factor		ρ (\$) (Corrected)	$\Delta\rho$ (\$)	k_{eff}	Δk_{eff}
		f	Δf				
EC1	-25.87	0.62	0.02	-16.04	0.51	0.894	0.003
EC2	-17.39	0.92	0.03	-16.00	0.52	0.894	0.003
EC3	-15.69	0.99	0.04	-15.33	0.62	0.897	0.004
EC4R	-11.24	1.28	0.05	-14.39	0.56	0.903	0.003
EC5R	-13.31	1.00	0.04	-13.31	0.53	0.910	0.003
EC6R	-15.43	1.11	0.04	-17.13	0.61	0.887	0.004
EC7R	-13.96	1.38	0.05	-19.26	0.69	0.875	0.004

3.3 Measurement of Neutron Multiplication Factor

The effective neutron multiplication factor (k_{eff}) is defined by the ratio of the rate of neutron production and the sum of the rate of absorption and the leakage. The system k_{eff} is related to the reactivity as follows:

$$k_{eff} = \frac{1}{(1-\rho)} \tag{3.2}$$

where, ρ is the system reactivity. Thus, the system k_{eff} can be measured using experimental value of ρ.

3.3.1 Estimation of Delayed Neutron Fraction

The reactivity in Area-ratio and Source-jerk method has been expressed in Dollar (\$) and the estimation of the system k_{eff} requires system β_{eff}. Thus, Monte Carlo simulation has been carried out to estimate the β_{eff} of BRAHMMA system. During the simulation, neutron multiplication of the system has been estimated in two steps with prompt neutrons and total neutrons. The β_{eff} is related to prompt neutron multiplication factor (k_p) and effective neutron multiplication factor (k_{eff}) as follows:

$$\beta_{eff} = 1 - \frac{k_p}{k_{eff}} \tag{3.3}$$

The simulation has been carried out using ENDF cross-section files and the estimated value of β_{eff} is 704±10 pcm. The delayed neutron fraction of natural Uranium is 650 pcm (Glasstone and Sesonske, 2004). The BRAHMMA is a thermal system and the delayed neutrons have higher importance due to its soft spectrum. Thus, the effective delayed neutron fraction in BRAHMMA is slightly higher compared to natural Uranium and has been used to estimate the k_{eff} .

3.3.2 Estimation of Neutron Generation Time

The mean neutron generation time (Λ) is defined by the average time spent by neutrons before absorption through fission process. It is related to the prompt neutron decay constant of the subcritical system as follow:

$$\alpha = \frac{\beta_{eff} - \rho}{\Lambda} \tag{3.4}$$

Thus, neutron generation time is essential for reactivity determination using Slope-fit method, which can be estimated by simulation or experimentally. In this regard, Kumar et al. (2017) estimated the neutron generation time using the diffusion theory-based code KINFIN, which solves the adjoint equation for the kinetic parameters. According to Kumar et al. (2017), the adjoint weighted neutron generation time in BRAHMMA subcritical system is 58.3 μs. Another way to estimate the neutron generation time is Monte-Carlo method. The estimated neutron generation time using Monte-Carlo is 83.8 μs which is higher compared to 58.3 μs estimated using KINFIN. This is due to the fact that the non-analog Monte-Carlo method uses non-adjoint technique for neutron generation time estimation.

On the other hand, neutron generation time has been estimated experimentally using PNS technique. The neutron generation time can be written using equations 2.10 and 3.4 as:

$$\Lambda = \left[\frac{1 - \left(\dfrac{\rho}{\beta_{eff}} \right)_{Area-ratio}}{\alpha_{Slope-fit}} \right] * \beta_{eff} \tag{3.5}$$

Therefore, the reactivity and prompt neutron decay time measured using Area-ratio and Slope-fit method respectively along with the estimated β_{eff} can be used to measure the prompt neutron generation time. Finally, the measured neutron generation time in BRAHMMA subcritical system is 59.71 μs, which is in good agreement with the estimation (58.3 μs) by Kumar et al. (2017) using diffusion theory-based code KINFIN.

3.3.3 Neutron Multiplication Factor of BRAHMMA

In Area-ratio and Source-jerk method, the k_{eff} has been estimated using the measured reactivity and β_{eff}. Whereas, in case of Slope-fit method the k_{eff} has been estimated using measured α along with β_{eff} and Λ. Finally, measured k_{eff} for different detector locations have been shown in Tables 3.1, 3.2 and 3.3 using Area-ratio, Slope-fit and Source-jerk method respectively. The k_{eff} has also been estimated using Monte-Carlo and diffusion theory-based code KINFIN. The estimated k_{eff} using Monte-Carlo and diffusion theory-based code are 0.890±0.001(Sinha et al., 2015) and 0.887±0.003 (Kumar et al., 2017) respectively. The variation of measured k_{eff} at different detector location using Area-ratio method has been shown in Figure 3.8. It has been observed that the measured k_{eff} considering the error bar at EC7, LC-C3 and LC-E5 is close to the theoretical value estimated using Monte-Carlo based method. Furthermore, other than EC1 and EC2, the estimated k_{eff} is higher compared to the theoretical value. In case of Slope-fit method, the measured k_{eff} is close to the theoretical estimate, whereas, Source-jerk method has a deviation from the theoretical estimate as shown in Figure 3.9. Thus, deterministic methods may be useful to estimate the reactivity in deep subcritical system BRAHMMA.

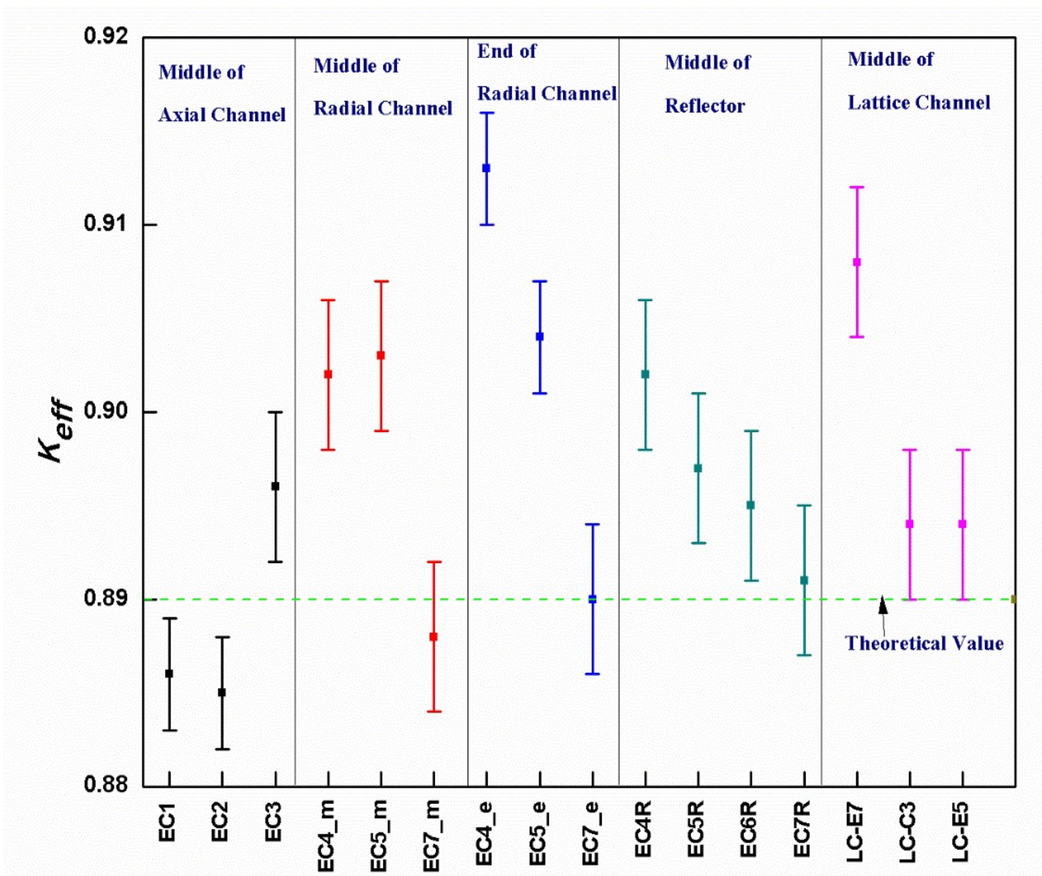

Figure 3.8. Measured k_{eff} using Area-ratio method at different detector locations.

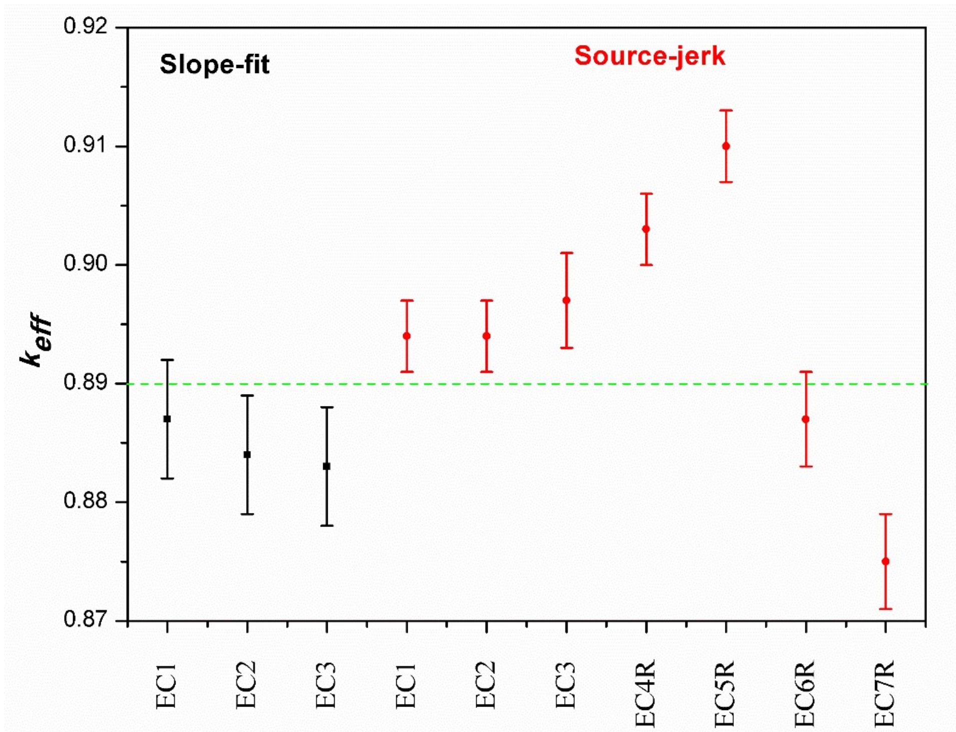

Figure 3.9. Measured k_{eff} using Slope-fit and Source-jerk method at different detector locations.

CHAPTER FOUR

EXPERIMENTAL VALIDATION OF NOISE THEORY DEVELOPED UNDER CONSIDERATION OF EXPONENTIALLY CORRELATED GAUSSIAN SOURCE CHARACTERISTICS AND DIRAC-DELTA PULSE

4.1 Introduction

Reactivity measurement in subcritical system using deterministic methods has been discussed in the previous chapter. These methods have some limitations, for example, in PNS techniques, the beam pulse should be 'OFF' for a time length depending upon the prompt neutron decay time of the subcritical system. This decay time in fast ADS will be very small (~µs), whereas, in thermal ADS the decay time will be comparatively higher (~ms). In case of fast ADS, the generated jerking for this very short period will give neutronic response, but no thermal response (Degweker & Rana, 2007). On the other hand, in thermal ADS, there will be neutronic response along with thermal recycle of the core and power fluctuation for this time duration, which is not at all desirable. Furthermore, the particle velocity at GeV energy will be comparable to velocity of light. Therefore, the synchronisation frequency of the accelerator with particles will be in Radio Frequency (RF) range. Hence, applicability of deterministic methods may be a serious technical issue. In such cases, noise methods can be helpful to infer the reactivity of subcritical system. Thus, the present research work has studied noise methods for reactivity measurement in subcritical system. However, several noise experiments have been carried out using D-T/D-D neutron generator under assumption of Poisson source characteristics. The assumption of Poisson source characteristics of accelerator-based neutron source is inappropriate due to internal fluctuations of beam current and accelerating voltage. Moreover, Degweker and Rana (2007) have postulated noise descriptors under assumption of Gaussian characteristics of accelerator-based neutron source.

Therefore, the present research work has made an attempt to validate this noise theory and reactivity measurement in BRAHMMA subcritical system using this postulate.

The present chapter will discuss the experimental validation of noise theory developed under consideration of exponentially correlated Gaussian source characteristics and Dirac-delta pulse. On the other hand, space dependent noise theory has been discussed by researchers considering Poisson and non-Poisson source characteristics (Williams, 1974; Degweker, 2003; Ballester & Muñoz-Cobo, 2005; Endo et al., 2006; Munoz-Cobo et al., 2011; Yamamoto, 2013, 2014). Furthermore, Szieberth et al. (2015) has discussed the space dependence of the measured reactivity due to detector and source location in a deep subcritical system (k_{eff}=0.92). The present chapter also discusses the space dependent noise due to asymmetry of the core in BRAHMMA subcritical system.

4.2 Review of Noise Theory Developed Under Consideration of Gaussian Source Characteristics

Present section will review the noise theory developed by Degweker and Rana (2007) for exponentially correlated Gaussian source characteristics. Let us consider a D-T neutron source having yield 10^{10} n/s. Under assumption of Poisson distribution of the source, the variance will be its mean (M), the standard deviation (Std) will be 10^5 n/s and the fluctuation (Std/M) must be ±0.001%. But it is practically impossible to get such kind of stability because of inherent fluctuations in beam current and accelerating voltage. Thus, such type of source cannot be assumed as Poisson character. On the other hand, if the accelerator is operating at a stable point and fluctuations are small, the source may be considered as Gaussian character. Furthermore, the assumption of random events in Poisson distribution is no longer valid for periodically chopped beam. Moreover, in case of spallation neutrons, which will be used in ADS system, neutron per incident proton is ~ 20-30 at incident proton energy of 1 GeV (Zucker et al., 1998).

Also, the spallation neutrons are correlated with each other because of cascade chain reaction. For the above-mentioned facts and proper estimation of reactivity, correlation factor of the external neutron source needs to be measured accurately. Thus, it is essential to study the source characteristics and noise experiments under consideration of exponentially correlated Gaussian source characteristics which are relevant for ADS system in future.

4.2.1 Theory of Variance to Mean Ratio and Two Time Probability Function

According to Degweker and Rana (2007), if the pulses are of short duration compared to all other time scales in the system and assuming the neutron pulses as a sum of Dirac-delta function, theoretical formulae for variance to mean ratio (*V/M*) and two-time probability function (*F(0,T)*) are written as follows:

$$
\begin{aligned}
\frac{V(T)}{M(T)} =\; & 1+\frac{\lambda_d m_1}{\alpha^2 T(1-e^{-\alpha/f})}\Bigg[\exp\left(\alpha\left(T-\frac{[fT]+1}{f}\right)\right)+\underset{1st-Term}{\exp\left(-\alpha\left(T-\frac{[fT]}{f}\right)\right)}+\exp\left(-\alpha\left(T+\frac{1}{f}\right)\right)-2e^{-\alpha/f}-e^{-\alpha T}\Bigg] \\
& -\left[\frac{\lambda_d m_1}{\alpha}\left[fT-2[fT]+\frac{[fT]([fT]+1)}{fT}\right]+\underset{2nd-Term}{\frac{\lambda_d}{m_1\alpha}\left\{(m_2+2m_1Y_1)+\Gamma^2\left(\frac{e^{-(\alpha+\beta)/f}}{1-e^{-(\alpha+\beta)/f}}-\frac{1}{1-e^{-(\alpha-\beta)/f}}\right)\right\}}*\left(1-\frac{1-e^{(-\alpha T)}}{\alpha T}\right)\right] \\
& +\frac{\lambda_d\Gamma'^2}{m_1T(1-e^{-(\alpha-\beta)/f})}*\left[\left(\frac{(\alpha T-1)(1-e^{-\alpha/f})}{\alpha^2}+\frac{e^{-\alpha/f}}{\alpha f}\right)*\left(\frac{1-e^{-\beta[fT]/f}}{1-e^{-\beta/f}}\right)-\left(\frac{1-e^{-\alpha/f}}{\alpha f}\right)*\left(\frac{e^{-\beta/f}(1-e^{-\beta[fT]/f})}{(1-e^{-\beta/f})^2}-\frac{[fT]e^{-\beta[fT]/f}}{1-e^{-\beta/f}}\right)\right] \\
& +\frac{\lambda_d\Gamma'^2 e^{-(\alpha+\beta)/f}}{m_1T(1-e^{-(\alpha+\beta)/f})}*\left[\left(\frac{(\alpha T+1)(e^{\alpha/f}-1)}{\alpha^2}-\frac{e^{\alpha/f}}{\alpha f}\right)*\left(\frac{1-e^{-\beta[fT]/f}}{1-e^{-\beta/f}}\right)-\left(\frac{e^{\alpha/f}-1}{\alpha f}\right)\left(\frac{e^{-\beta/f}(1-e^{-\beta[fT]/f})}{(1-e^{-\beta/f})^2}-\frac{[fT]e^{-\beta[fT]/f}}{1-e^{-\beta/f}}\right)\right] \\
& +\frac{\lambda_d\Gamma'^2}{\alpha^2 m_1 T}\left(\frac{[\alpha(T-[fT]/f)-(1-e^{-\alpha(T-[fT]/f)})]}{1-e^{-(\alpha-\beta)/f}}+\frac{e^{-(\alpha+\beta)/f}[e^{\alpha(T-[fT]/f)}-1-\alpha(T-[fT]/f)]}{1-e^{-(\alpha+\beta)/f}}\right)e^{-\beta[fT]/f}
\end{aligned}
\tag{4.1}
$$

$$
F(0,T)=\frac{f\lambda_d^2}{2\alpha}\left[\begin{aligned}
&\underset{1st-Term}{\frac{m_1^2}{1-e^{-\alpha/f}}\left\{e^{-\alpha/f}e^{\alpha(T-[fT]/f)}+e^{-\alpha(T-[fT]/f)}\right\}}+\underset{2nd-Term}{\left(m_2-m_1^2+2m_1Y_1\right)e^{-\alpha T}} \\
&+\Gamma'^2\left\{\left(\frac{e^{-(\alpha+\beta)/f}e^{\alpha(T-[fT]/f)}}{1-e^{-(\alpha+\beta)/f}}+\frac{e^{-\alpha(T-[fT]/f)}}{1-e^{-(\alpha-\beta)/f}}\right)e^{-\beta[fT]/f}+\left(\frac{e^{-(\alpha+\beta)/f}}{1-e^{-(\alpha+\beta)/f}}-\frac{1}{1-e^{-(\alpha-\beta)/f}}\right)e^{-\alpha T}\right\}
\end{aligned}\right]
\tag{4.2}
$$

where, *V(T)* and *M(T)* are the variance and mean respectively for gate width *T*, λ_d is the probability of detection per second. Furthermore, m_1 and m_2 are the first and second moment of source multiplicity distribution, α is the prompt neutron decay constant, Γ'^2 is the variance of the number of neutrons in a pulse, β is the source correlation factor, f is the frequency of the external source, $[fT]$ represents the floor integer and Y_1 a constant which is represented by equation 4.3. The first term of the above equations represents the uncorrelated oscillatory part due to the periodicity of source. The second term has two parts of which first part represents the source multiplicity and the second represents the correlated chain multiplication. The remaining terms represent the correlated source neutrons.

$$Y_1 = \frac{\lambda_f \langle \nu(\nu-1) \rangle}{2\alpha} \tag{4.3}$$

In equation 4.3, λ_f is the probability of fission per second, v is the number of neutrons per fission. The prompt neutron decay constant (α) is related with reactivity (ρ), delayed neutron fraction (β_{eff}) and neutron generation time (Λ) as:

$$\alpha = \frac{\beta_{eff} - \rho}{\Lambda} \tag{4.4}$$

For $\beta >> f$, above formulae are simplified to equations under consideration of Gaussian and uncorrelated external neutron source (Degweker, 2003). In such cases the V/M is given by:

$$\begin{aligned}\frac{V(T)}{M(T)} = 1 + \frac{\lambda_d m_1}{\alpha^2 T(1-e^{-\alpha/f})}\Bigg[& \underbrace{\exp\left(\alpha\left(T - \frac{[fT]+1}{f}\right)\right) + \exp\left(-\alpha\left(T - \frac{[fT]}{f}\right)\right) + \exp\left(-\alpha\left(T + \frac{1}{f}\right)\right) - 2e^{-\alpha/f} - e^{-\alpha T}}_{1st-Term}\Bigg] \\ - \Bigg[& \underbrace{\frac{\lambda_d m_1}{\alpha}\left[fT - 2[fT] + \frac{[fT]([fT]+1)}{fT}\right]}_{2nd-Term} + \frac{\lambda_d \{m_2 + 2m_1 Y_1\}}{m_1 \alpha} * \left(1 - \frac{1-e^{(-\alpha T)}}{\alpha T}\right)\Bigg]\end{aligned} \tag{4.5}$$

and the two time probability function ($F(0,T)$) is given by:

$$F(0,T) = \frac{f\lambda_d^2}{2\alpha}\left[\underbrace{\frac{m_1^2}{1-e^{-\alpha/f}}\left\{e^{-\alpha/f}e^{\alpha(T-[fT]/f)} + e^{-\alpha(T-[fT]/f)}\right\}}_{1st-Term} + \underbrace{\left(m_2 - m_1^2 + 2m_1 Y_1\right)}_{2nd-Term}e^{-\alpha T}\right] \tag{4.6}$$

The above formulae have two terms. The first term represents the uncorrelated part and it is periodic in nature. The period of the uncorrelated part is same as the external neutron source. The second term has two parts of which first part represents the multiplication of external neutron source and second part represents the correlated fission reaction.

In case, $f >> \alpha$, the above formulae reduce to much simplified form. In such case, the *V/M* is given by:

$$\frac{V(T)}{M(T)} = 1 + \frac{\lambda_d \left\{ m_2 - m_1{}^2 + 2m_1 Y_1 \right\}}{m_1 \alpha} * \left(1 - \frac{1 - e^{(-\alpha T)}}{\alpha T} \right) \tag{4.7}$$

and two-time probability function ($F(0,T)$) is given by:

$$F(0,T) = \frac{f^2 \lambda_d^2 m_1^2}{\alpha^2} + \frac{f \lambda_d^2}{2\alpha} \left(m_2 - m_1^2 + 2m_1 Y_1 \right) e^{-\alpha T} \tag{4.8}$$

The prompt neutron decay constant can be determined by least square fitting of equations 4.7 and 4.8. The ρ can be calculated from the measured value of α using β_{eff} and Λ.

4.2.2 Auto Power Spectral Density

Variance to mean ratio and two-time probability function discussed in section 4.2.1 are used to describe the reactor noise in time domain. An alternative approach of noise analysis can be made through power spectral density. The power spectral density is defined by the Fourier transform of auto correlation function (*ACF*). Thus, *APSD* is given as:

$$\Phi(\omega) = \int_{-\infty}^{\infty} ACF(T) e^{-i\omega T} dT \tag{4.9}$$

The *APSD* gives the frequency distribution of the reactor noise. According to Degweker and Rana (2007), the *APSD* is as follows:

$$\Phi(\omega) = H(\omega) \left[\frac{\left\langle q^2 \right\rangle f m_1 \lambda_d}{\alpha} + \left\langle q \right\rangle^2 \xi(\omega) \right] \tag{4.10}$$

where, q is the number of charges per neutron detection, ω is the angular frequency.

In equation 4.10, *H(ω)* is the Fourier transform of detector response and *ξ(ω)* is the Fourier transform of $F(0,T)-\bar{i}^2$. *F(0,T)* is the two time probability function given by equation 4.2 and *i* is the detector current. The first term of the equation 4.10 represents power spectral density of detector white noise and second term represents spectral density of correlated and uncorrelated (fission and source) part. Finally, *APSD* is given by:

$$\Phi(\omega)=\frac{\langle q^2\rangle fm_1\lambda_d}{\alpha}H(\omega)+\langle q\rangle^2 f\lambda_d^2H(\omega)\left\{\sum_{n\neq 0}\frac{4\pi fm_1^2\delta(\omega-2n\pi f)}{\alpha^2+(2n\pi f)^2}\right\}+\langle q\rangle^2 f\lambda_d^2H(\omega)\frac{2m_1Y_1}{\omega^2+\alpha^2}$$
$$+\frac{\langle q\rangle^2 f\lambda_d^2H(\omega)(m_2-m_1^2)}{\omega^2+\alpha^2}+\frac{\langle q\rangle^2 f\lambda_d^2H(\omega)\Gamma'^2}{\omega^2+\alpha^2}\left(\frac{e^{-(\alpha+\beta)/f}}{1-e^{-(\alpha+\beta)/f}}-\frac{1}{1-e^{-(\alpha-\beta)/f}}\right)+ \tag{4.11}$$
$$\langle q\rangle^2 f\lambda_d^2H(\omega)\Gamma'^2\frac{[2(e^{-(\alpha+2\beta)/f}-e^{-\alpha/f})\cos(\omega/f)+(1+e^{-2\alpha/f})(1-e^{-2\beta/f})]}{(\omega^2+\alpha^2)(1-2e^{-\beta/f}\cos(\omega/f)+e^{-2\beta/f})(1-e^{-(\alpha+\beta)/f})(1-e^{-(\alpha-\beta)/f})}$$

The first term of *APSD* represents the detector white noise and the second term represents discrete lines corresponding to the integer multiple of source frequency which comes from the periodic uncorrelated part of correlation function. While the third term represents the reactor power spectral density and the remaining terms represent the non-Poisson source characteristics.

In case of, *β>>f*, the above equation reduces to simple form as follows:

$$\Phi(\omega)=\frac{\langle q^2\rangle fm_1\lambda_d}{\alpha}H(\omega)+\langle q\rangle^2 f\lambda_d^2H(\omega)\left\{\sum_{n\neq 0}\frac{4\pi fm_1^2\delta(\omega-2n\pi f)}{\alpha^2+(2n\pi f)^2}\right\}+\langle q\rangle^2 f\lambda_d^2H(\omega)\frac{m_2-m_1^2+2m_1Y_1}{\omega^2+\alpha^2} \tag{4.12}$$

The least square fitting of the above equation with the measured *APSD* will give the prompt neutron decay constant of subcritical system.

4.3 Experimental Setup

The experimental setup consists of three parts, Purnima Neutron Generator (PNG), BRAHMMA subcritical system and detectors with data acquisition system. Details of the BRAHMMA, PNG and data acquisition system have been discussed in chapter two.

4.4 Location of Detectors

In deep subcritical system, reactivity measurement is challenging due to the presence of higher order modes (Suzaki, 1991; Rana et al., 2013) which can be eliminated by placing detectors at designated locations based on the system modal analysis (Rana et al., 2013).

According to Rana et al. (2013) the two time probability function is given by:

$$P(t_1, t_2)\delta t_1 \delta t_2 = \left(\delta t_1 \int \Sigma_{d1}\varphi(r,\Omega,E)drd\Omega dE\,dt\right)\left(\delta t_2 \int \Sigma_{d2}\varphi(r,\Omega,E)drd\Omega dEdt\right)$$

$$+\overline{\nu(\nu-1)} \int \begin{bmatrix} \Sigma_f * \varphi(r,\Omega,E)\left(\delta t_1 \int \frac{\chi(E')}{4\Pi} G_{z1}(r,\Omega' E', t, 1,1)d\Omega' dE'\right) * \\ \left(\delta t_2 \int \frac{\chi(E')}{4\Pi} G_{z2}(r,\Omega' E', t, 1,1)d\Omega' dE'\right) \end{bmatrix} drd\Omega dEdt \qquad (4.13)$$

where, G_{z1} and G_{z2} are the Green's function (backward) representing the expected number of counts due to a single neutron released at (r, Ω, E) in delta function detectors $\Sigma_{d1}\delta(t-t_1)$ and $\Sigma_{d1}\delta(t-t_2)$ at time t_1 and t_2 respectively. Authors have discussed the solution for G_{z1} and G_{z2} along with the final form of the second term of equation 4.13. The first term of the equation 4.13 is the product of the counts at different time and is the uncorrelated part, whereas, the second part has a spatial integral over the flux and the product of two neutrons importance functions. Thus, the symmetric arrangement of detectors with respect to the source will cancel out the contribution of asymmetric modes. The postulate of mode cancellation has been validated experimentally by Kumar et al. (2017) using symmetric arrangement of detectors based on the modal analysis of BRAHMMA. During the present work, ^{3}He detectors (Number: 8 Nos, Diameter: 2.438 cm and Length: 10 cm) have been placed on the zeros of the first symmetric modes along the axial and transverse direction as discussed by Kumar et al. (2017) in BRAHMMA subcritical system. Two symmetric detector configurations are available for experiments along lattice channels, namely 8-DET R1 (D4, D10, J4 and J10) and 8-DET R2 (B7, L7, G2 and G12) as shown in Figure 4.2 (Kumar et al., 2017). First symmetric modes have nodes at Z=±18.5 cm along lattice channels. Detectors are also at the symmetric locations with respect to the source which is at the centre of the subcritical system as shown in Figure

4.1 and 4.2. Therefore, this arrangement will eliminate all anti-symmetric modes along with first symmetric modes in the measured correlation function and the modal contamination in the measured prompt neutron decay constant will be minimum. Radial distance of these two configurations (8-DET R1 and 8-DET R2) from the centre are 20.36 cm and 24.0 cm respectively. The radial distance of 8-DET R2 configuration is higher compared to 8-DET R1 from the external source. As a result, source contribution will be less compared to fission neutron in 8-DET R2 set.

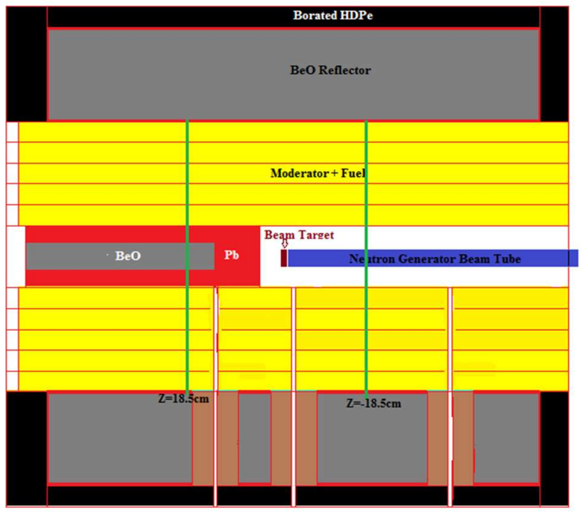

Figure 4.1. Schematic representation of detectors location (at Z=±18.5 cm) along axial direction.

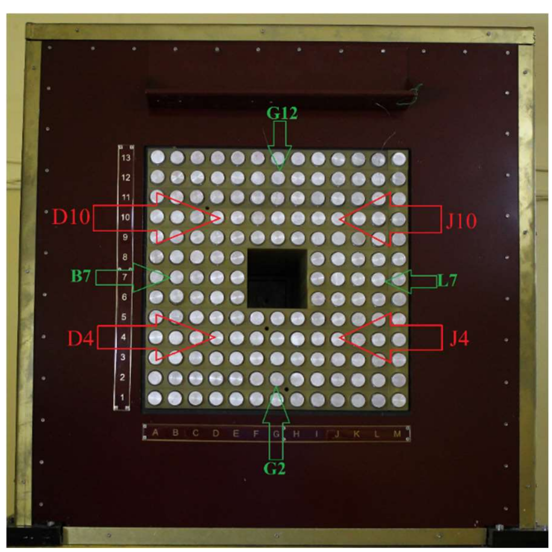

Figure 4.2. Schematic representation of different detector configurations along radial direction.

4.5 Validation Experiment of Data Acquisition System and Analysis Tools

During noise experiments, TTL output from preamplifiers have been added in a TTL adder unit and data have been acquired by a time stamp data acquisition system as discussed in section 2.2.4. Kumar et al. (2015) had validated the data acquisition system using Am-Be neutron source. But the present research has been carried out using preamplifiers MRS-2000 (Mesytek) and data analysis tools have also been developed for various noise descriptors. Thus, the data acquisition system along with MRS-2000 and data analysis tools for *V/M* and *ACV* methods have been tested using isotopic neutron source (Am-Be ~30 mCi). The *V/M* and *ACV* have been analysed using time stamped data as discussed in sections 2.3.2.1 and 2.3.2.2. In Figure 4.3, it can be seen that the *V/M-1* for isotopic source is close to zero, independent of time segment and follows Poisson distribution as expected for isotopic source. Furthermore, the measured *ACV* indicates that the neutrons are randomly distributed and uncorrelated. The *V/M-1* and *ACV* agree with the theoretical consideration of Poisson distribution for isotopic source and the data acquisition system including analysis tools perform satisfactorily.

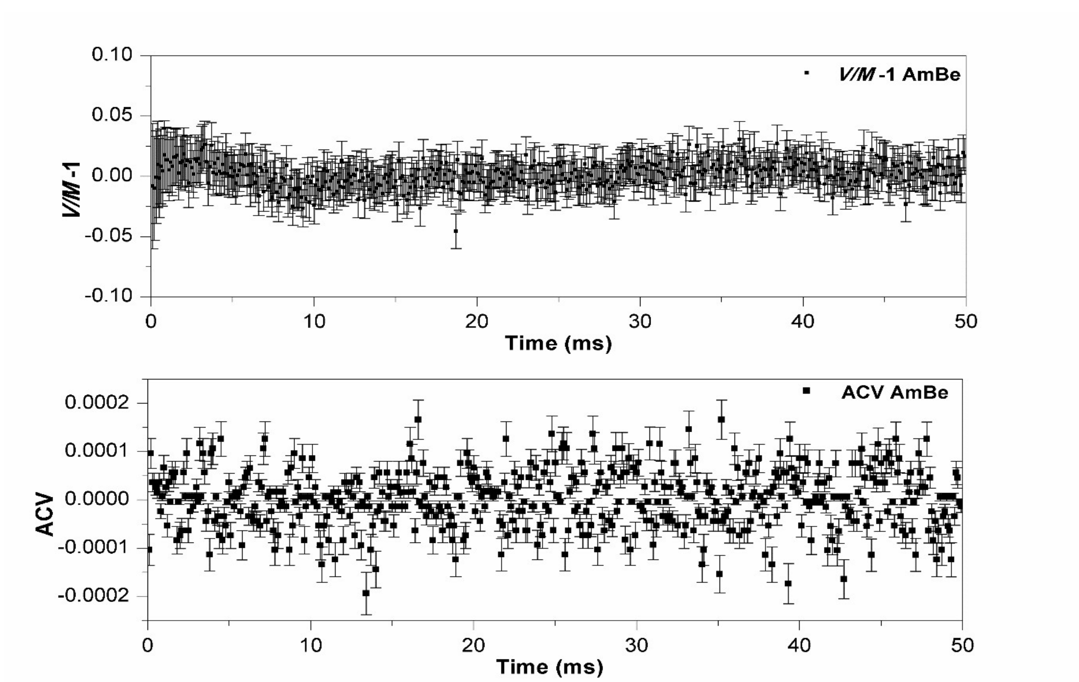

Figure 4.3. Measured *V/M*-1 and *ACV* for Am-Be neutron source.

4.6 Experimental Results

In the present section, experiments with D-T neutrons from PNG and BRAHMMA subcritical system and results have been discussed.

Experiments have been performed in two steps. The first step of the experiment consists of source characterisation and correlation factor measurement for D-T neutrons. During source characterization, a ^3He detector (length: 10 cm, diameter: 2.438 cm, sensitivity: 18 cps/nv) has been used at distance of 10 cm from the beam target. The ^3He detector has been placed inside a Perspex cylinder followed by 2 mm cadmium sheet. The Perspex has been used to thermalise the 14.1 MeV neutrons and the cadmium to stop the scattered thermal neutrons from surroundings entering the detector. In the second step, noise experiments in BRAHMMA have been performed using PNG and eight ^3He detectors. The duty cycle of the neutron generator has been selected 10% during the entire experiment to maintain the neutron yield. Data have been acquired in asynchronous mode that is the start of data acquisition system is not synchronised with the neutron pulse.

4.6.1 Source Characterisation and Correlation Factor Measurement

D-T source neutrons have been detected using ^3He detector and time stamp data acquisition system. Time stamped data have been converted into Counts Per Second (CPS) to study the source fluctuation. Normalised CPS at different source frequencies have been shown in Figure 4.4. Preliminary statistical analysis, for example, mean, standard deviation (Std) has been carried out for each set of data and have been presented in Table 4.1. According to the Mean and standard deviation (Std) in Table 4.1, the observed source fluctuations (Std/Mean) are around 2.0-2.41%. Whereas, in case of Poisson characteristics, the standard deviation must be square root of mean. Fluctuations considering the source as Poisson character have been presented in Table 4.2. It has been observed that the measured fluctuation of CPS and the fluctuation considering the source as Poisson character are different. Thus, the source cannot be considered as Poisson character. Moreover, the measured *V/M-1* at different source frequencies have been shown in Figures 4.5 and 4.6. Within the inset portion of Figure 4.5, it can be seen that the *V/M*-1 at low frequencies (1 and 2 kHz) show oscillation for lower time segment and the periodicity of the oscillation is same as the source pulse. Additionally, the *V/M-1* has an asymptotic value which is close to 0.1 after few milliseconds (Figure 4.5). Whereas at accelerator frequency 4 kHz, mild periodicity has been observed for initial 0.6 ms as shown in inset of Figure 4.6. Furthermore, at high frequencies (8 and 10kHz), the *V/M-1* is close to 0.1 irrespective of time segment (Figure 4.6). Therefore, the neutron source having fluctuation greater than 2% and non-zero *V/M*-1 cannot be assumed as Poisson character.

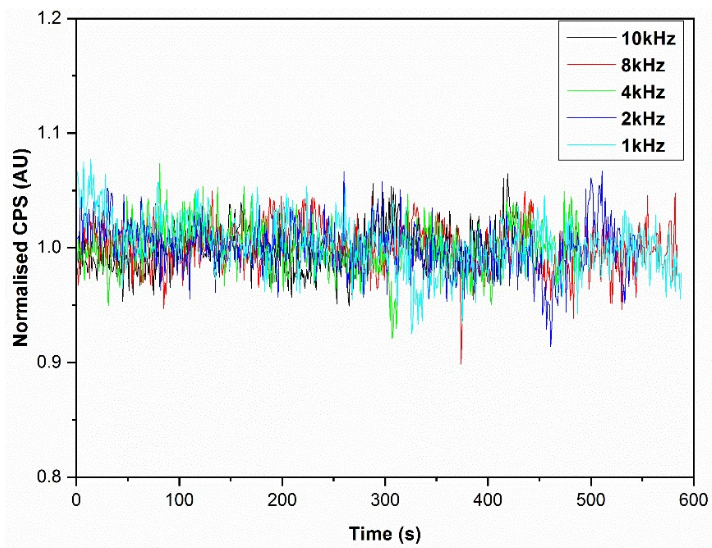

Figure 4.4. Normalised CPS at different source frequencies.

Table 4.1. *Statistical variation of CPS at different accelerator frequency.*

Accelerator frequency (kHz)	N total	Mean	Standard deviation	Sum	Minimum	Median	Max
10	429	4437.14452	88.64748	1.90354E6	4212	4432	4724
8	584	4421.60616	89.96721	2.58222E6	3973	4419.5	4641
4	489	4223.86299	90.18242	2.06547E6	3890	4225	4534
2	549	3995.05282	88.57781	2.19328E6	3651	3998	4263
1	702	3827.68519	92.36284	2.68703E6	3541	3827.5	4124

Table 4.2. *Observed and theoretical standard deviation to mean ratio at different accelerator frequencies.*

Accelerator frequency (kHz)	Std/Mean (%)	
	Observed	Theoretical (Poisson)
10.0	2.0	1.5
8.0	2.03	1.5
4.0	2.13	1.5
2.0	2.21	1.6
1.0	2.41	1.6

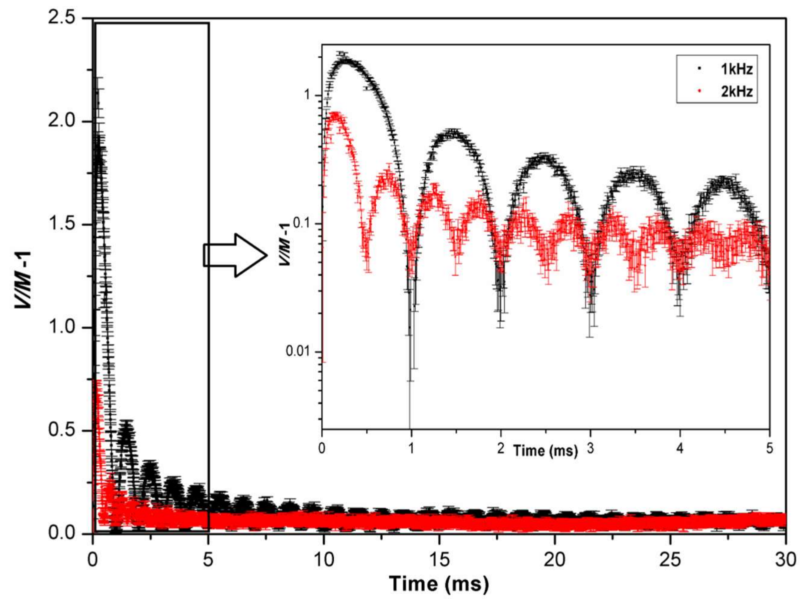

Figure 4.5. V/M-1 plot at 1 and 2 kHz for D-T neutrons and the inset shows the marked region in Log scale.

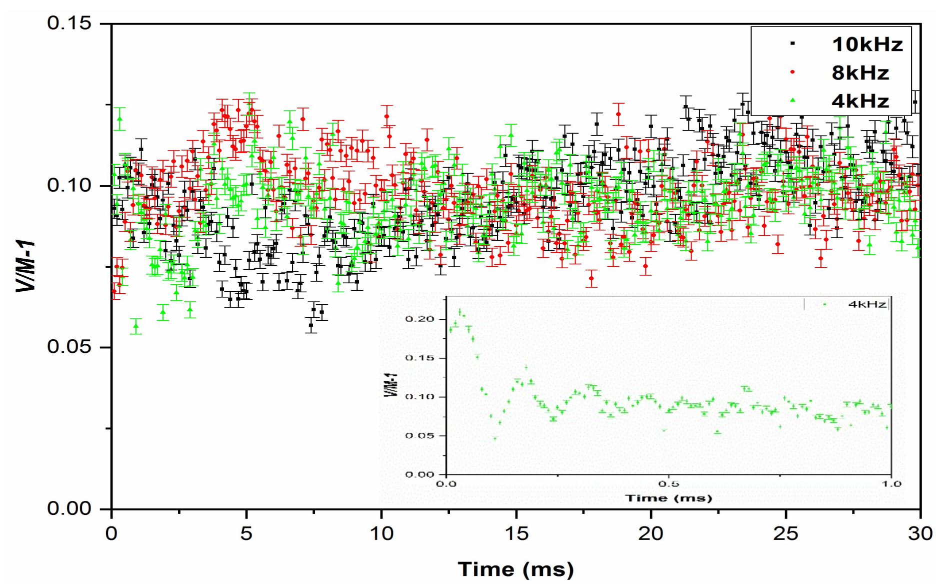

Figure 4.6. V/M-1 plot at 4, 8 and 10 kHz for D-T neutrons and the inset shows 0 to 1ms at 4 kHz.

In next step, data have been analysed using ACV method and the measured ACV for different source frequencies have been shown in Figure 4.7. The measured ACV has periodicity corresponding to the source frequency and has exponential decay following the neutron pulse. Therefore, the decay constant of correlated source neutrons (or source correlation factor) has been estimated from the exponential decay of the measured ACV for different accelerator frequencies as shown in Figure 4.8. The measured source correlation factor and correlation time at different frequencies have been presented in Table 4.3. In case of low frequency (1 kHz), the correlation factor is 13.77 ms^{-1}, whereas, in the case of high frequency (10 kHz), the correlation factor is 50.44 ms^{-1} (Table 4.3). Apart from this, the error in source correlation factor (Table 4.3) also increases with accelerator frequency. This can be attributed to the decay of ACV in high frequency which is sharp and the number of data points is also less as shown in Figure 4.8. The variation of the source correlation factor can be analysed qualitatively by observing the decay of ACV (Figure 4.8). It can be inferred that the decay is longer in case of low frequencies due to the larger pulse width of PNG. Furthermore, Degweker and Rana (2007) stated that there might be short term correlation (less than few seconds) which could materially affect measurements if the pulse repetition frequency is high. The observed variation of source correlation time agrees with the assumption of Degweker and Rana (2007). Moreover, the noise theory under discussion, had been developed under consideration that the source pulse should be Dirac-delta function, which is also a requirement for source correlation time measurement (Degweker & Rana, 2007). In PNG, the available minimum pulse width is 10 μs. So, the finite width of neutron pulse will be included in the decay of ACV and it will smear out the correlation factor. Additionally, ^{3}He detector encapsulated by a Perspex cylinder has been used to slowdown the fast neutrons and it will introduce delay in their detection. The slowing down time of 2 MeV neutrons in water moderator is 2.7±0.4 μs (Möller & Sjöstrand, 1963). Moreover, Nellis (1977) has calculated the average slowing down time of 14 MeV neutron to thermal energy in CH_2 which is 4.7 μs. However, the measured source correlation time is large compared to the slowing down time of 14 MeV neutrons in Perspex and it can be inferred that major contribution to the measured source correlation factor is due to the decay of the neutron population. Moreover, the source correlation factor will be higher compared to the measured value in ideal situation.

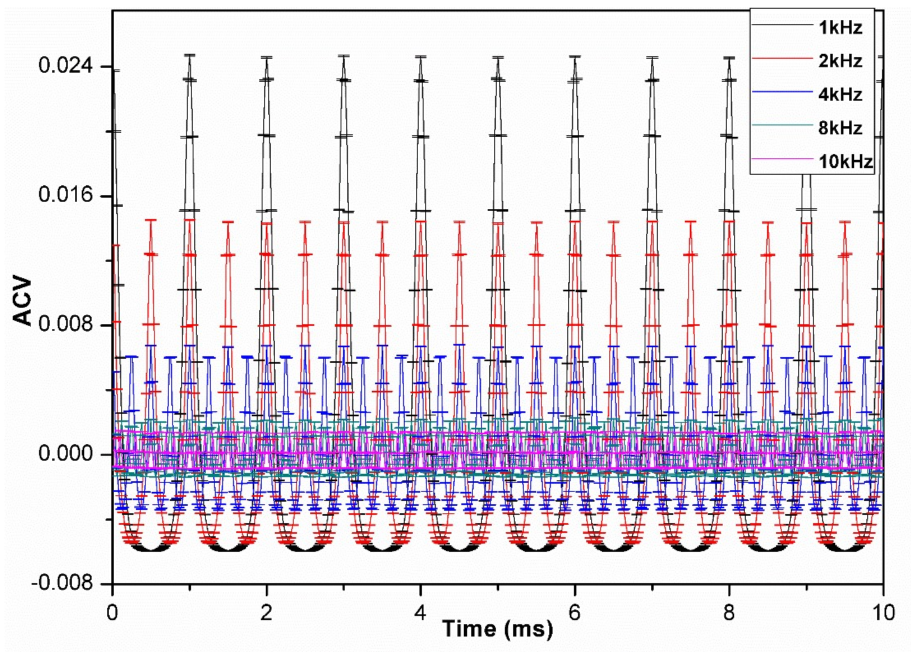

Figure 4.7. ACV plot for D-T neutrons at different source frequencies.

Table 4.3. *Source correlation factor (β) at different source frequency.*

Sr. No.	Accelerator Frequency (kHz)	Pulse Width (μs)	Source Correlation Factor(*β*) (ms^{-1})	Correlation time (*1/β*) (μs)
1	1.0	100.0	13.77±0.39	72.6±2.1
2	2.0	50.0	16.76±0.35	59.6±1.2
3	4.0	25.0	22.22±0.83	45.4±1.7
4	8.0	12.5	43.32±4.55	23.1±2.4
5	10.0	10.0	50.44±10.76	19.8±4.2

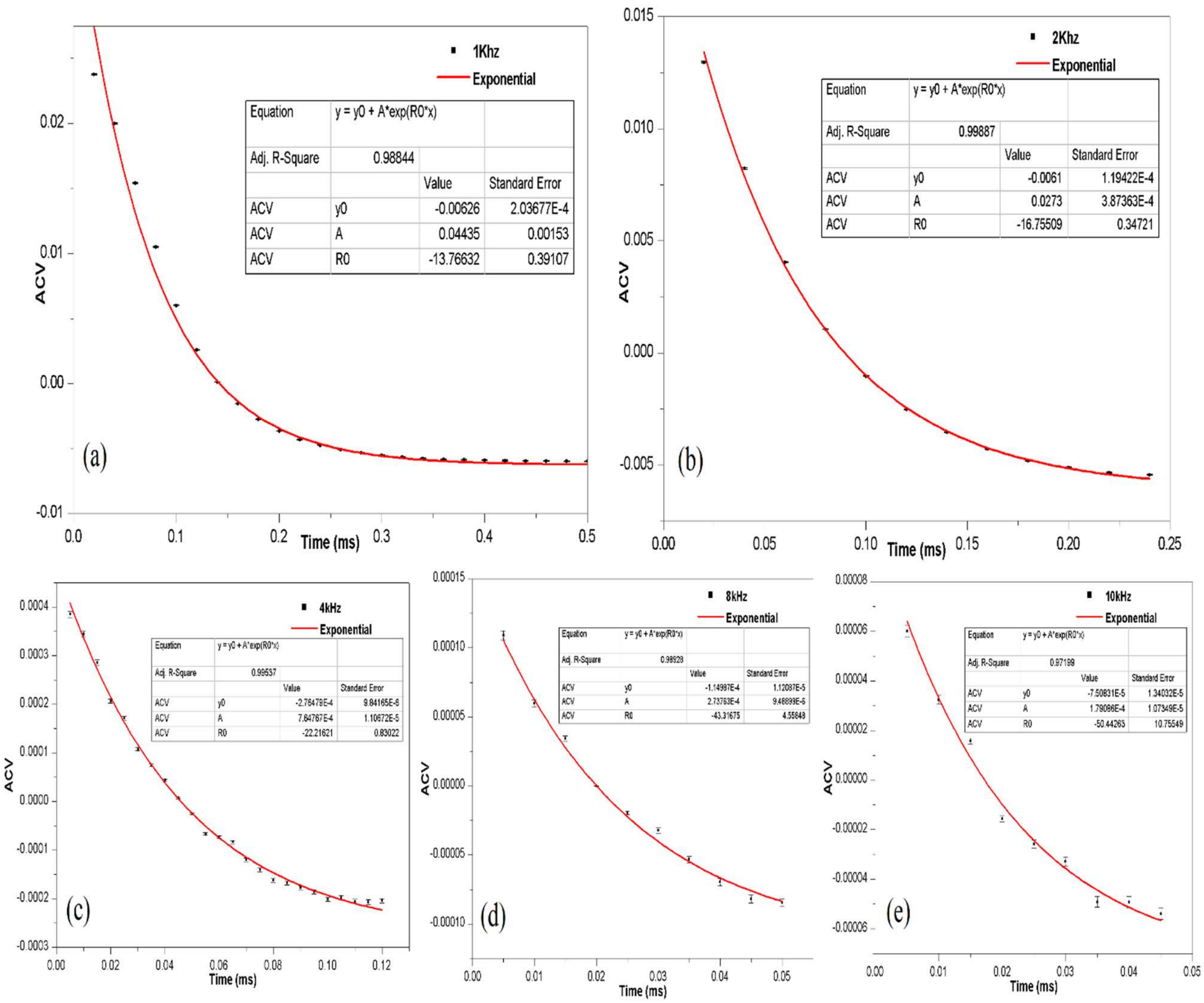

Figure 4.8. Estimation of source correlation factor from *ACV* at different source frequencies, (a)1 kHz, (b)2 kHz, (c)4 kHz, (d)8 kHz, (e)10 kHz.

4.6.2 Prompt Neutron Decay Constant

The measured source correlation factor for PNG at 10 kHz is 50.44 ms^{-1}. Thus, the time correlation between source emissions, or source correlation factor, decay much faster than the decay of prompt neutron chain (α~2.31 ms^{-1}) of BRAHMMA. Furthermore, source frequencies (f) 4, 8 and 10 kHz are large compared to the prompt neutron decay constant (α) of

BRAHMMA. Therefore, equations 4.7, 4.8 and 4.12 have been used in case of *V/M*, *ACV* and *APSD* respectively as discussed in section 4.2.

Finally, noise experiments in BRAHMMA subcritical system have been carried out with D-T neutron source. Three different detector configurations have been used during experiments, namely 8 detectors set (8 Det) and two 4 detectors sets placed at transverse planes at Z=-18.5 cm (4F Det, F indicating Forward in subcritical assembly) and +18.5 cm (4B Det, B indicating Backward in subcritical assembly). Data have been analysed using *V/M*, *ACV* and *APSD* method. The measured *V/M*-1 at different accelerator frequencies have been shown in Figures 4.9 4.10 and 4.11. The error bar in *V/M* has been estimated using the analytical approach proposed by Endo and Yamamoto (2019). But, the bunching method as proposed by Misawa et al. (1990) has not been used in the present research work. The prompt neutron decay constant for different detector configurations has been obtained by fitting *V/M*-1 to equation 4.7 based on the accelerator frequency and measured source correlation factor. During fitting, a constant term has been used to incorporate the dead time effect of detectors (Soule et al., 2004). The measured prompt neutron decay constant and other fitting parameters with the error bar, estimated for different detector sets at different frequencies have been presented in Table 4.4. The prompt neutron decay constant in case of 8 Det set is close to theoretical value ($2.310 \pm 0.058\ ms^{-1}$) (Kumar et al., 2017), whereas, in case of 4F and 4B Det set, the decay constant is relatively high. Moreover, the error bar of prompt neutron decay with 8 Det set (Table 4.4) is significantly small compared to 4F and 4B Det set. This can be explained qualitatively by modal effects at different detector sets during experiments. In case of 8 detectors, higher order modes have insignificant contribution, whereas, in case of 4F and 4B set, anti-symmetric modes have significant contribution to the prompt neutron decay. Similarly, the Adj. R-Square is higher for 8 detectors compared with 4F and 4B Det set (Figures 4.9-4.11, Table 4.4), which indicates that the fitting model is more accurate for 8 detectors.

Table 4.4. *Prompt neutron decay constant measured using V/M method.*

Accelerator Frequency (kHz)	Detector configuration	Correlated Amplitude (A)	Prompt neutron decay (B) (ms^{-1})	Additional constant (C)	Adj. R-Square
10.0	8 Det	0.37763±0.00203	2.31345±0.03810	-0.00328±0.00218	0.99334
	4F Det	0.23765±0.0015	2.52902±0.04482	0.02513±0.00162	0.99192
	4B Det	0.22740±0.00152	2.56301±0.05001	-0.00077±0.00163	0.99093
8.0	8 Det	0.32022±0.00125	2.37041±0.02384	-0.02859±0.00137	0.99629
	4F Det	0.23008±0.00185	2.51021±0.05856	-0.02520±0.00199	0.98782
	4B Det	0.16876 ±0.0018	2.62510±0.08806	-0.01777±0.00192	0.98217
4.0	8 Det	0.29215±0.00135	2.42874±0.03249	0.01594±0.00145	0.99537
	4F Det	0.20907±0.00143	2.65378±0.05161	0.02874±0.00153	0.99151
	4B Det	0.17505±0.00134	2.56872±0.07144	-0.00580±0.00142	0.99034

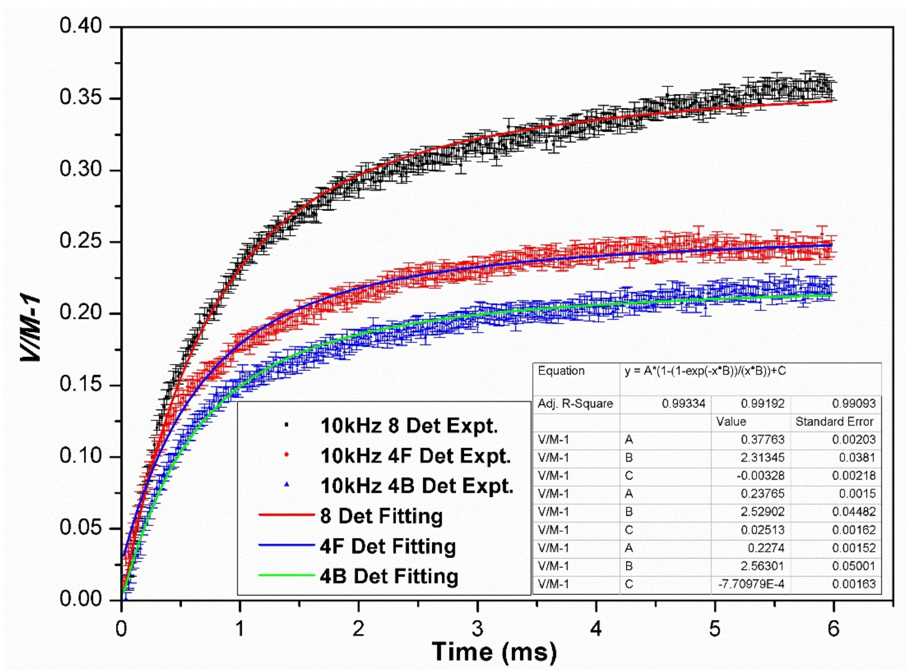

Figure 4.9. V/M-1 plot for different detector set at 10 kHz.

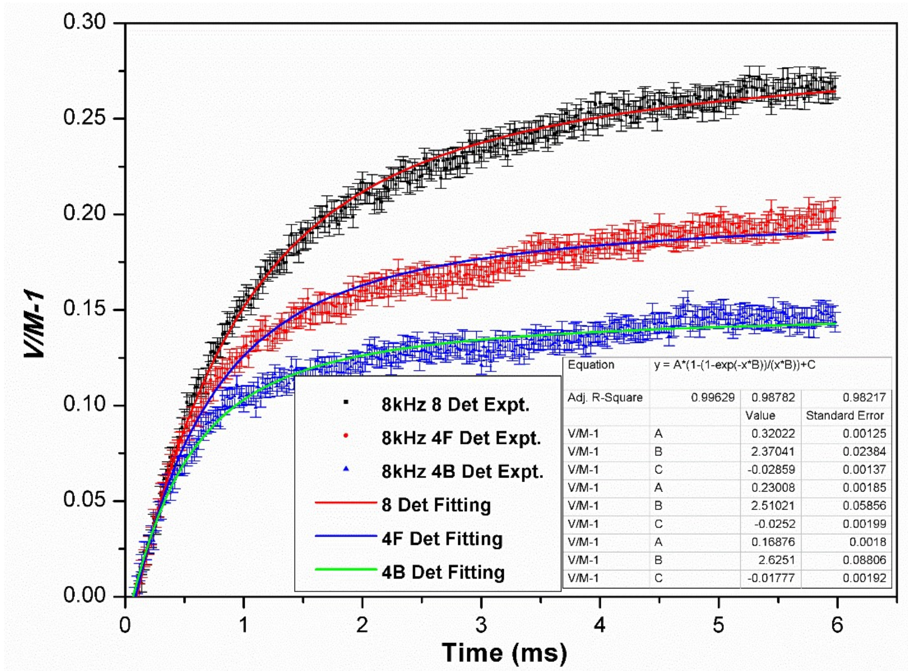

Figure 4.10. V/M-1 plot for different detector set at 8 kHz.

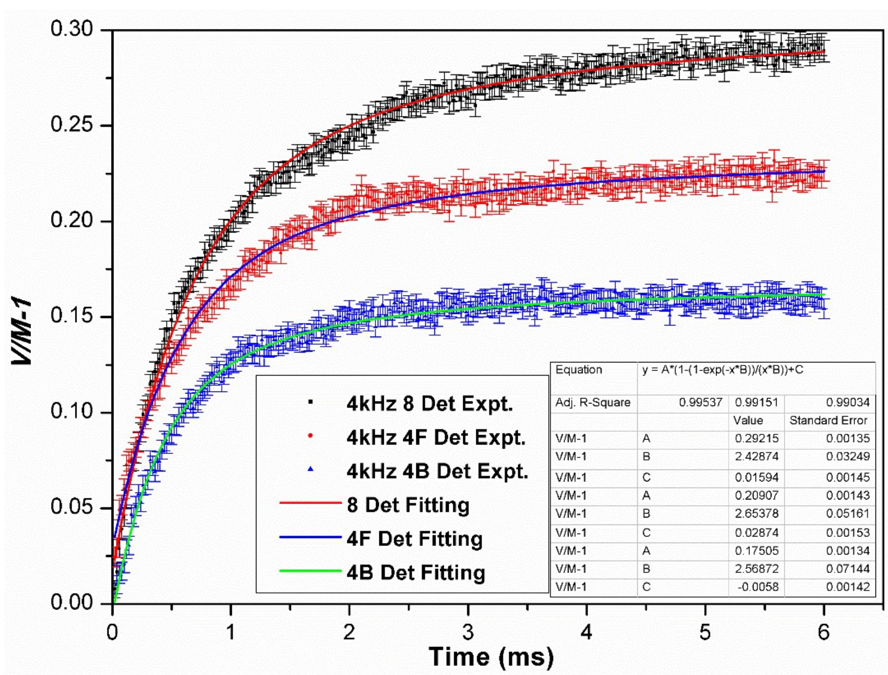

Figure 4.11. V/M-1 plot for different detector set at 4 kHz.

In Figures 4.9-4.11, the correlated amplitude of *V/M*-1 are different for 4F and 4B Det at different frequencies, though their time evolution remains same. The noise theory under discussion had been developed considering space independent point kinetic model. In the present subcritical system, at Z=±18.5 cm, the 1st symmetric mode in axial and transverse direction has zeros (Kumar et al., 2017). Due to this fact, 8 Det set (as mentioned in section 4.4) will cancel 1st symmetric modes and all anti-symmetric modes. On the other hand, the 2nd and higher symmetric modes and anti-symmetric modes in axial direction have contribution to the measured noise descriptors for 4F and 4B Det set. Higher modes will die away much faster compared to the fundamental mode (Kumar et al., 2017; Yamamoto, 2013, 2014). As a result, the major portion of correlated amplitude for higher gate width will be contributed by the fundamental mode (Kumar et al., 2017). Therefore, the correlated amplitude should be same in case of 4F and 4B Det set under symmetric flux distribution. But, the measured flux in axial direction is asymmetric and has different value at Z=±18.5 cm as shown in Figure 4.12. This indicates the space dependency of neutron population within system and several authors have also discussed space dependent noise theory (Williams, 1974; Ballester & Muñoz-Cobo, 2005; Muñoz-Cobo et al., 2011; Yamamoto, 2013, 2014) with space dependent correlated amplitude in *V/M* and Rossi-alpha. Therefore, due to the design asymmetry in axial direction (Z) in BRAHMMA, the measured *V/M* at Z=±18.5 cm with 4F and 4B Det set showed different value of correlated amplitude. Incorporating spatial corrections, Williams (1974) has proposed space dependent noise theory under fundamental mode approach and the *V/M* ratio is given by equation 4.14.

$$\frac{V(T)}{M(T)} = 1 + \frac{\varepsilon\lambda_f \left\langle \nu\Sigma_f \right\rangle \left\langle \nu(\nu-1) \right\rangle}{(1+M^2B^2)\alpha^2} \underbrace{\left\{ \frac{F_{00}\Psi_0^2(r_0)}{f(r_0)} \right\}}_{Spatial-correction} * \left(1 - \frac{1-e^{(-\alpha T)}}{\alpha T} \right) \tag{4.14}$$

where, ε is the detector efficiency, Σ_f is the macroscopic fission cross section, $\Psi_0(r_0)$ is the flux in fundamental mode, B is the geometrical buckling, M is the migration length, $f(r_0)$ is the neutron density and F_{00} is given by:

$$F_{00} = \int_v f(r_0)\Psi_0(r_0)\Psi_{0'}(r_0)dr_0 \tag{4.15}$$

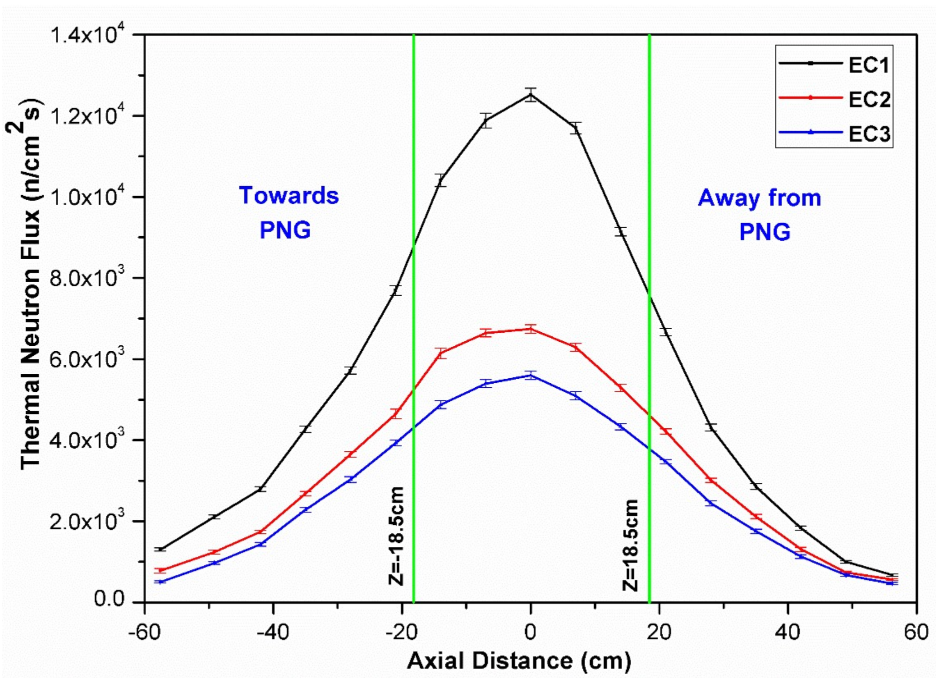

Figure 4.12. Thermal flux profile along axial channels (EC1-EC3) (Shukla et al., 2015).

The quantitative analysis of the postulate is out of the scope of the present study and will be the subject of the future work.

The prompt neutron decay constant which has been obtained by *V/M* method using 8 detector set indicates that, for BRAHMMA point model space-independent analysis is adequate to obtain the prompt neutron decay constant. Here onwards, 8 Det data have been presented using *ACV* and *APSD* method for prompt neutron decay constant. The prompt neutron decay constant has been obtained by fitting the measured *ACV* with equation 4.8. The measured *ACV* at frequencies 10 and 8 kHz have been shown in Figures 4.13 and 4.14 respectively. Furthermore, the *APSD* has been obtained from Fourier transform of the measured *ACV* and

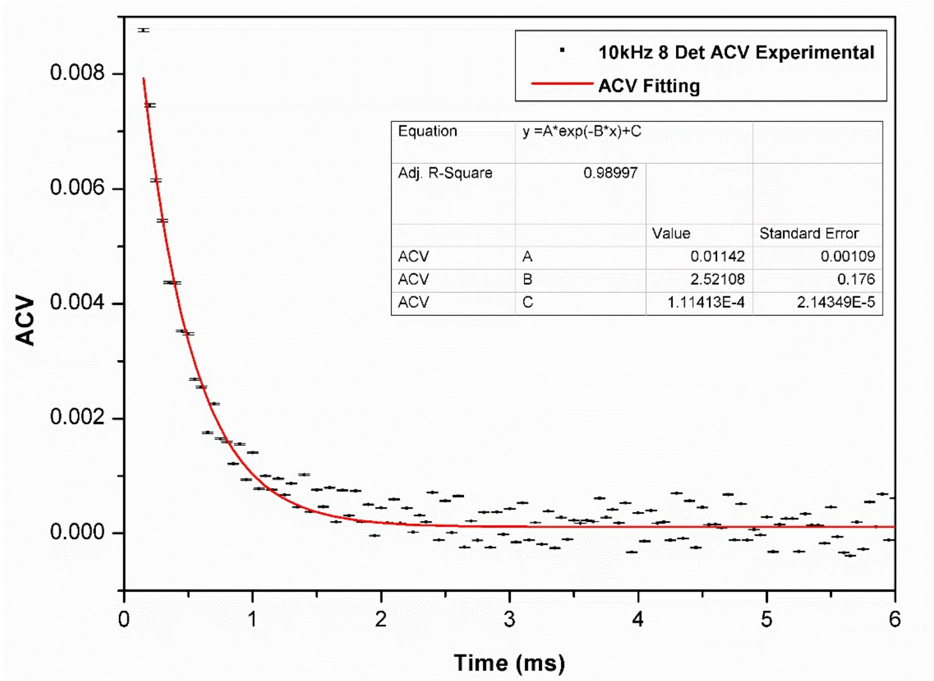

Figure 4.13. ACV plot for 8 Det at 10 kHz.

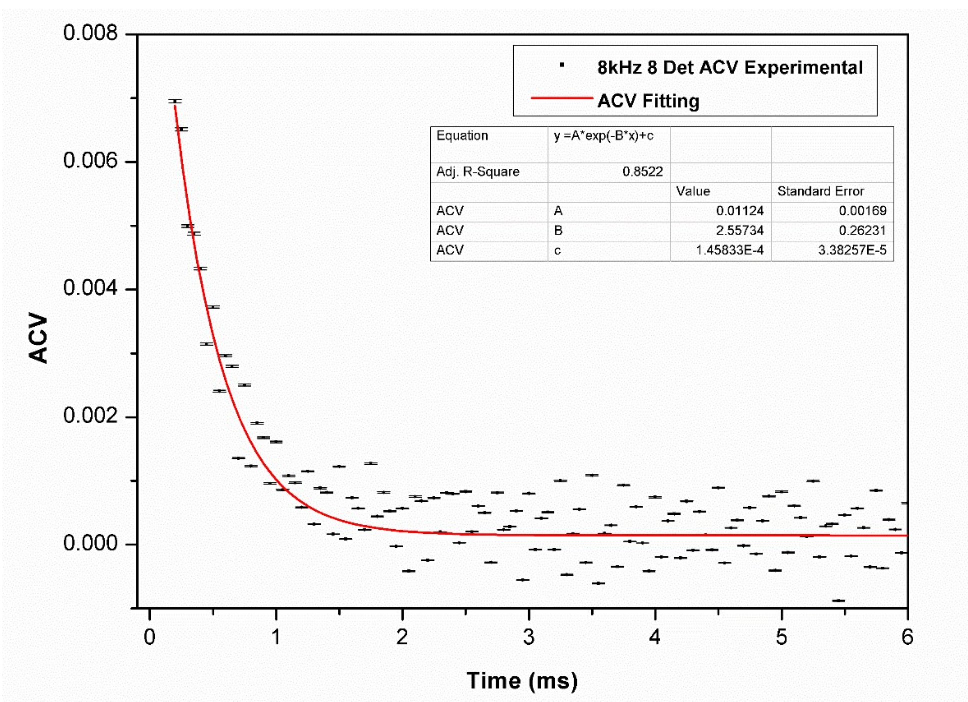

Figure 4.14. ACV plot for 8 Det at 8 kHz.

measured *APSD* at different frequencies have been shown in Figures 4.15-4.17. Moreover, results obtained by *APSD* shows peaks at integer multiple of source frequency, which corresponds to the periodic uncorrelated part in *ACV*. The first and third terms of equation 4.12 have been used for fitting of the measured *APSD*. The data points corresponding to the integer multiple of source frequency have been masked to avoid the second term of equation 4.12. Prompt neutron decay constant has been obtained by least square fitting of rest of the data points. The prompt neutron decay constant obtained from *ACV* and *APSD* method have been presented in Table 4.5.

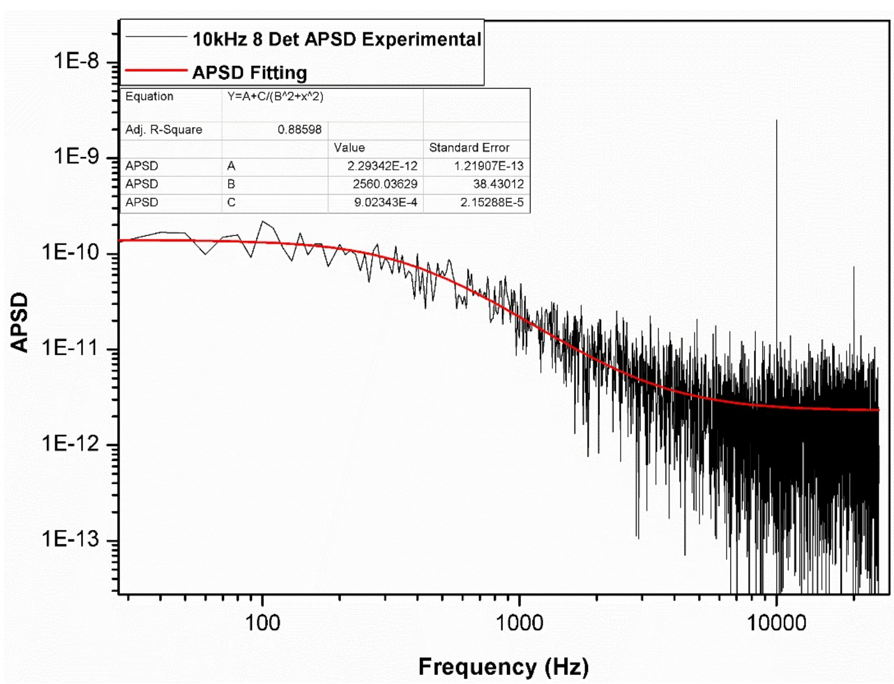

Figure 4.15. APSD plot at 10 kHz.

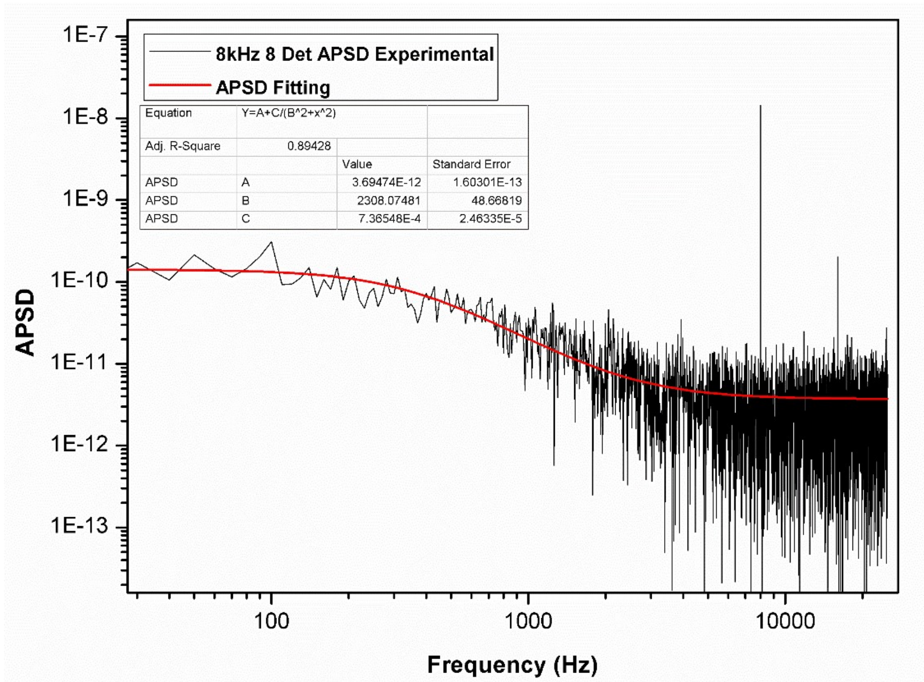

Figure 4.16. APSD plot at 8 kHz.

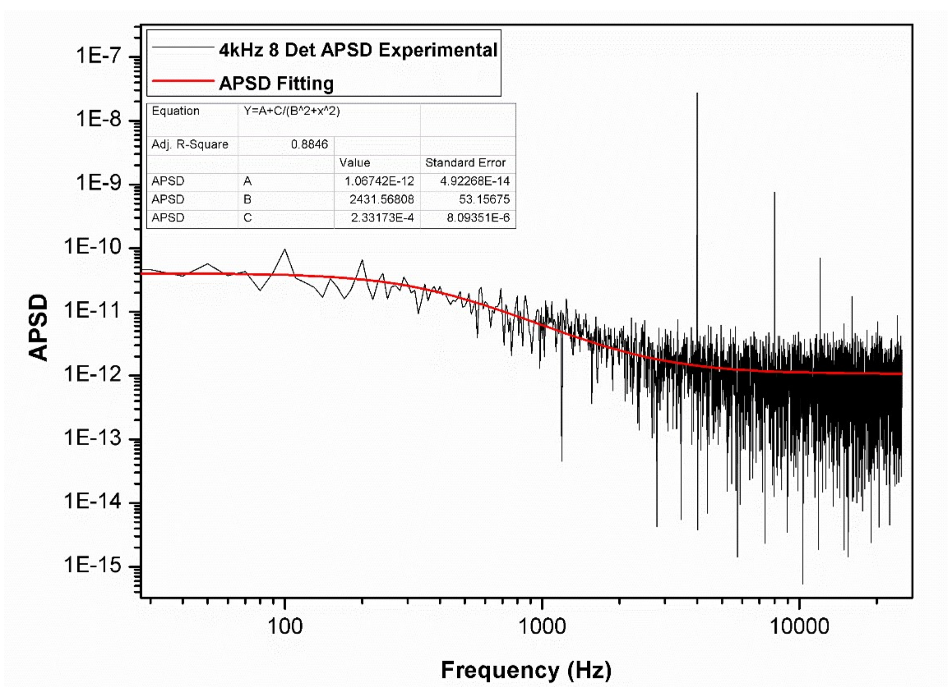

Figure 4.17. APSD plot at 4 kHz.

Table 4.5. *Prompt neutron decay constant measured using ACV and APSD method using 8Det set.*

Methods	Fitting parameter	Accelerator Frequency (kHz)		
		10.0	8.0	4.0
ACV	Correlated Amplitude (A)	0.01142 ±0.00109	0.01124 ±0.00169	-
	Prompt neutron decay (B) (ms^{-1})	2.52108 ±0.17600	2.55734 ±0.26231	-
	Uncorrelated Amplitude (C)	0.00011 ±0.00002	0.00014 ±0.00003	-
	Adj. R-Square	0.98997	0.85220	
APSD	Detector white spectrum (A)	2.29342E-12 ±1.21907E-13	3.69474E-12 ±1.60301E-13	1.06742E-12 ±4.92268E-14
	Prompt neutron decay (B) (s^{-1})	2560.04 ±38.43	2308.07 ±48.67	2431.57 ±53.15
	Correlated Amplitude (C)	9.02343E-4 ±2.15288E-5	7.36548E-4 ±2.46335E-5	2.33173E-4 ±8.09351E-6
	Adj. R-Square	0.88598	0.89428	0.88460

The measured prompt neutron decay constant using various noise methods are in good agreement with the theoretical value. Finally, prompt neutron decay constant along with β_{eff} (0.00704) and Λ (59.71 μs) can be used to infer the reactivity and neutron multiplication factor (k_{eff}) of the subcritical system.

4.6.3 Analysis of Experimental Data with the Exact Theoretical Postulate

Previous sections have studied the noise theory developed under consideration of exponentially correlated Gaussian source characteristics for reactivity measurement in ADS. The decay of the correlated neutron sources (or source correlation factor) is crucial for accurate measurement of prompt neutron decay constant and reactivity. Thus, the actual behaviour of the accelerator-based neutron source has been studied experimentally and an approach has been made for application of more general noise theory involving the non-Poisson character with experimental evidences. According to experimental observations of source correlation factor and accelerator frequencies, the research has used simplified noise descriptors. Furthermore, the present section has made an attempt for rigorous analysis of the measured correlation factor with the exact noise descriptor as proposed by authors. The fitting of the measured *ACV* at 10 kHz with equation 4.2 has been shown in Figure 4.18. The prompt neutron decay constant according to this analysis is 2.596±0.117 ms^{-1} and the Adj. R-Square value is 0.9604, whereas, the Adj. R-Square value is 0.98997 for fitting with equation 4.8 as presented in Table 4.5. This difference can be attributed to the absence of uncorrelated oscillatory part of equation 4.2 in experimental observation due to the high accelerator frequency. Moreover, the source correlation time is very small compared to the prompt neutron decay time of BRAHMMA. Therefore, the fitting of the measured *ACV* with equation 4.8 is more appropriate according to the source parameters (source correlation factor and accelerator frequency).

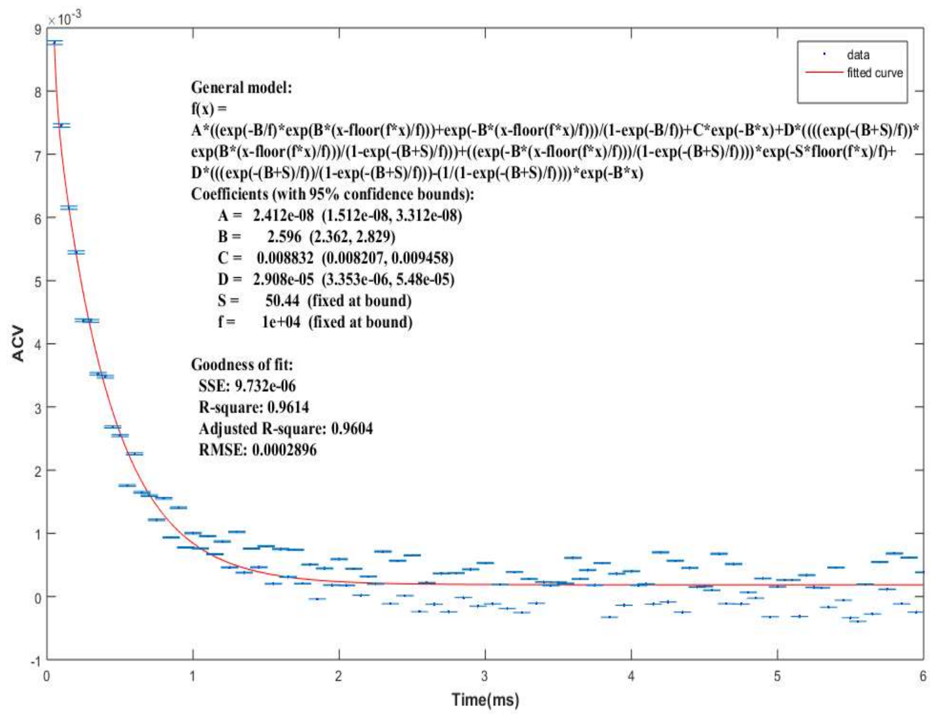

Figure 4.18. Analysis of measured *ACV* using equation 4.2.

CHAPTER FIVE

PULSE SHAPE MEASUREMENT AND EXPERIMENTAL VALIDATION OF NOISE THEORY DEVELOPED UNDER CONSIDERATION OF FINITE PULSE WIDTH

5.1 Introduction

The experimental validation of the noise theory developed by Degweker and Rana (2007) under assumption of exponentially correlated Gaussian source characteristics has been discussed in previous chapter. The theoretical assumption that the accelerator-based neutron source does not follow Poisson characteristics (Degweker & Rana, 2007) has been validated using D-T neutron generator. It has been observed that the external neutron source has fluctuation ~2-2.5% and measured V/M-1 has an asymptotic value of 0.1. Furthermore, previous chapter has also discussed noise experiments under consideration of external source as exponentially correlated Gaussian character having very small pulse width (Dirac-delta function) compared to the prompt neutron decay time ($1/\alpha$) along with accelerator frequency (f) that is large compared to prompt neutron decay constant (α).

However, there could be situation when the pulse width is comparable to $1/\alpha$. In this perspective, Degweker and Rana (2007) also postulated noise descriptors for different pulse shape (Rectangular, Gaussian) with finite width. Authors have also considered different cases for source correlation time, accelerator pulse width and frequency. Hence, it is essential to measure the source correlation time and pulse shape before validation of this noise theory developed under the condition of finite pulse width. Furthermore, in case of $f < \alpha$, the fission chain induced by external neutron source will die away between consecutive pulses. Thus, the correlation of fission neutrons from one pulse to the next pulse will be very small and will be reflected in measured variance to mean ratio (V/M) and two time probability function.

However, very little experimental works in this direction have been reported to describe how the noise descriptors behave for a wide range of accelerator frequencies with fixed subcriticality and source strength (10% duty cycle at the present research). In D-T neutron generator, the pulse shape was found out to be rectangular and is described in the present chapter. Hence, for validation purpose, the theoretical postulate for finite and rectangular pulse has been considered and reviewed in the following sections.

5.2 Review of Noise Theory Developed Under Consideration of Gaussian Source Characteristics along with Finite Rectangular Pulse Width

The present section provides the theoretical review of various noise descriptors under the assumption that the beam pulse having rectangular shape and its width is large compared to the source correlation time as postulated by Degweker and Rana (2007).

5.2.1 Theory of Variance to Mean Ratio and Two Time Probability Function

According to Degweker and Rana (2007), for variation of the current *I(t)* as periodic sum of narrow pulse train $\varepsilon(t-t_n)$ at time t_n with exponential correlation of the current fluctuation, theoretical formulae for one time probability ($F_1(t)$) and two time probability ($F_2(0,T)$) distributions are written as follows:

$$F_1(t) = \bar{I}\,\bar{\nu}_{sp}\lambda_d f \int_{-1/f}^{0} dt_0 \sum_{n=0}^{\infty} \varepsilon(t - t_0 + n/f) e^{\alpha t} dt \tag{5.1}$$

$$\begin{aligned} F_2(0,T) = {} & \bar{\nu}_{sp}^2 \lambda_d^2 f \int_{-1/f}^{0} dt_0 \sum_{n=0}^{\infty}\sum_{m=0}^{\infty}\int_{-\infty}^{\infty}\int_{-\infty}^{\infty} \varepsilon(t_1 - t_0 + n/f) * \varepsilon(t_2 - t_0 + m/f) * \left(\langle I\rangle^2 + \Gamma^2 e^{-\beta|t_1 - t_2|}\right) e^{\alpha t_1} e^{\alpha(t_2 - T)} dt_1 dt_2 \\ & + \langle I\rangle \lambda_d^2 f \int_{-1/f}^{0} dt_0 \sum_{n=0}^{\infty}\int_{-\infty}^{\infty} \varepsilon(t - t_0 + n/f)\left(2Y_1\bar{\nu}_{sp} e^{\alpha t}(1 - e^{\alpha t}) * e^{-\alpha T} + \langle \nu_{sp}(\nu_{sp} - 1)\rangle e^{\alpha(2t - T)}\right) dt \end{aligned} \tag{5.2}$$

where, $\Gamma^2 = \langle I^2 \rangle - \langle I \rangle^2$, I is the mean beam current, v_{sp} is the number of neutrons produced per ion, f is frequency of the external source, λ_d is the probability of detection per second, α is the prompt neutron decay constant, β is the source correlation factor and Y_1, a constant given by:

$$Y_1 = \frac{\lambda_f \langle \nu(\nu-1) \rangle}{2\alpha} \tag{5.3}$$

where, λ_f is the probability of fission per second, v is the number of neutrons per fission.

Let us consider a rectangular pulse defined by:

$$\varepsilon(t) = rect(\frac{g}{\sigma}) \tag{5.4}$$

where, g and σ are pulse amplitude and width respectively. If the correlation time ($1/\beta$) of the current fluctuation is much smaller than the pulse width, the circumstance corresponds to the Poisson source characteristics as described by Degweker and Rana (2007) and the noise descriptors will be same as derived by Pázsit et al. (2005). In such case, the $F_1(t)$ is given by:

$$F_1(t) = \frac{\langle I \rangle g \lambda_d \bar{v}_{sp} f}{\alpha} = \frac{\lambda_d f m_1}{\alpha} \tag{5.5}$$

where, $m_1 = \langle I \rangle g \bar{v}_{sp}$ is the mean number of neutrons per source pulse.

The two time probability is given by:

$$F_2(0,T) = \frac{m_1 \lambda_d^2 f}{2\alpha} \left[\underbrace{\frac{\langle \nu(\nu-1) \rangle \lambda_f}{\alpha} + \frac{\langle v_{sp}(v_{sp}-1) \rangle}{\bar{v}_{sp}}}_{1st-Term} \right] e^{-\alpha T} + \frac{m_1^2 \lambda_d^2 f^2}{\alpha^2} \left[\underbrace{\sum_{n=1}^{\infty} \frac{4\alpha^2 (1-\cos(\omega_n \sigma)) \cos(\omega_n T)}{\sigma^2 \omega_n^2 (\omega_n^2 + \alpha^2)}}_{2nd-Term} + 1 \right] \tag{5.6}$$

where, v is the number of neutrons produced per fission, λ_f is the probability of fission per second and $\omega_n = 2\pi n f$, where n is the positive integer denoting cycle number.

The V/M is derived as usual by integration of the above equation as follows (Williams, 1974):

$$\frac{V(T)}{M(T)} = 1 - F_1 T + \frac{2}{F_1 T} \int_0^T (T-\tau) F_2(0,\tau) d\tau \tag{5.7}$$

The final expression of *V/M* is given by:

$$\frac{V(T)}{M(T)} = 1 + \underbrace{\left(\frac{\lambda_d \lambda_f \langle \nu(\nu-1) \rangle}{\alpha^2} + \frac{\lambda_d \langle \nu_{sp}(\nu_{sp}-1) \rangle}{\alpha \bar{\nu}_{sp}}\right)\left(1 - \frac{1-e^{-\alpha T}}{\alpha T}\right)}_{1st-Term} + \underbrace{\frac{4 m_1 \lambda_d \alpha}{\sigma^2 T f}\left[\sum_{n=1}^{\infty} \frac{(1-\cos(\omega_n \sigma))\sin^2(\omega_n T/2)}{n^2 \pi^2 \omega_n^2 (\omega_n^2 + \alpha^2)}\right]}_{2nd-Term} \quad (5.8)$$

The above formulae (equation 5.6 and 5.8) have two terms. The first term represents the correlated part and the second term represents the uncorrelated part which is periodic in nature. Least square fitting of equations 5.6 and 5.8 will give the prompt neutron decay constant of subcritical system.

5.2.2 Auto Power Spectral Density

Auto Power Spectral Density analysis is another state of art of reactor noise analysis. *APSD* is given by the Fourier analysis of the Auto Correlation function. The *APSD* has been discussed elaborately in previous chapter and the final equation of *APSD* is given by:

$$\begin{aligned} APSD(\omega) &= \frac{\langle q^2 \rangle f m_1 \lambda_d}{\alpha} H(\omega) + \langle q \rangle^2 f \lambda_d^2 H(\omega) \left\{ \sum_{n \neq 0} \frac{4\pi f m_1^2 \delta(\omega - \omega_n)}{\alpha^2 + \omega_n^2} \right\} \\ &+ \langle q \rangle^2 f \lambda_d^2 H(\omega) \frac{m_2 - m_1^2 + 2 m_1 Y_1}{\omega^2 + \alpha^2} \end{aligned} \quad (5.9)$$

Least square fitting of the measured *APSD* with above equation will give α of subcritical system.

5.3 Experimental Setup and Location of Detectors

The experimental set up and detectors' location have been discussed in previous chapter and the same have been used during noise experiments with finite pulse width.

5.4 Source Characterisation

The theoretical reviews of *V/M* and two-time probability function have been discussed in section 5.2.1 under consideration of rectangular pulse shape and the source correlation time is small compared to pulse width. The present section describes measurements related to source correlation time and pulse shape characterisation.

The decay time of correlated source neutrons (*1/β*) has been measured using ^{3}He detector (length: 10.0 cm, diameter: 2.438 cm) and time stamp data acquisition system. The ^{3}He detector, encapsulated by Perspex cylinder followed by 2 mm Cadmium, has been placed at a distance of 10 cm from the beam target of the PNG. Perspex has been used to thermalize the 14.1 MeV neutrons and Cadmium to stop scattered thermal neutrons from surroundings. Moreover, the Pulse shape of PNG has been characterised by ACCT, which has been introduced in the D^+ beam path.

5.4.1 Study of Source Correlation Time for Different Pulse Width

Degweker and Rana (2007) have postulated the noise theory for different pulse width (Dirac-delta pulse and finite pulse width) and the previous chapter has discussed noise experiments for Dirac-delta pulse. In case of finite pulse width, Degweker and Rana (2007) have considered different cases depending on the source correlation time ($1/\beta$), accelerator pulse width (σ) and pulse period ($1/f$) ($1/\beta<<\sigma$, $\sigma<<1/\beta<<1/f$ and $1/\beta>>\sigma$). The section 5.2.1 has discussed only the noise theory postulated under consideration of source correlation time much small compared to the accelerator pulse width. Therefore, before further noise experiments, it is essential to measure the σ and $1/\beta$ to determine suitable noise descriptors as postulated by Degweker and Rana (2007).

For measurement of source correlation time, time stamped data have been analysed using *ACV* method. The source correlation factor along with source correlation time have been estimated from the exponential decay of the measured *ACV* for different accelerator frequencies (10 kHz to 1 kHz) and have been discussed in previous chapter (section 4.6.1). As an example, the source correlation time and pulse width for accelerator frequency 2 kHz are

59.6±1.2 μs and 50.0 μs respectively, whereas for accelerator frequency 1 kHz, these values are 72.6±2.1 μs and 100.0 μs respectively. Therefore, the source correlation time is small compared to the pulse width at 1 kHz, whereas, it is large at accelerator frequency 2 kHz. Furthermore, this variation does not accomplish any of the criteria as mentioned in previous paragraph. On the other hand, in the previous chapter (section 4.6.1), it has inferred that the finite width of the neutron pulse will smear out the correlation time and the higher pulse width at lower accelerator frequency will slow down the decay.

To understand the behaviour of source correlation time with accelerator pulse width and fulfilment of the assumption as discussed in section 5.2.1, source correlation factor and correlation time have been studied for different pulse width at accelerator frequency 1 kHz. The accelerator frequency 1 kHz has been chosen as the pulse width can be varied from 100 μs to 10 μs, whereas, this is not possible at 2 kHz. Time stamped data have been analysed using *ACV* method as shown in Figure 5.1 and the source correlation time has been estimated from the exponential decay (Figure 5.2). In case of 100 μs pulse width, the source correlation time is 72.5 μs, whereas, in case of 10 μs pulse width, the correlation time is 52.4 μs (Table 5.1). Hence, the higher pulse width has a significant contribution to the decay of *ACV* and the correlation time of source neutrons smear out with higher pulse width.

The source correlation time should be independent of the pulse width, but experimental observations suggest the opposite. The contribution of the pulse width in measured source correlation time is a subject of future study with theoretical model. Furthermore, the slowing down time of 14.1 MeV neutrons in Perspex (Nellis, 1977) and the measured fall time of pulsed beam as mentioned in section 5.4.2 have not been considered during the present research work. Based on these observed variations of source correlation time with pulse width, further noise studies have been carried out considering source correlation time is small compared to the beam pulse width.

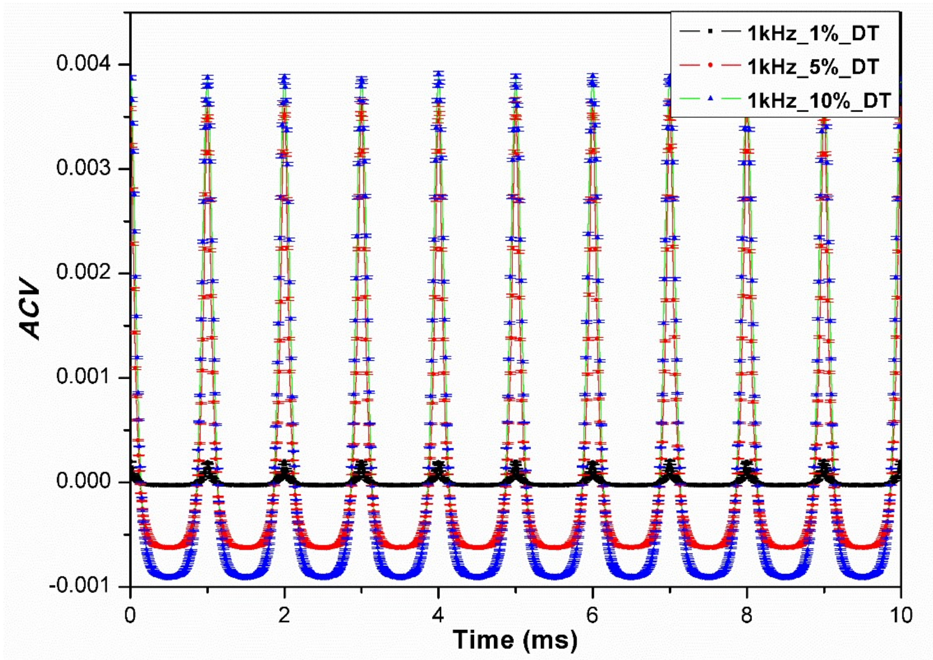

Figure 5.1. Evolution of the measured *ACV* at different pulse width at 1 kHz accelerator frequency.

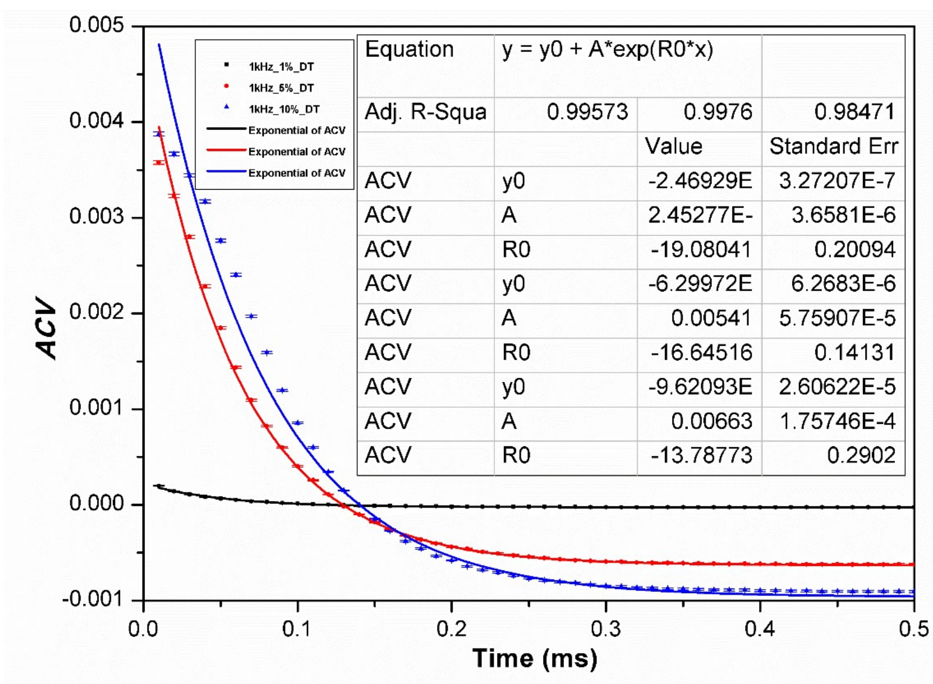

Figure 5.2. Estimation of source correlation factor and time for different pulse width at 1 kHz (figure 5.2 is a subset of figure 5.1 with exponential fitting).

Table 5.1. *Variation of source correlation time with pulse width at 1 kHz.*

Sr. No.	Pulse Width (μs)	Source correlation factor (β) (ms^{-1})	Source correlation time ($1/\beta$) (μs)
1	100.0	13.79±0.29	72.5±1.5
2	50.0	16.65±0.14	60.1±0.1
3	10.0	19.08±0.20	52.4±0.1

5.4.2 Pulse Shape Characterisation

In case of high frequencies (10, 8 and 4 kHz), pulse period (100, 125 and 250 μs respectively) and width (10% of period) are small compared to the prompt neutron decay time ($1/\alpha$~433 μs) of BRAHMMA. Under such a situation, the fission chain triggered by source pulse will overlap with each other and experimental results as discussed in previous chapter have shown that the noise descriptors will be similar to continuous neutron source. On the other hand, in case of $f \leq \alpha$, the pulse width is comparable to $1/\alpha$ and cannot be assumed as delta function. Therefore, it is necessary to consider the pulse shape and finite width of the external source during noise experiments. So, the pulsed D^+ beam profile has been measured for noise experiments.

An ACCT has been introduced in the beam path to measure the pulse shape. The ACCT output is fed into a high impedance device as shown in Figure 5.3. Pulse shape, as seen in oscilloscope, at different accelerator frequencies have been shown in Figures 5.4-5.8 and the measured pulse widths have been presented in Table 5.2. It has been observed that the rise and fall time of the ACCT output is approximately 1 μs and the beam profile maintains constant amplitude irrespective of the accelerator frequency. Hence, the pulse shape can be concluded as rectangular and the theoretical consideration made by Degweker and Rana (2007) as discussed in section 5.2.1, has been implemented for further noise studies in ADS.

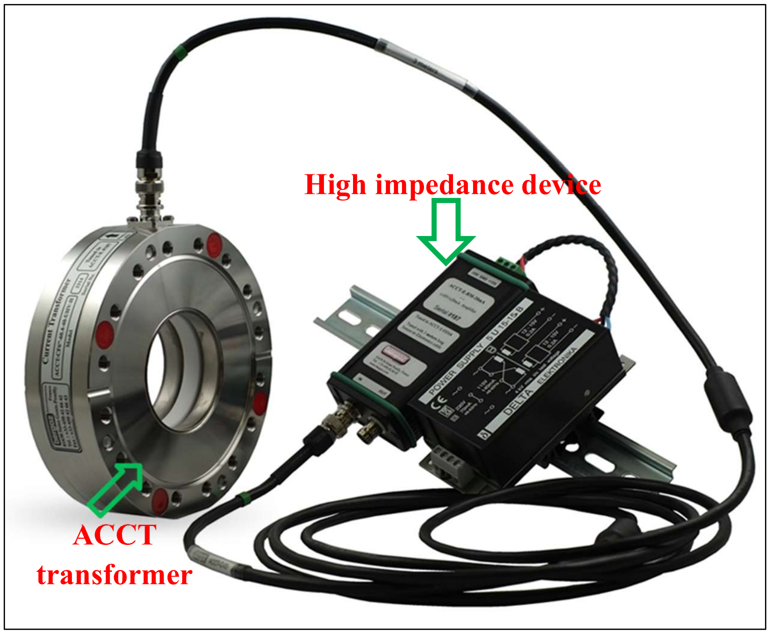

Figure 5.3. ACCT and high impedance device (Bergoz Instrumentation) for beam profile measurement.

Table 5.2. *Pulse width measured using ACCT at different source frequencies.*

Sr. No.	Accelerator frequency (kHz)	Time period (µs)	Pulse width (µs)	
			Set value	Measured using ACCT
1	4.00	250.0	25.0	24.746
2	2.00	500.0	50.0	49.651
3	1.25	800.0	80.0	79.760
4	1.00	1000.0	100.0	99.860
5	0.80	1250.0	125.0	124.820

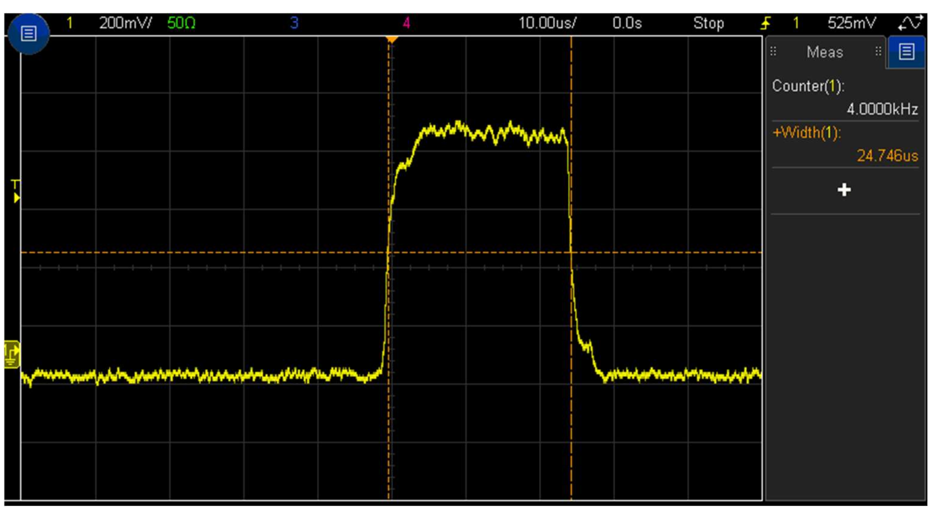

Figure 5.4. Measured pulse shape and pulse width at 4 kHz.

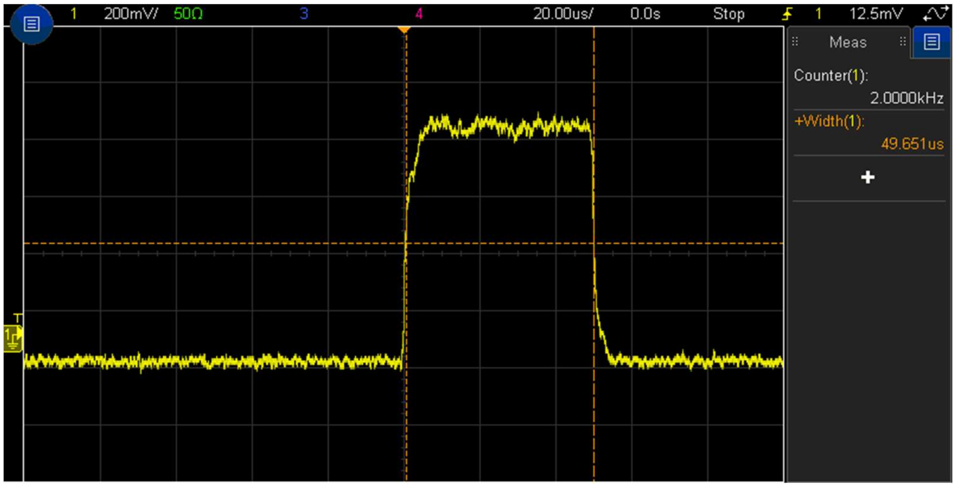

Figure 5.5. Measured pulse shape and pulse width at 2 kHz.

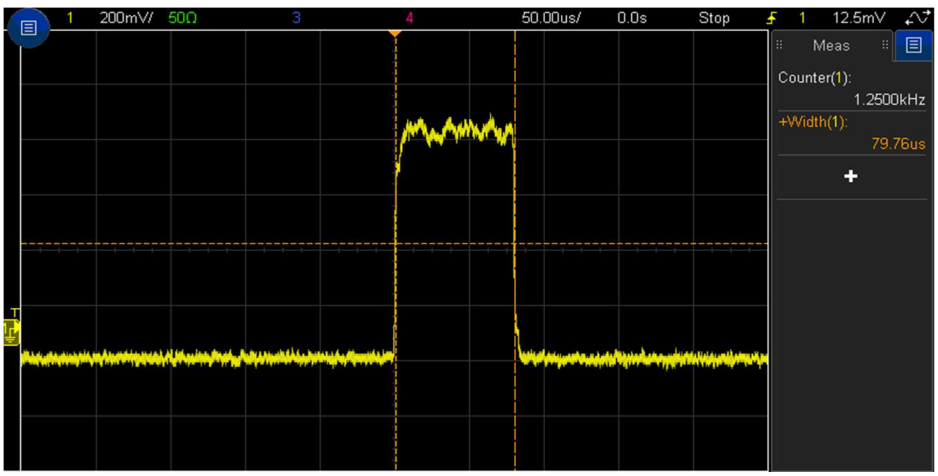

Figure 5.6. Measured pulse shape and pulse width at 1.25 kHz.

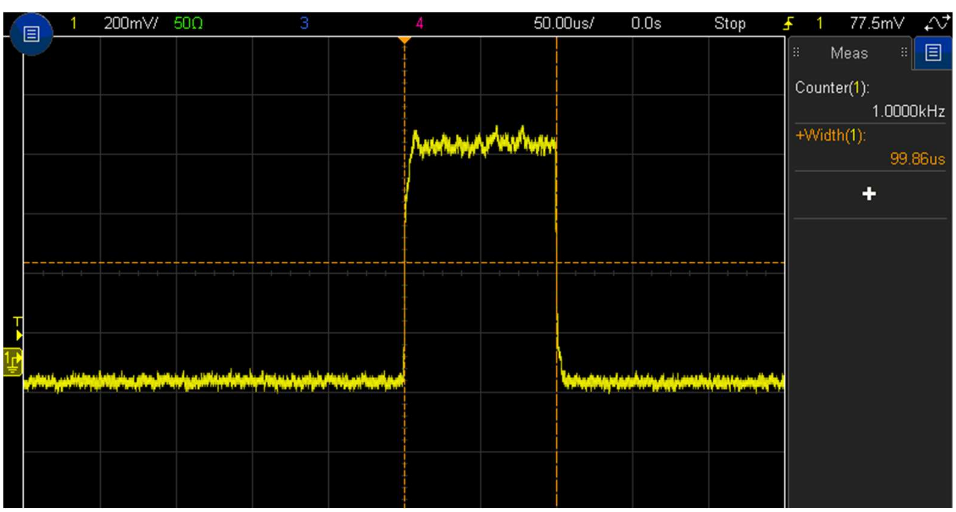

Figure 5.7. Measured pulse shape and pulse width at 1 kHz.

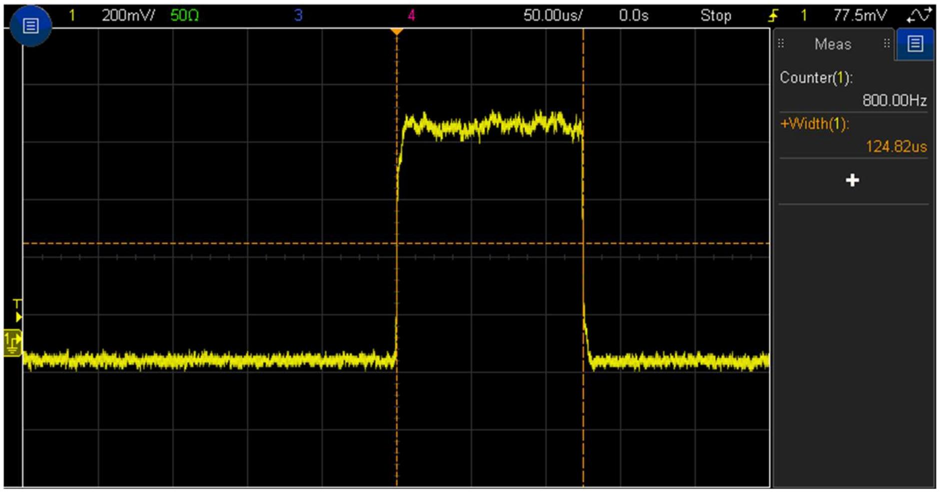

Figure 5.8. Measured pulse shape and pulse width at 800 Hz.

5.5 Experimental Results

The zero-power noise in BRAHMMA subcritical system which originates from statistical fluctuation of various nuclear events has been studied using PNG and time stamp data acquisition system. Time stamped data have been analysed using various methods such as *V/M*, *ACV* and *APSD*. In *V/M*, time stamped data have been segmented for gate width say, *T* and corresponding variance to mean ratio and error bar as postulated by Endo and Yamamoto (2019) have been estimated as function of *T*. The measured *V/M*-1 at accelerator frequency 2 kHz has been shown in Figure 5.9. It has been observed that small oscillation arises at 2 kHz and Figure 5.9 shows the fitting of the measured *V/M*-1 with the first term of equation 5.8, that is correlated part only. It has also been observed that the fitting model deviates from the experimental observation (Adj. R-Square=0.98178) and the prompt neutron decay constant (1.79818 ms^{-1}) is less compared with the theoretical value (2.310 ms^{-1}). In the next step, the second term of equation 5.8, which is the uncorrelated part, has been taken into account along with correlated part. As the second term of equation 5.8 is a Fourier series, it is very difficult to fit an infinite series with the measured *V/M*-1 and one needs to truncate it over finite terms. The evolution of fitting with number of higher order terms have been shown in Figures 5.10-

5.14 along with the Adj. R-Square value. The fitting parameters, such as, prompt neutron decay constant as mentioned by parameter B and Adj. R-Square value have been presents in Table 5.3. It can also be seen that for n=4, the Adj. R-Square value of the fitting is maximum and the measured α is in good agreement with the theoretical value (2.310 ms^{-1}).

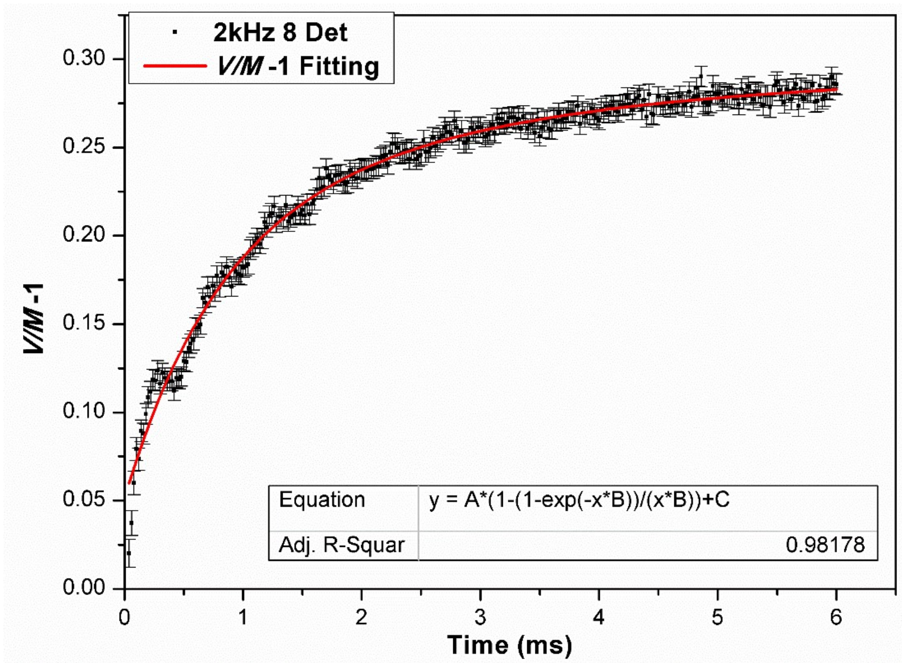

Figure 5.9. Fitting of measured *V/M* with correlated part of equation 5.8.

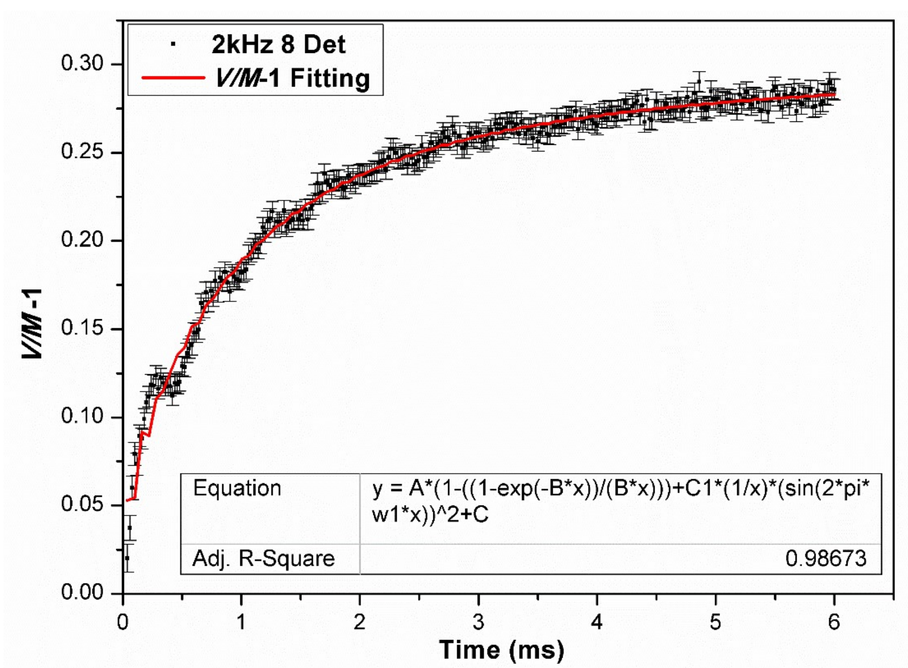

Figure 5.10. Fitting of measured *V/M* with correlated part along with 1st term (n=1) of uncorrelated part of equation 5.8.

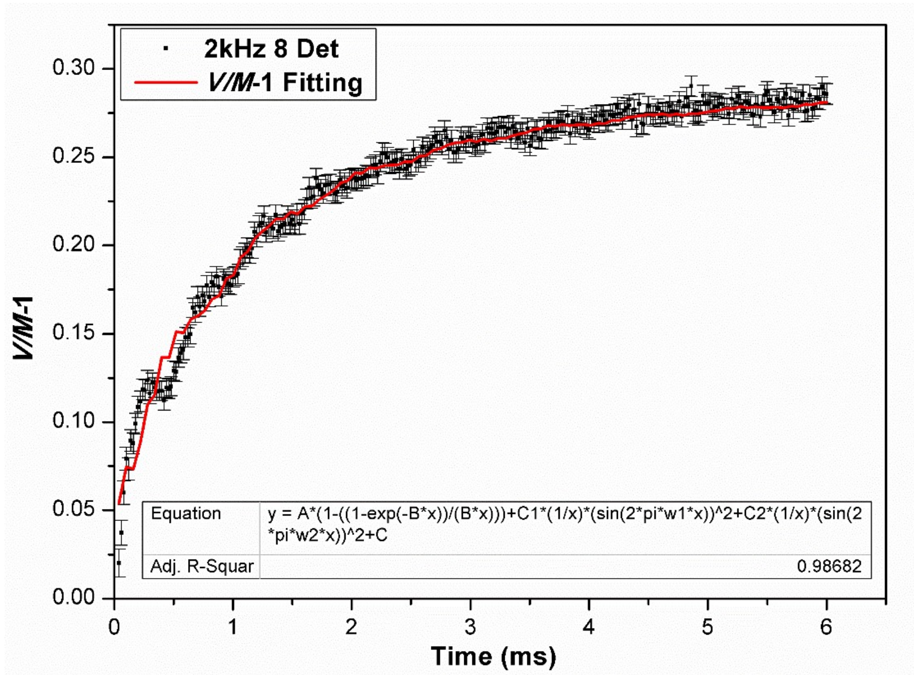

Figure 5.11. Fitting of measured *V/M* with correlated part along with uncorrelated parts (n=2) of equation 5.8.

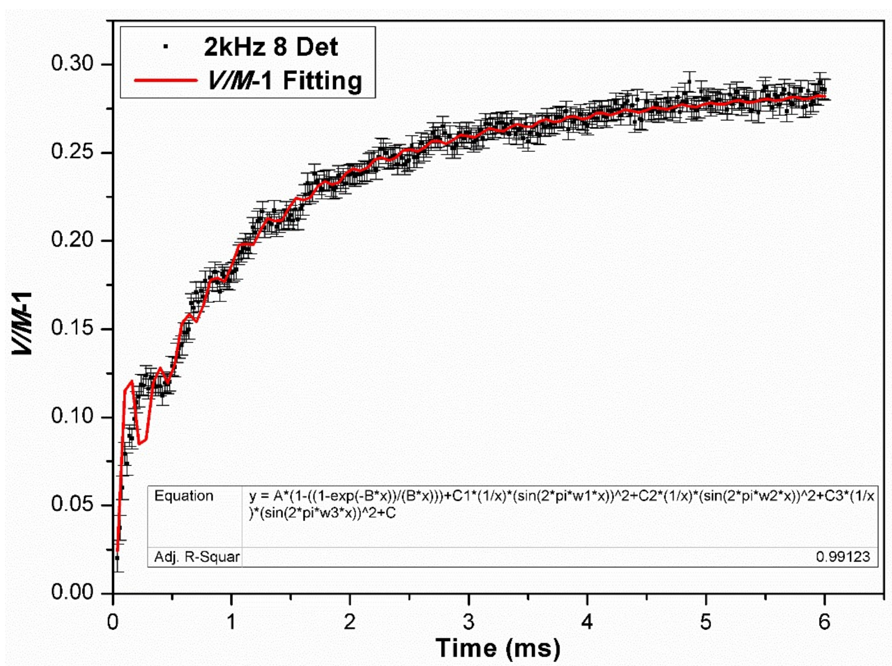

Figure 5.12. Fitting of measured *V/M* with correlated part along with uncorrelated parts (n=3) of equation 5.8.

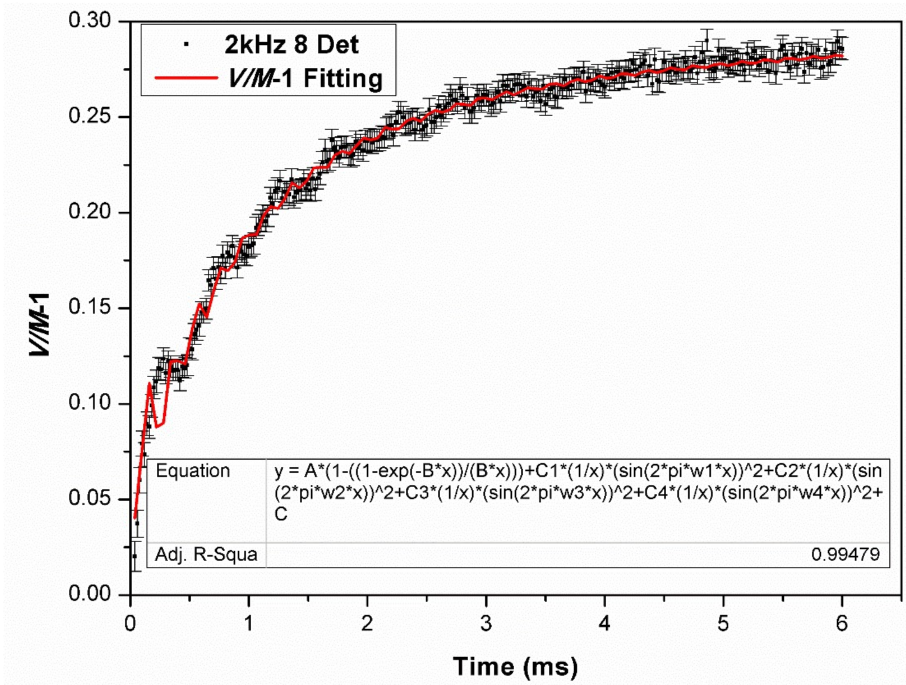

Figure 5.13. Fitting of measured *V/M* with correlated part along with uncorrelated parts (n=4) of equation 5.8.

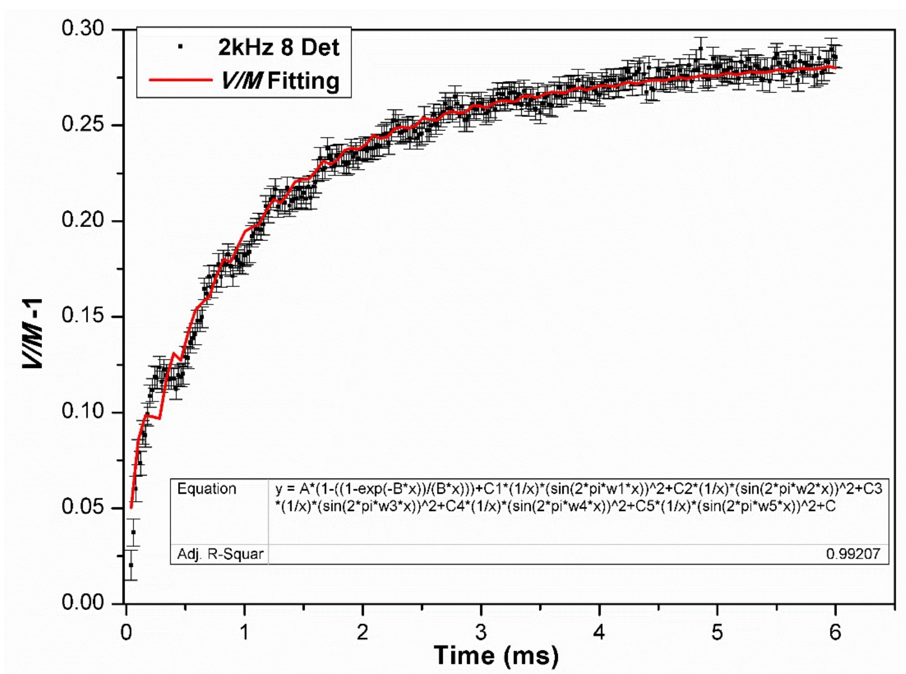

Figure 5.14. Fitting of measured *V/M* with correlated part along with uncorrelated parts (n=5) of equation 5.8.

Table 5.3. *The fitting parameters and Adj. R-Square value with number of terms in Fourier series during least square fitting.*

Sr. No.	Fitting Parameters	Number of terms in Fourier series (n)					
		0	1	2	3	4	5
1	A	0.25555 ±0.00184	0.24649 ±0.00303	0.28486 ±0.00576	0.288360 ±0.00522	0.28332 ±0.00365	0.27799 ±0.00501
2	B (ms^{-1})	1.79818 ±0.03770	1.92937 ±0.04761	2.05141 ±0.06712	2.15441 ±0.05914	2.34243 ±0.04305	2.19994 ±0.06124
3	C	0.05096 ±0.00207	0.06046 ±0.00342	0.01766 ±0.00623	0.01563 ±0.00562	0.02116 ±0.00396	0.02286 ±0.00537
4	C1	-	0.00282 ±0.00053	0.00861 ±0.00111	0.00980 ±0.00091	0.00730 ±0.00007	-0.00166 ±0.00076
5	C2	-	-	0.00400 ±0.00077	0.00162 ±0.00047	0.00895 ±0.00072	0.00656 ±0.00259
6	C3	-	-	-	0.00088 ±0.00065	0.00912 ±0.00004	0.00099 ±0.00009
7	C4	-	-	-	-	0.00012 ±0.00006	0.00010 ±0.00006
8	C5	-	-	-	-	-	0.00182 ±0.00271
9	w1 (Hz)	-	1998.02 ±1.28	2000.96 ±0.66	2099.11 ±0.50	2172.87 ±7.19	2086.87 ±4.19
10	w2 (Hz)	-	-	3998.56 ±1.73	3728.12 ±11.59	3523.98 ±0.94	3951.01 ±1.33
11	w3 (Hz)	-	-	-	6223.04 ±13.97	6613.58 ±12.58	5469.69 ±175.66
12	w4 (Hz)	-	-	-	-	8052.35 ±9.89	7634.87 ±197.62
13	w5 (Hz)	-	-	-	-	-	9122.40 ±107.75
14	Adj. R-Square	0.98178	0.98673	0.98682	0.99123	0.99479	0.99207

Furthermore, experimental data at accelerator frequencies 1.25 kHz, 1 kHz, 800 Hz, 250 Hz and 100 Hz have also been analysed using *V/M* method. Results have been discussed to address how does *V/M*-1 look at $f<\alpha$. The correlated amplitude (A) and the prompt neutron decay constant (B) have been mentioned in Figures 5.15-5.17 for further discussion. The amplitude (A) of correlated neutrons at different frequencies have been presented in Table 5.4. It has been observed that the correlated amplitude decreases with accelerator frequency although source strength has been maintained at the same level (10% duty cycle) throughout the experiments. This can be explained qualitatively by the time evolution of neutron population in subcritical core. After the source pulse, the neutron population will rise to a peak and then decay until the arrival of the next source pulse. For very high frequency ($f>>\alpha$), the decay may be negligible and the source may be considered as quasi continuous. Nevertheless, for low frequency, this assumption is inappropriate and the prompt neutron will die away before arrival of next pulse. As an example, the prompt neutron decay time ($1/\alpha$) in case of BRAHMMA is approximately 433 μs. So, in case of f=2 kHz, the time period is 500 μs, as a result, the correlation between neutron pulses will be less compared to high frequencies (10, 8 and 4 kHz). Similarly, for frequencies of 1 kHz or less, the correlation between prompt neutrons will decrease. Moreover, the amplitude of the uncorrelated higher order terms of Fourier series will increase with decreasing frequency as the uncorrelated amplitude is inversely proportional to $\omega_n^2(\omega_n^2+\alpha^2)$ (equation 5.8). As a result, the ratio of the correlated to the uncorrelated amplitude will decrease and least square fitting of the V/M-1 will demand higher order terms for fitting convergence of the experimental observation. The measured V/M-1 at different accelerator frequencies have been shown in Figure 5.15-5.17. It has been observed that the amplitude of the oscillation increases as the frequency decreases which is in good agreement with the theoretical assumption (equation 5.8) and the correlated amplitude decreases as presented in Table 5.4 (the star marked data have been taken from Table 4.4). Furthermore, V/M-1 at accelerator frequencies 250 Hz and 100 Hz have been shown in Figure 5.18 and the inset of Figure 5.18 (in Log scale) shows that the oscillation is higher and the correlated amplitude of V/M-1 decreases at 100 Hz.

However, the present study discusses the noise experiments under mode cancellation of prompt neutrons only and delayed neutrons have not been considered during theoretical development (Degweker & Rana, 2007) and system modal analysis (Kumar et al., 2017). Since, for f=250 Hz and 100 Hz the V/M saturates at higher gate width, the contribution from delayed neutrons needs to be considered and this is a subject of future study.

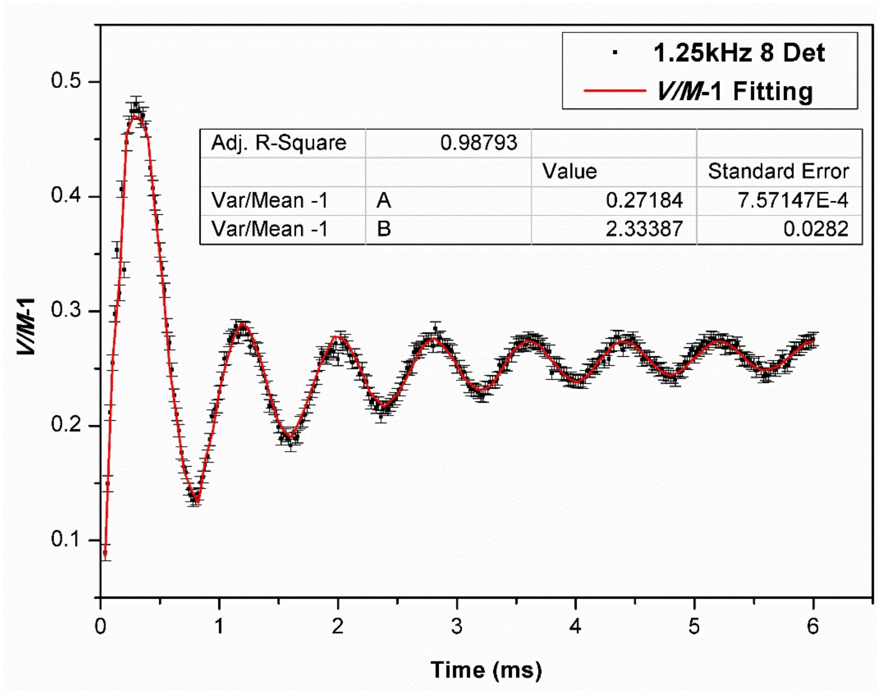

Figure 5.15. V/M-1 plot at accelerator frequency 1.25 kHz.

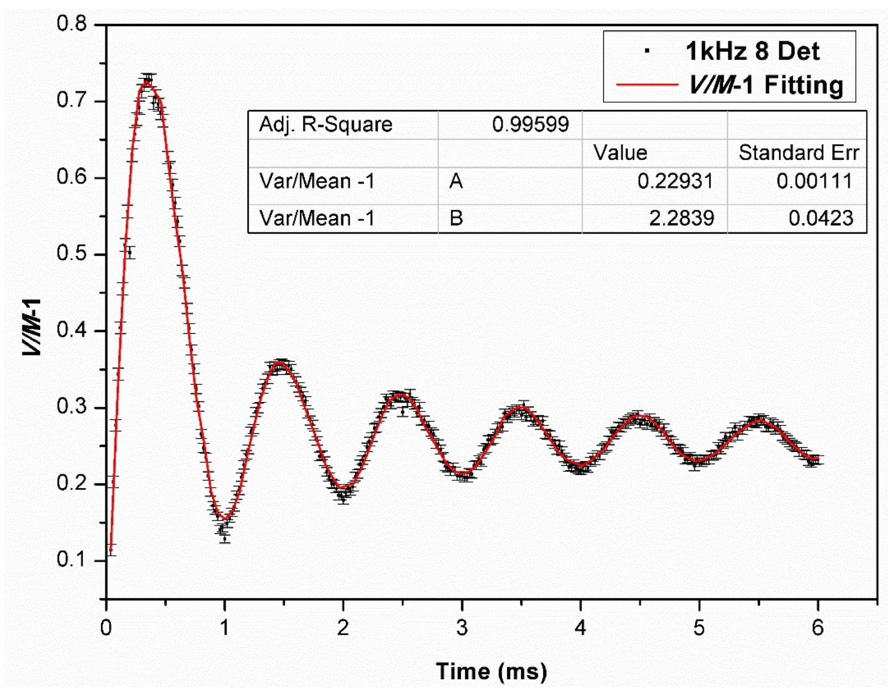

Figure 5.16. V/M-1 plot at accelerator frequency 1 kHz.

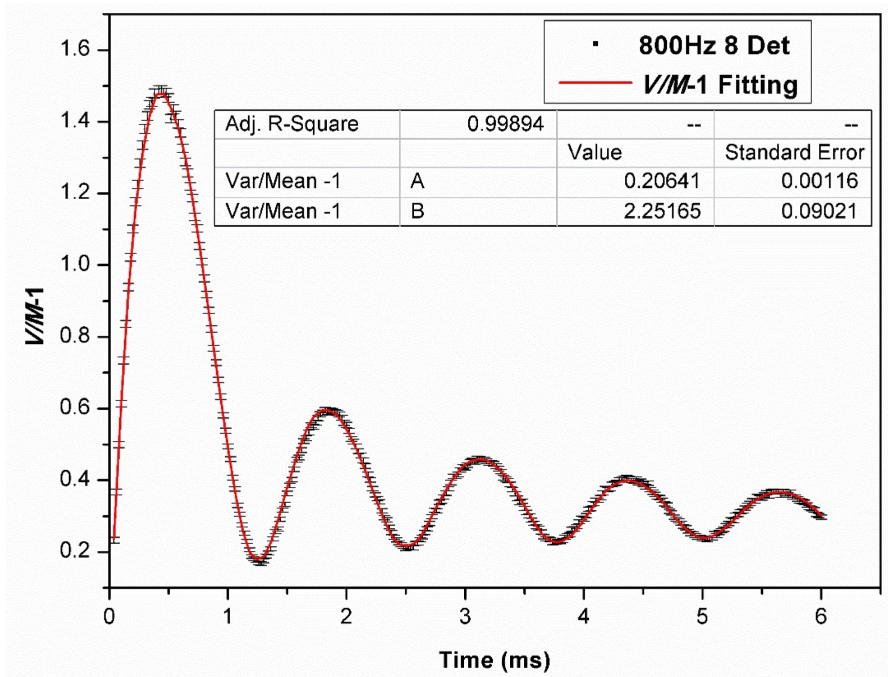

Figure 5.17. V/M-1 plot at accelerator frequency 800 Hz.

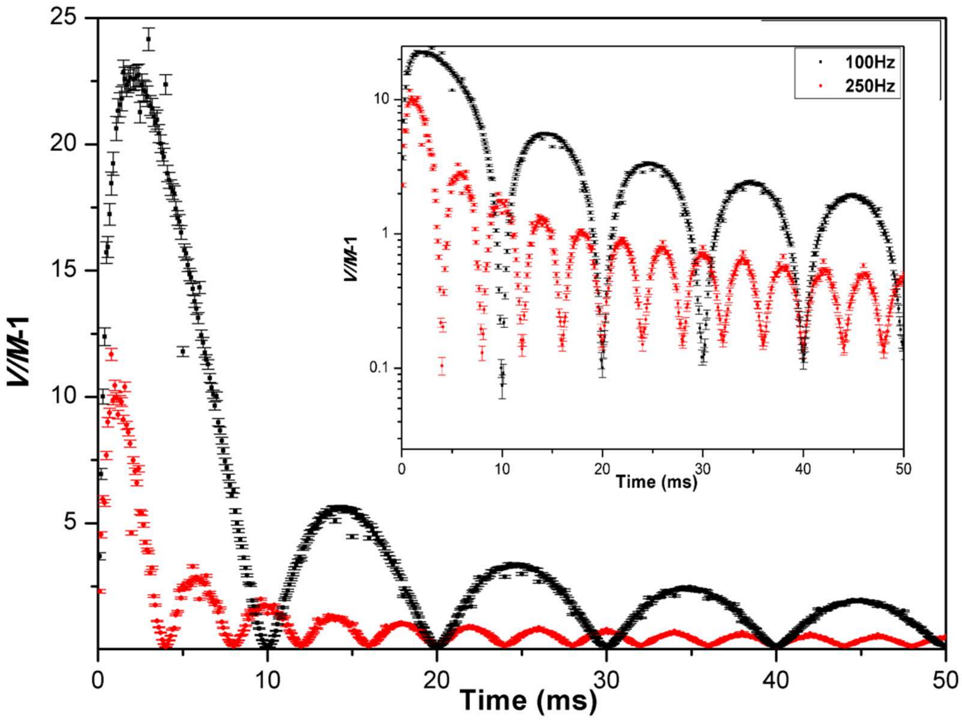

Figure 5.18. V/M-1 plot at accelerator frequencies 250 Hz and 100 Hz (inset in Log scale).

Table 5.4. *Variation of correlated amplitude (A) with accelerator frequency in V/M.*

Sr. No.	Accelerator frequency (kHz)	Correlated amplitude (A)
1	10.00*	0.37763±0.00203
2	8.00*	0.32022±0.00125
3	4.00*	0.29215±0.00135
4	2.00	0.28332±0.00365
5	1.25	0.27184±0.00076
6	1.00	0.22931±0.00111
7	0.80	0.20641±0.00116

In the next step, time stamped data have been analysed using *ACV* method and prompt neutron decay constant has been obtained by fitting the measured *ACV* with equation 5.6. The behaviour of *ACV* along with its correlated and uncorrelated part have been shown in Figure 5.19 for f=10, 8 and 4 kHz. In Figure 5.19, it can be seen that at f=10 kHz, the correlated part of the measured *ACV* after 1 ms is small due to the die away of correlated neutron chain and contains constant uncorrelated part only. Also, the oscillation of the uncorrelated part increases as f decreases. On the other hand, for *V/M-1*, oscillation starts at 2 kHz and increases for lower frequencies. This can be explained qualitatively with the help of equations 5.6 and 5.8. In case of *V/M* and *ACV,* the uncorrelated part is proportional to $\sin^2(\omega_n T/2)$ and $\cos(\omega_n T)$ respectively. The cosine function has higher oscillation compared to $\sin^2$ function and there is a damping factor which is proportional to *1/T* in case of *V/M*. The measured *ACV* at different accelerator frequencies (4 kHz-800 Hz) have been shown in Figures 5.20-5.24. Iterative method, as discussed in case of *V/M*, has been followed to fit the measured *ACV* with equation 5.6. Similar to *V/M* method, the uncorrelated oscillation enhances with lower accelerator frequency as shown in Figures 5.20-5.24 and number of higher order terms of Fourier series increases for accurate fitting of the measured *ACV*.

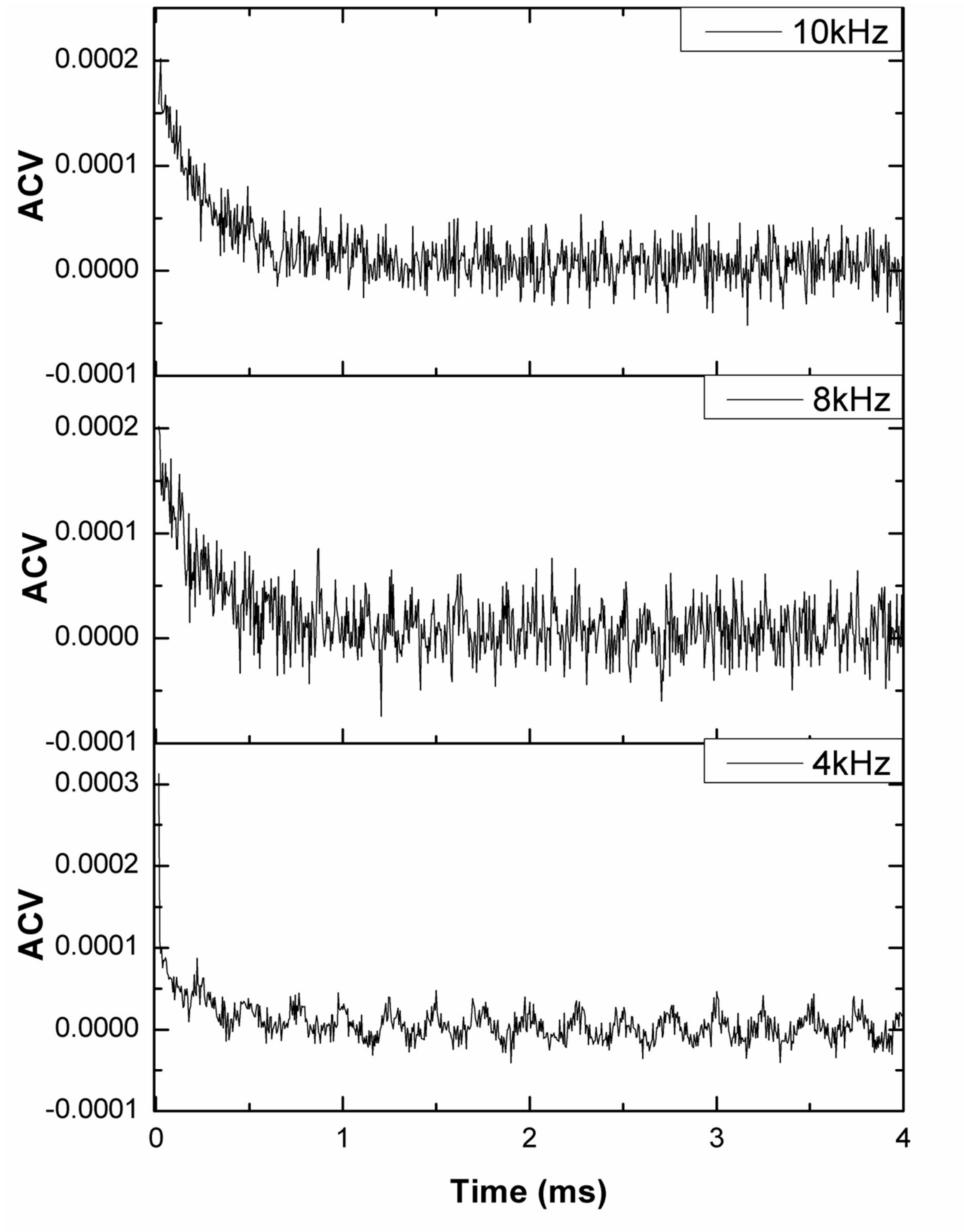

Figure 5.19. Variation of measured *ACV* with accelerator frequency (10, 8 and 4 kHz).

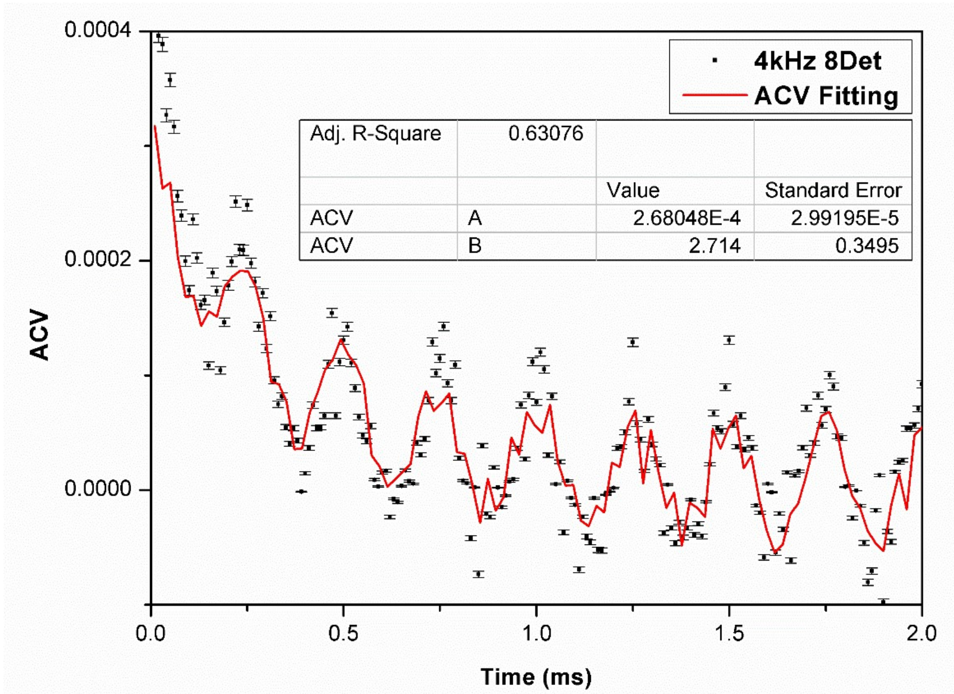

Figure 5.20. ACV plot at accelerator frequency 4 kHz.

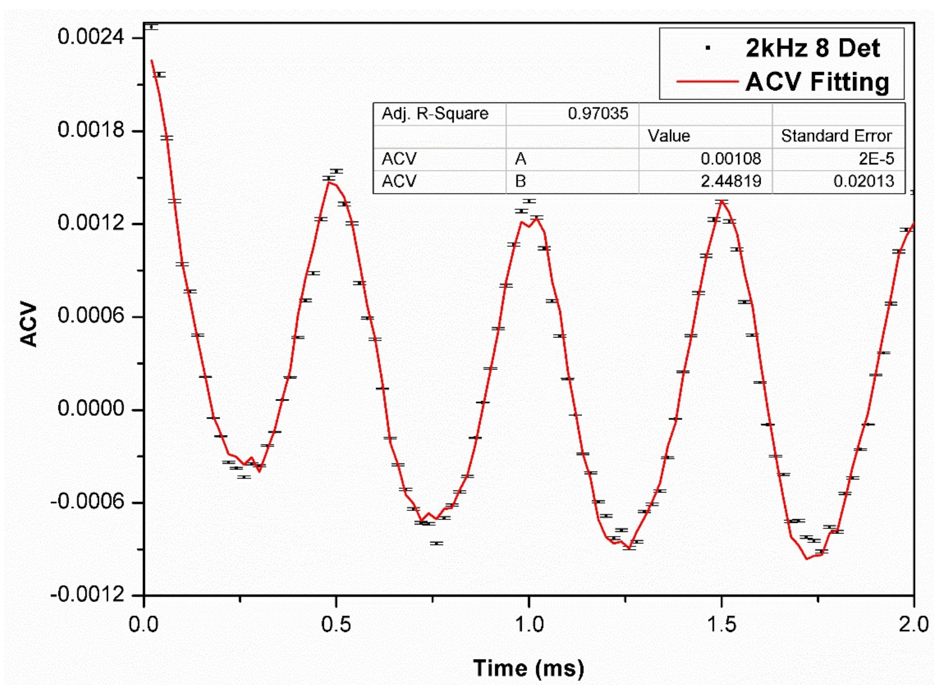

Figure 5.21. ACV plot at accelerator frequency 2 kHz.

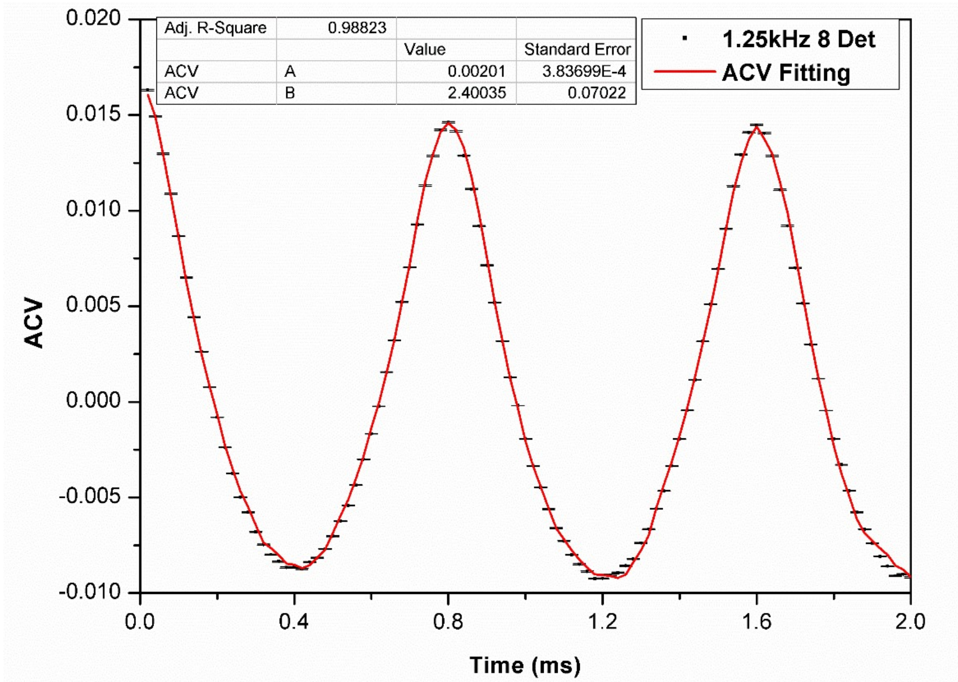

Figure 5.22. ACV plot at accelerator frequency 1.25 kHz.

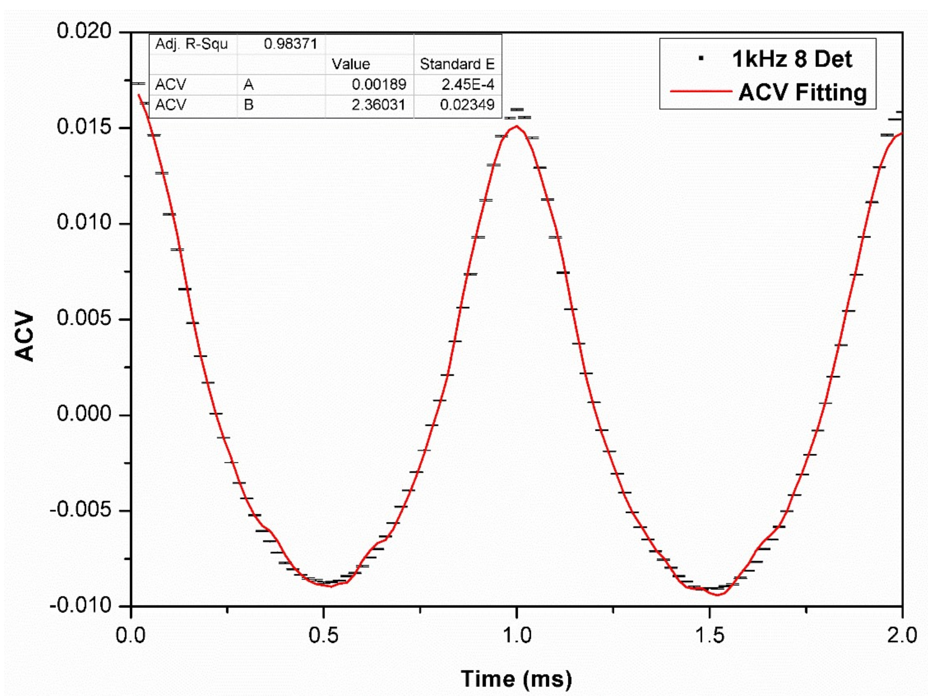

Figure 5.23. ACV plot at accelerator frequency 1 kHz.

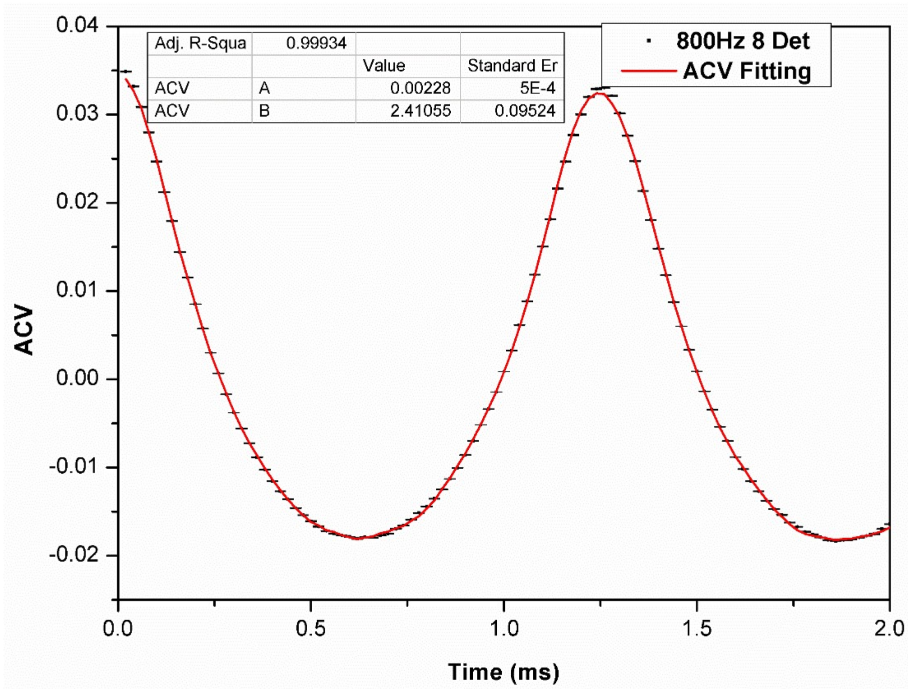

Figure 5.24. ACV plot at accelerator frequency 800 Hz.

Finally, the frequency distribution of the measured reactor noise has been obtained from the Fourier transform of measured *ACV* and the measured *APSD* at different frequencies (2 kHz-100 Hz) have been shown in Figures 5.25-5.30. The measured *APSD* shows peak at integer multiple of source frequency. Theoretically speaking, peaks are Dirac-delta function and amplitude is inversely proportional to $1/(\omega_n^2+\alpha^2)$, which represents the uncorrelated oscillation of *ACV*. Data points correspond to delta function have been masked and the first and third term of equation 5.9 have been used for fitting of *APSD*. The prompt neutron decay constant has been estimated by least square fitting of the rest of the data points. The prompt neutron decay constant measured by different noise methods has been presented in Table 5.5.

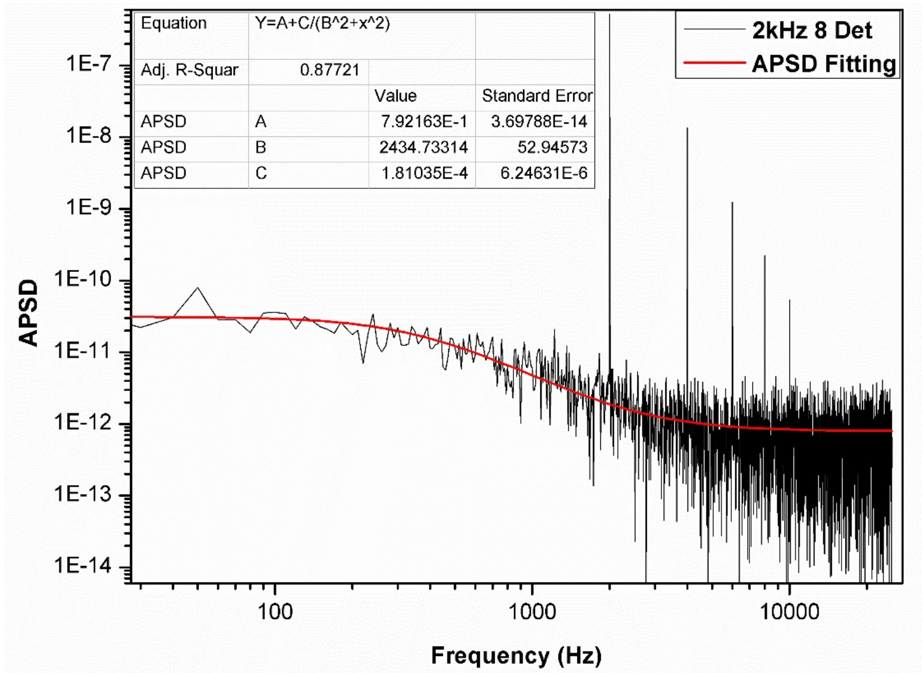

Figure 5.25. APSD plot at accelerator frequency 2 kHz.

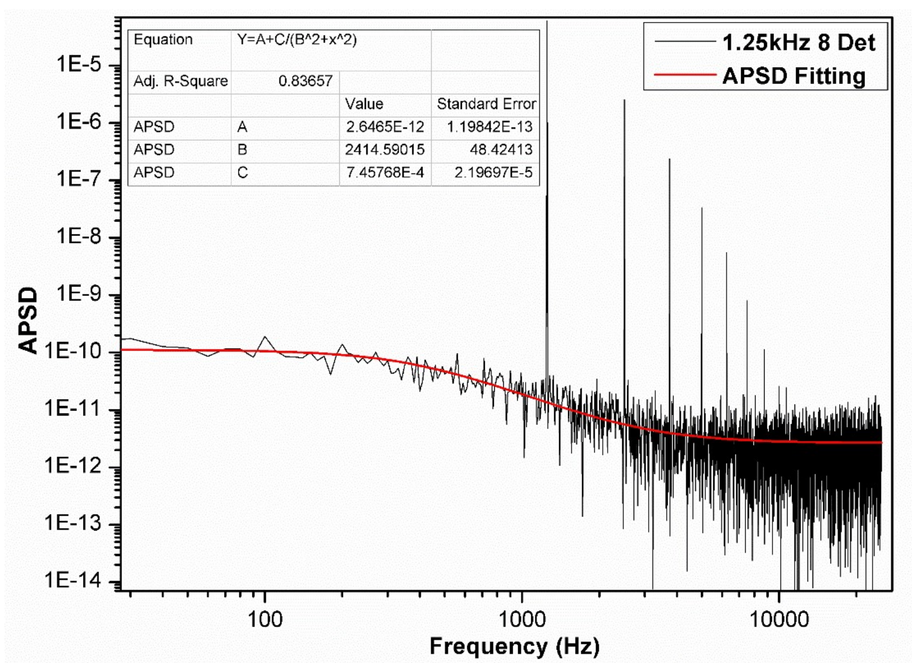

Figure 5.26. APSD plot at accelerator frequency 1.25 kHz.

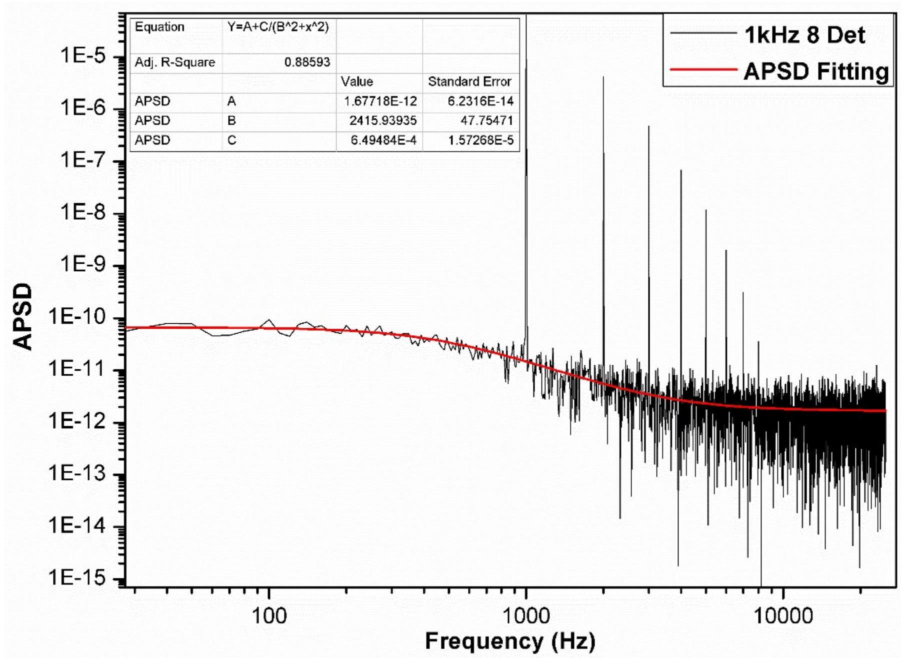

Figure 5.27. APSD plot at accelerator frequency 1 kHz.

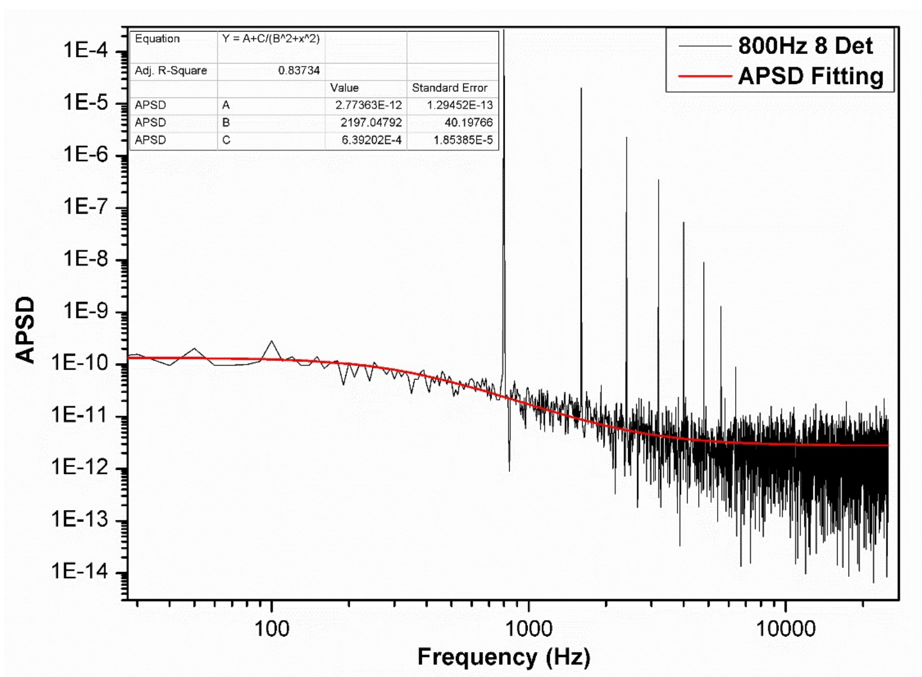

Figure 5.28. APSD plot at accelerator frequency 800 Hz.

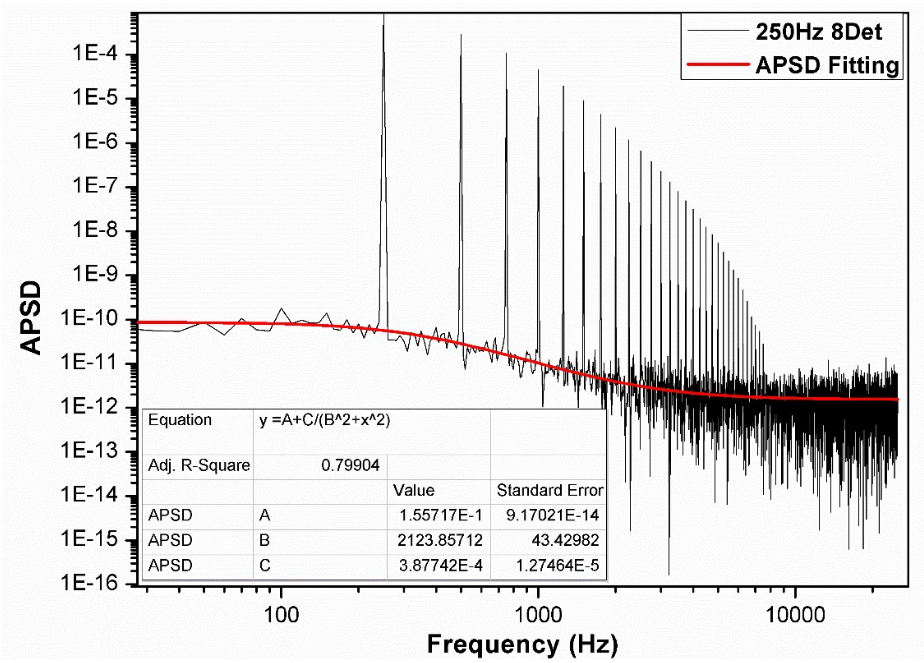

Figure 5.29. APSD plot at accelerator frequency 250 Hz.

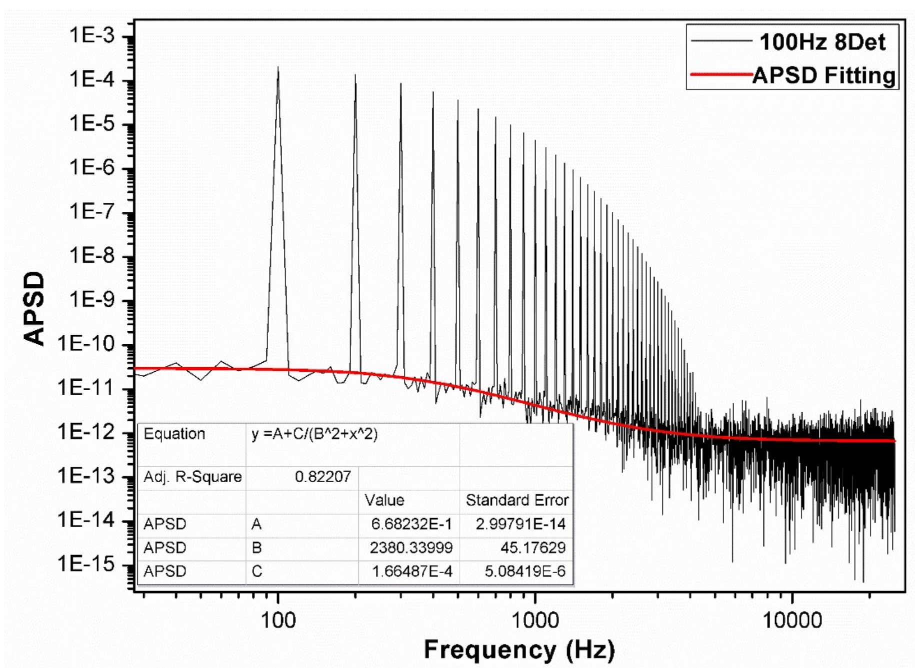

Figure 5.30. APSD plot at accelerator frequency 100 Hz.

Table 5.5. *Prompt neutron decay constant measured using different noise methods.*

Sr. No.	Accelerator frequency (kHz)	*V/M*		*ACV*		*APSD*	
		α (ms^{-1})	Adj. R-Square	α (ms^{-1})	Adj. R-Square	α(s^{-1})	Adj. R-Square
1	4.00	-	-	2.71400 ±0.34950	0.63076	-	-
2	2.00	2.34243 ±0.04305	0.99479	2.44819 ±0.02013	0.97035	2434.7 ±52.9	0.87721
3	1.25	2.33387 ±0.02820	0.98793	2.40035 ±0.07022	0.98823	2414.6 ±48.4	0.83657
4	1.00	2.28390 ±0.04230	0.99599	2.36031 ±0.02349	0.98371	2415.9 ±47.8	0.88593
5	0.80	2.25165 ±0.09021	0.99894	2.41055 ±0.09524	0.99934	2197.1 ±40.2	0.83734
6	0.25	-	-	-	-	2123.9 ±43.4	0.79904
7	0.10	-	-	-	-	2380.3 ±45.2	0.82207

The measured prompt neutron decay constant using the noise theory developed under consideration of exponentially correlated Gaussian source character along with finite pulse width are close to the theoretical value (2.310 ms^{-1}). However, in case of 4 kHz, the measured prompt neutron decay constant using *ACV* has large variation compared with the theoretical estimate and the Adj. R-Square value is 0.63076. The measured *ACV* has random oscillation and it was difficult to fit with the analytical equation as shown in Figure 5.20. This may be attributed to change in the correlation property of neutrons when *1/f* approaches *1/α* and this is a subject of future study.

CHAPTER SIX

DEVELOPEMNT OF AN ADVANCED TIME STAMP DATA ACQUISITION SYSTEM FOR FURTHER NOISE EXPERIMENTS

6.1 Introduction

Time stamp data acquisition system is an indispensable component for carrying out noise experiments. Noise experiments presented in previous chapters have been carried out using the time stamp data acquisition system developed by Kumar et al. (2015) using NI6602 time stamp card and VISUAL BASIC. The development of the data acquisition system has configured only one channel for time stamp. The data can be stored using dynamic memory allocation and the data acquisition system has capability to acquire a maximum sample length of 10 million. The programme estimates array size depending on the input event rate and acquisition time specified by user. At the end of the acquisition, the data acquired in buffer is stored in a file. The data file consists of two columns. The first column consists of sequence of detection events and the second column consists the corresponding detection time in μs. The present data acquisition system has been very useful for noise experiments in our subcritical system.

However, some limitations have been experienced during noise experiments using this time stamp data acquisition system. These are as follows:

1. **Limitation of sample length**

   The maximum sample length of 10 million was a major technical limitation during noise experiments in BRAHMMA using PNG. As discussed in section 2.3.2.1, the time duration of measurement should be high compared to the characteristics time of the system and number of samples should also be large for any statistical analysis. On the other hand, higher yield of D-T reaction and detectors with higher sensitivity used during the noise experiments are the constraints for longer data acquisition duration. Therefore, during noise experiments, the PNG has been operated at lower operating parameters (HV: 80 kV, Current: 60 μA) to acquire data for longer time.

2. Number of inputs for time stamp

The data acquisition system which has been used during noise experiments had configured only one channel for time stamp, whereas, it can access maximum three channels in Direct Memory Access (DMA) mode for acquisition. Therefore, time stamp data in different detector configuration, for example, 8DET, 4F DET and 4B DET can be acquired simultaneously by further development.

3. Mode of acquisition

The present data acquisition system has software start only and the start of the acquisition is in asynchronous mode with PNG. Thus, the present research work has been carried out in asynchronous mode only. However, the NI6602 has the capability to start the acquisition with external trigger, for example, with trigger pulse from PNG.

4. Real time visualisation of source strength stability

As discussed in section 2.3.2.2, the noise theory is based on "Ergodic hypothesis", which states that in steady state, the ensemble average and time average are same. Thus, during noise experiments the external neutron source should be stable as much as possible, to avoid any fluctuation of neutron population in subcritical system. However, the data acquisition system developed by Kumar et al. (2015) has no scope for real time assessment of source stability. The stability of the source has been assessed using another MCS or during data analysis by conversion of time stamped data in CPS.

Hence, all the above-mentioned facts pave the way to develop an advanced time stamp data acquisition system to overcome the shortfalls faced during noise experiments in BRAHMMA subcritical system.

6.2 Description of NI6602 Time Stamp Data Acquisition System

Based on the above-mentioned shortfalls, an advanced time stamp data acquisition system has been developed using NI6602 time stamp system, which consists of a Peripheral Component Interconnect (PCI) card, a BNC connector box as shown in Figures 6.1 and 6.2. The PCI card and connector box are connected by a 68-channel shielded cable. The salient features of the NI6602 are as follows:

Figure 6.1. NI6602 PCI card (National Instruments).

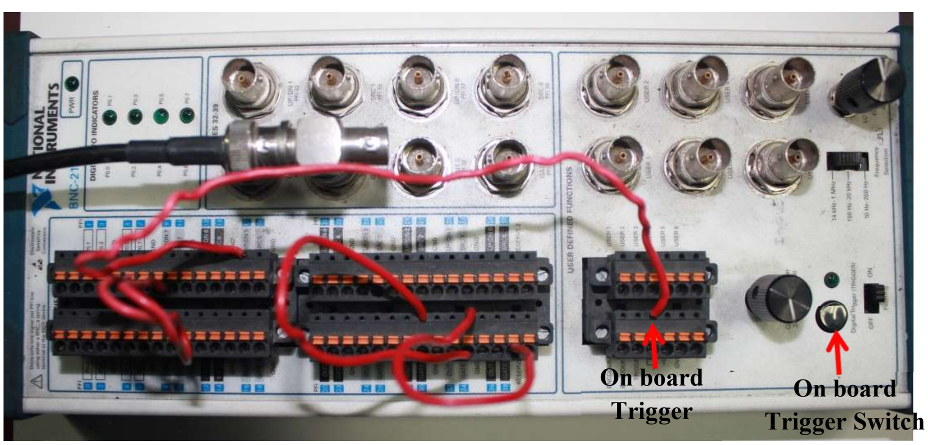

Figure 6.2. BNC connector box for I/O.

- **Compatibility**: The NI6602 is compatible with TTL or CMOS logic.
- **Number of channels**: The NI6602 has total 32 digital I/O channels and out of 32 channels, 8 channels are dedicated for timing I/O. It has 7 trigger lines, one Real Time System Integration (RTSI) clock, 8 programmable pulse train generator and filter I/O. The card can access maximum 3 channels in DMA mode.
- **Sampling frequency**: The card uses sampling frequency of 80 MHz for time stamp. According to Nyquist–Shannon sampling theorem, the sampling frequency should be twice of maximum sample frequency. Therefore, the card can be safely used up to 40 MHz input frequency and the corresponding time resolution is 25 ns.

6.3 User Interface

The NI6602 PCI card has options for programming using C, VISUAL BASIC and LabVIEW. Kumar et al. (2015) had used VISUAL BASIC for programming the time stamp card. Whereas, present development has been carried out using LabVIEW student edition 32 bit and NI-DAQ driver package (National Instruments, 2019). NI6602 can transfer data for maximum three channels in DMA mode. So, during the present development, three timing inputs (GATE0, GATE1 and GATE2) have been used for data acquisition. GATE0 has been defined for real time visualisation of the source strength stability as discussed in section 6.1. GATE1 and GATE2 have been defined for time stamp acquisition. The Graphical User Interface (GUI) of the developed time stamp Data Acquisition (DAQ) system has been shown in Figure 6.3. User needs to define 'File Path' and 'File name' before starting the acquisition. The present DAQ has options of 'ON' and 'OFF' for GATE1 (Cntr1) and GATE2 (Cntr2) during acquisition. The graphics on the right-hand side in Figure 6.3 is for visualisation of the CPS plot and the box bellow the graphics shows the current CPS value. The programme requires the 'Data Size' in million to be collected during acquisition as shown in Figure 6.3. 'Cntr1' and 'Cntr2' shows the number of data collected during acquisition. 'Initiated' indicates the arrival of the trigger pulse and start of the acquisition. 'Elapsed Time' indicates total acquisition time. The PFI19 has been defined for trigger input, whereas, PFI12 has been used for sample clock for CPS and connected with PFI11. During noise experiments in synchronous mode, the trigger pulse is to be connected to PFI19. On the other hand, during noise experiments in asynchronous mode, the on-board trigger as shown in Figure 6.2 is to be connected with PFI19.

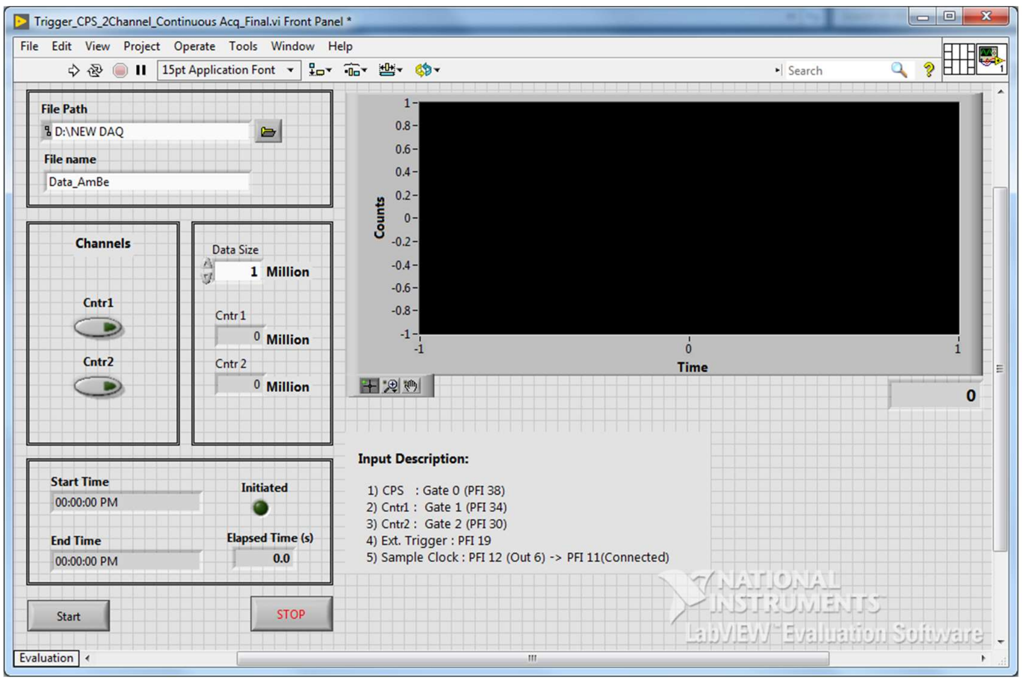

Figure 6.3. GUI for time stamp DAQ.

The LabVIEW programme stores the data at pre-defined file path location on arrival of each 1 million data. As an example, for 50 million data 50 data files will be generated, which makes the data management easier as per requirement. The DAQ stores period interval of the input events which has been presented in Table 6.1. The first and second column represents the date and time of experiment whereas the third column represents the period in second. The programme measures the number of source clock between two consecutive rising edges of GATE input and corresponding period (P1) as shown in Figure 6.4.

Table 6.1. *Representation of acquired data using Am-Be neutron source.*

AmBe TS1.txt - Notepad

File Edit Format View Help

04-12-2019	19:06:59	0.000300437500
04-12-2019	19:06:59	0.000070937500
04-12-2019	19:06:59	0.000126175000
04-12-2019	19:06:59	0.001710212500
04-12-2019	19:06:59	0.001431600000
04-12-2019	19:06:59	0.000269025000
04-12-2019	19:06:59	0.000130312500
04-12-2019	19:06:59	0.000143787500
04-12-2019	19:06:59	0.000722862500
04-12-2019	19:06:59	0.001442912500
04-12-2019	19:06:59	0.000524562500
04-12-2019	19:06:59	0.001736125000
04-12-2019	19:06:59	0.000155587500
04-12-2019	19:06:59	0.000465675000
04-12-2019	19:06:59	0.002982462500
04-12-2019	19:06:59	0.000740250000
04-12-2019	19:06:59	0.000759000000
04-12-2019	19:06:59	0.001207687500
04-12-2019	19:06:59	0.000051437500
04-12-2019	19:06:59	0.002968462500
04-12-2019	19:06:59	0.002531187500
04-12-2019	19:06:59	0.002608387500
04-12-2019	19:06:59	0.000753537500
04-12-2019	19:06:59	0.002824350000
04-12-2019	19:06:59	0.000768925000
04-12-2019	19:06:59	0.000837162500
04-12-2019	19:06:59	0.003152362500
04-12-2019	19:06:59	0.001940012500
04-12-2019	19:06:59	0.000546450000
04-12-2019	19:06:59	0.003921712500
04-12-2019	19:06:59	0.000583875000
04-12-2019	19:06:59	0.001767262500
04-12-2019	19:06:59	0.001408037500
04-12-2019	19:06:59	0.000966375000
04-12-2019	19:06:59	0.000448337500
04-12-2019	19:06:59	0.001990800000
04-12-2019	19:06:59	0.003746887500
04-12-2019	19:06:59	0.000800425000
04-12-2019	19:06:59	0.000853975000
04-12-2019	19:06:59	0.004470525000
04-12-2019	19:06:59	0.001467187500

Therefore, the data file will represent the periodicity of consecutive neutron detections, whereas, the first period indicates the time interval between trigger and first event.

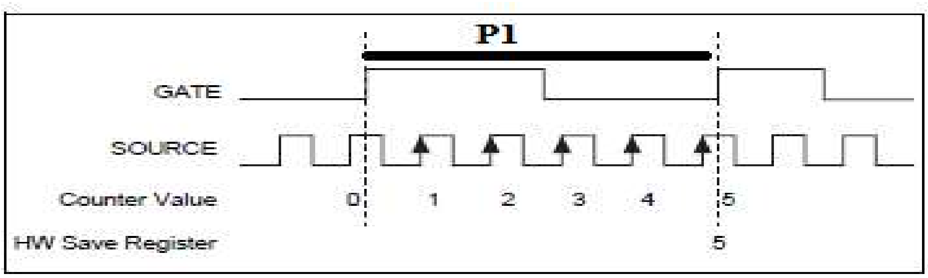

Figure 6.4. Schematic representation of period measurement (National Instruments).

6.4 Validation Experiments for DAQ

The performance of newly developed time stamp data acquisition system has been tested with pulse generator and isotopic neutron source. Initial testing for periodicity measurement, external trigger and data archiving have been performed with pulse generator. Furthermore, it is important to ensure that there is no loss of data during data archiving. This has been tested with pulse generator with predefined N million events at frequency of 1 MHz. It has been observed that the total number of events registered in multiple files is exactly same as the input events (N million) and there is no loss of data during data transfer and archive.

In the next step, the time stamp data acquisition has been tested with ^{3}He detector (Active length: 50 cm, Diameter: 2.5 cm, Sensitivity: 65 cps/nv), Preamplifier (MRS200) and Am-Be neutron source (30 mCi). Time stamped data have been analysed using *V/M* and *ACV* methods as discussed in sections 2.3.2.1 and 2.3.2.2 respectively. The measured *ACV* and *V/M* for Am-Be neutron source have been shown in Figure 6.5. The measured *V/M*-1 is close to zero and independent of gate width as expected for Poisson source characteristics. For isotopic source, the measured *ACV* is random and uncorrelated. Therefore, the measured *V/M* and *ACV* agree with Poisson characteristics of isotopic neutron source. Hence, the newly developed time stamp data acquisition system performs pleasantly.

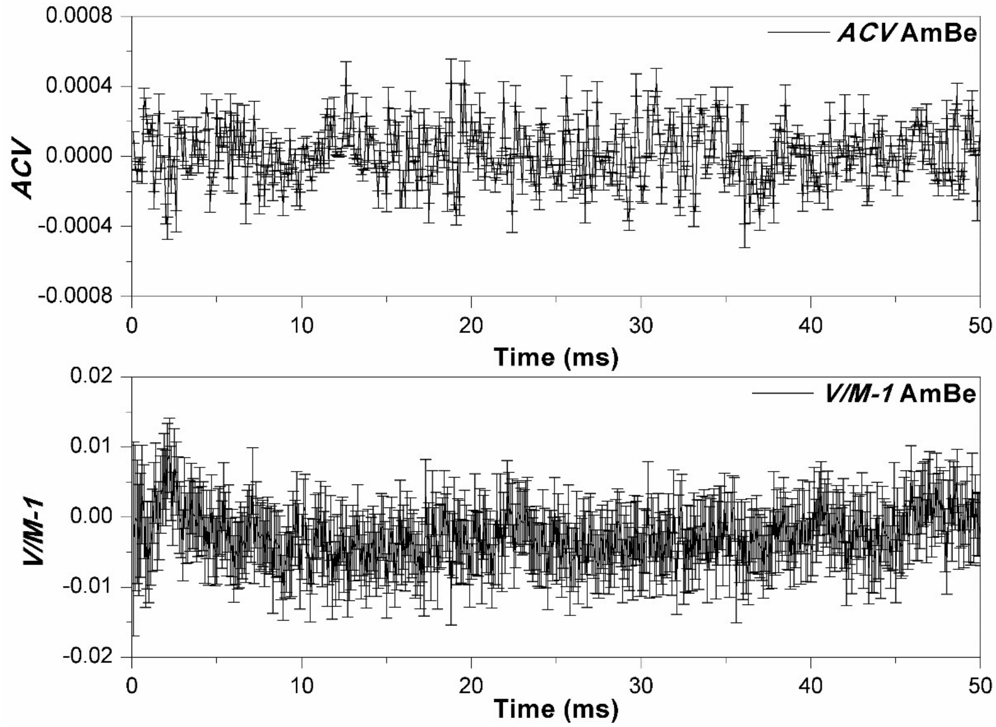

Figure 6.5. ACV and *V/M*-1 plot for Am-Be neutron source measured with newly developed time stamp data acquisition system.

6.5 Testing with Neutron Generator

The newly developed time stamp data acquisition system has also been tested with D-D and D-T neutron generator (PNG). During the testing of DAQ with PNG, the ^{3}He detector has been placed at a distance of 10 cm from the beam target. The detector has been encapsulated by HDPe followed by Cadmium. HDPe has been used to thermalise the fast neutron and Cadmium to stop the streaming of scattered neutrons inside detector. In D-D mode neutron generator has been operated at acceleration voltage of 200 KV and beam current of 200 μA. Time stamped data have been converted in CPS and shown in Figure 6.6. Whereas, in case of D-T mode neutron generator has been operated at 100 kV and 100 μA and the corresponding CPS plot has been shown in Figure 6.7. The newly developed time stamp data acquisition system performs pleasantly with D-D and D-T neutrons.

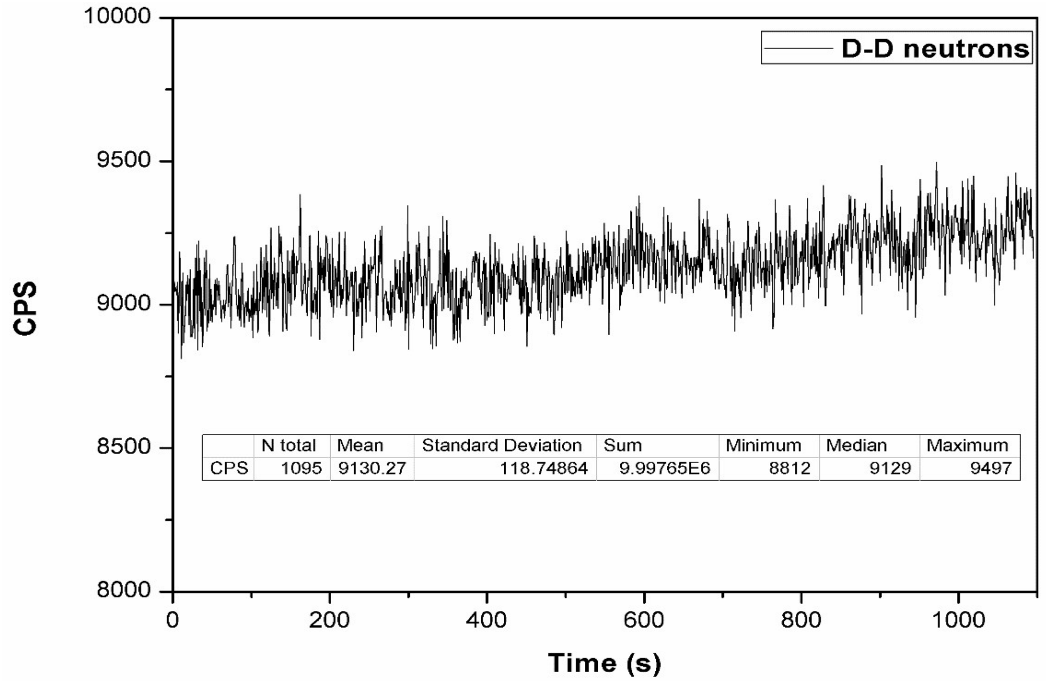

Figure 6.6. CPS plot of D-D neutrons calculated using time stamp data.

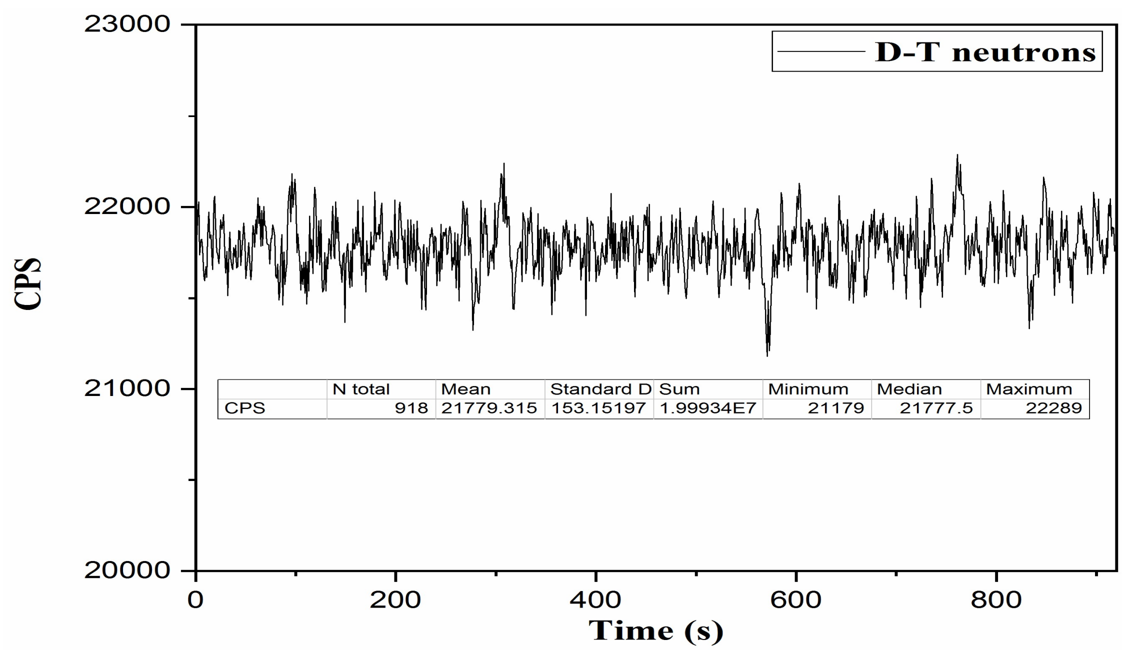

Figure 6.7. CPS plot of D-T neutrons calculated using time stamp data.

Thesis Highlight

Name of the Student: Nirmal Kumar Ray

Name of the CI: Bhabha Atomic Research Centre   Enrolment No.: PHYS01201604021

Thesis Title: Reactivity Measurement Using Deterministic and Noise Methods in BRAHMMA Subcritical System

Discipline: Physical Sciences   Sub-Area of Discipline: Accelerator Driven Subcritical system

Date of viva voce: March 03, 2021

Accelerator Driven Subcritical (ADS) system has the potential for future power production based on reserved Thorium in India. In such system, power can be maximised for a certain accelerator beam power by reducing the subcriticality. Although, the reactor core will be subcritical, still there is a chance of criticality due to accumulation of ^{233}U as a result of breeding. Therefore, reactivity measurement is essential for commercial, control and safety purpose.

The study has focused on reactivity measurement in a deep subcritical system namely, **B**eO **R**eflected **A**nd **H**DPe **M**oderated **M**ultiplying **A**ssembly (BRAHMMA), commissioned in Bhabha Atomic Research Centre, India. Initially, reactivity measurement experiments have been carried out using deterministic methods, for example, Area-ratio, Slope-fit and Source-jerk based on the perturbation of external D-T neutron source. But, deterministic methods are not suitable for reactivity measurement during continuous operation of ADS due to thermal recycle of the core and power fluctuation. On the other hand, noise methods based on correlation technique are robust and useful for reactivity measurement during continuous operation of ADS. In this context, a noise theory assuming the accelerator-based neutron source as exponentially correlated Gaussian character had been developed by Degweker and Rana (2007) for reactivity measurement in ADS. First-ever experimental validation of this noise theory has been carried out using D-T neutron generator and BRAHMMA subcritical system. As a part of validation experiments, a methodology has been developed to study the statistical properties of accelerator-based neutron source for noise experiments. Then validation experiments have been carried out for different pulse shape using various noise descriptors, for example, Feynman-alpha, Auto Covariance and Auto Power Spectral Density. The measured prompt neutron decay constant of the subcritical system are in good agreement with the theoretical estimate. Furthermore, variations of noise descriptors with accelerator parameter(s) have also been studied for a fixed subcriticality. Based on his research output, the ADS community will certainly be benefited in carrying out reactivity measurement using noise methods using accelerator based non-Poisson neutron source.

Time stamp data acquisition system is essential to conduct noise experiments as noise descriptors are based on the time signature of neutron detection. The time stamp data acquisition system used in the present study had some limitations, such as single input for time stamp, maximum sample of 10 million and asynchronous mode only. Hence, an advanced time stamp data acquisition system has been developed with incorporation of more features, such as three input channels, trigger input, data archiving for high sample length and real-time visualisation of source stability for further noise experiments.

References

Abbondanno, U. et al. (2002). Neutron capture measurements at the CERN-nTOF facility for ADS applications. *http://dababneh.com/Articles/csgs11_proc_FG.pdf.*

Abderrahim, H. A., Baeten, P., De Bruyn, D., & Fernandez, R. (2012). MYRRHA–A multi-purpose fast spectrum research reactor. Energy conversion and management, 63, 4-10.

Andriamonje, S., Angelopoulos, A., Apostolakis, A., Attale, F., Brillard, L., Buono, S., ... & Charalambous, S. (1995). Experimental determination of the energy generated in nuclear cascades by a high energy beam. Physics Letters B, 348(3-4), 697-709.

Arnould, H., Bompas, C. A., Del Moral, R., Lacoste, V., Vlachoudis, V., Aleixandre, J., ... & Andriamonje, S. (1999). Experimental verification of neutron phenomenology in lead and transmutation by adiabatic resonance crossing in accelerator driven systems. Physics Letters B, 458(2-3), 167-180.

Bajpai, S., Roy, T., Ray, N., Kashyap, Y., Shukla, M., Patel, T., & Sinha, A. (2015). Evaluation of spatial correction factors for BRAHMMA subcritical assembly. *Nuclear Science and Engineering*, *181*(3), 361-367.

Ballester, D., and Muñoz-Cobo, J. L. (2005). Feynman-Y function for a subcritical assembly with intrinsic spontaneous fissions driven by external pulsed sources. Annals of Nuclear Energy, 32(5), 493-519.

Ballester, D., and Muñoz-Cobo, J. L. (2006). The pulsing CPSD method for subcritical assemblies driven by spontaneous and pulsed sources. Annals of Nuclear Energy, 33(3), 281-288.

Ballester, D., Muñoz-Cobo, J. L., and Kloosterman, J. L. (2005). On the applicability of the pulsing Feynman-α method: Validation with MUSE experiments. Annals of Nuclear Energy, 32(13), 1476-1494.

Bécares, V., Villamarín, D., Fernández-Ordóñez, M., Gonzalez-Romero, E. M., Berglöf, C., Bournos, V., ... & Serafimovich, I. (2013). Validation of ADS reactivity monitoring techniques in the Yalina-Booster subcritical assembly. Annals of Nuclear Energy, 53, 331-341.

Bell, G. I., & Glasstone, S. (1970). *Nuclear reactor theory* (No. TID-25606). US Atomic Energy Commission, Washington, DC (United States).

Berglöf, C., Fernández-Ordóñez, M., Villamarín, D., Bécares, V., González-Romero, E. M., Bournos, V., ... & Fokov, Y. (2010). Spatial and source multiplication effects on the area ratio reactivity determination method in a strongly heterogeneous subcritical system. Nuclear science and engineering, 166(2), 134-144.

Berglöf, C., Fernández-Ordóñez, M., Villamarín, D., Bécares, V., González-Romero, E. M., Bournos, V., & Muñoz-Cobo, J. L. (2011). Auto-correlation and variance-to-mean measurements in a subcritical core obeying multiple alpha-modes. Annals of Nuclear Energy, 38(2-3), 194-202.

Bergoz Instrumentation, ACCT. Retrieved from: http://www.bergoz.com/en/acct?=6.

Bharatiya Nabhikiya Vidyut Nigam Limited (BHAVINI). Project, About us. Retrieved from: http://www.bhavini.nic.in/Userpages/CompanyView.aspx.

Billebaud, A., Brissot, R., Le Brun, C., Liatard, E., & Vollaire, J. (2007). Prompt multiplication factor measurements in subcritical systems: From MUSE experiment to a demonstration ADS. Progress in Nuclear Energy, 49(2), 142-160.

Bowman, C. D. (1998). Accelerator-driven systems for nuclear waste transmutation. Annual Review of Nuclear and Particle Science, 48(1), 505-556.

Bowman, C. D. (2000). Once-through thermal-spectrum accelerator-driven light water reactor waste destruction without reprocessing. *Nuclear Technology*, *132*(1), 66-93.

Bowman, C. D., Arthur, E. D., Lisowski, P. W., Lawrence, G. P., Jensen, R. J., Anderson, J. L., ... & Engel, L. N. (1992). Nuclear energy generation and waste transmutation using an accelerator-driven intense thermal neutron source. *Nuclear Instruments and Methods in Physics Research Section A: Accelerators, Spectrometers, Detectors and Associated Equipment*, *320*(1-2), 336-367.

Cao, Y., & Lee, J. C. (2010). Spatial corrections for pulsed-neutron reactivity measurements. Nuclear Science and Engineering, 165(3), 270-282.

Carta, M., & D'angelo, A. (1999). Subcriticality-level evaluation in accelerator-driven systems by harmonic modulation of the external source. Nuclear Science and Engineering, 133(3), 282-292.

Country Nuclear Fuel Cycle Profiles (2005). Technical Reports Series 425. Vienna: International Atomic Energy Agency.

De Bruyn, D., Abderrahim, H. A., Baeten, P., & Leysen, P. (2015). The MYRRHA ADS project in Belgium enters the front end engineering phase. Physics Procedia, 66, 75-84.

Degweker, S. B. (2000). Some variants of the Feynman alpha method in critical and accelerator driven sub critical systems. Annals of Nuclear Energy, 27(14), 1245-1257.

Degweker, S. B. (2003). Reactor noise in accelerator driven systems. Annals of Nuclear Energy, 30(2), 223-243.

Degweker, S. B., and Rana, Y. S. (2007). Reactor noise in accelerator driven systems–II. Annals of Nuclear Energy, 34(6), 463-482.

Degweker, S. B., Bhagwat, P. V., Krishnagopal, S., & Sinha, A. (2017). Physics and technology for development of accelerator driven systems in India. Progress in Nuclear Energy, 101, 53-81.

Dragt, J. B. (1973). On the Applicability of Sjöstrand's Area Method for Reactivity Measurement by the Pulsed-Neutron Technique. Nuclear Science and Engineering, 50(3), 216-219.

Dudley, B. (2019). BP statistical review of world energy. Retrieved from: https://www.bp.com/en/global/corporate/energy-economics/statistical-review-of-world-energy.html.

Endo, T., and Yamamoto, A. (2019). Comparison of theoretical formulae and bootstrap method for statistical error estimation of Feynman-α method. Annals of Nuclear Energy, 124, 606-615.

Endo, T., Yamane, Y., and Yamamoto, A. (2006). Space and energy dependent theoretical formula for the third order neutron correlation technique. Annals of Nuclear Energy, 33(6), 521-537.

Ferrari, A. and Sala, P. R. (1996). The Physics of High-energy Reactions. Proceedings of the *Workshop on Nuclear Reaction Data and Nuclear Reactors Physics, Design and Safety,*

Fokau, A., Zhang, Y., Ishida, S., & Wallenius, J. (2010). A source efficient ADS for minor actinides burning. Annals of Nuclear Energy, 37(4), 540-545.

Gabrielli, F., Carta, M., D'Angelo, A., Maschek, W., & Rineiski, A. (2008). Inferring the reactivity in accelerator driven systems: Corrective spatial factors for Source-Jerk and area methods. Progress in Nuclear Energy, 50(2-6), 370-376.

Gajda, P., Janczyszyn, J., & Pohorecki, W. (2013). Correction methods for pulsed neutron source reactivity measurement in accelerator driven systems. Nukleonika, 58.

Glasstone, S., & Sesonske, A. (2004). Nuclear Reactor Engineering. *Van Nostrand Reinhold, NJ*, *19*, 15.

Goeckermann, R. H., & Perlman, I. (1948). Characteristics of Bismuth Fission with High Energy Particles. *Physical Review*, *73*(9), 1127.

Gohar, Y., Aliberti, G., Bolshinsky, I., Kiyavitskaya, H., Talamo, A. (2009). YALINA booster subcritical assembly conversion. Trans. Am. Nucl. Soc. 101, 39–40.

Gozani, T. (1962). A modified procedure for the evaluation of pulsed source experiments in subcritical reactors. Nukleonik (West Germany) Discontinued with vol. 12, 4.

Grancea, L., & Hanly, A. (2018). Uranium 2018: Resources, Production and Demand (No. NEA--7413). Organisation for Economic Co-Operation and Development.

Grover, R. B., & Chandra, S. (2006). Scenario for growth of electricity in India. *Energy Policy*, *34*(17), 2834-2847.

Humphrey, U. E., & Khandaker, M. U. (2018). Viability of thorium-based nuclear fuel cycle for the next generation nuclear reactor: Issues and prospects. Renewable and Sustainable Energy Reviews, 97, 259-275.

IAEA, Preliminary Nuclear Power Facts and Figures for 2019. (2019) Retrieved from: https://www.iaea.org/newscenter/news/preliminary-nuclear-power-facts-and-figures-for-2019.

Jammes, C., Geslot, B., & Imel, G. (2006). Advantage of the area-ratio pulsed neutron source technique for ADS reactivity calibration. Nuclear Instruments and Methods in Physics Research Section A: Accelerators, Spectrometers, Detectors and Associated Equipment, 562(2), 778-784.

Jammes, C., Geslot, B., Rosa, R., Imel, G., & Fougeras, P. (2005). Comparison of reactivity estimations obtained from rod-drop and pulsed neutron source experiments. Annals of Nuclear Energy, 32(10), 1131-1145.

Janczyszyn, J. (2013). On the Sjöstrand method of reactivity measurement. Annals of Nuclear Energy, 60, 374-376.

Kadi, Y., & Herrera-Martinez, A. (2006). Energy amplifier systems: Simulation and experiments in the field. *Nuclear Instruments and Methods in Physics Research Section A: Accelerators, Spectrometers, Detectors and Associated Equipment*, *562*(2), 573-577.

Kadi, Y., & Revol, J. P. (2003). Design of an accelerator-driven system for the destruction of nuclear waste (No. INIS-XA--900).

Kapoor, S. S. (2002). Accelerator-driven sub-critical reactor system (ADS) for nuclear energy generation. *Pramana*, *59*(6), 941-950.

Kitamura, Y., Pázsit, I., Wright, J., Yamamoto, A., and Yamane, Y. (2005). Calculation of the pulsed Feynman-and Rossi-alpha formulae with delayed neutrons. Annals of Nuclear Energy, 32(7), 671-692.

Kitamura, Y., Taguchi, K., Misawa, T., Pázsit, I., Yamamoto, A., Yamane, Y., ... and Oigawa, H. (2006a). Calculation of the stochastic pulsed Rossi-alpha formula and its experimental verification. Progress in Nuclear Energy, 48(1), 37-50.

Kitamura, Y., Taguchi, K., Yamamoto, A., Yamane, Y., Misawa, T., Ichihara, C., ... and Oigawa, H. (2006b). Application of variance-to-mean technique to subcriticality monitoring for accelerator-driven subcritical reactor. International Journal of Nuclear Energy Science and Technology, 2(3), 266-284.

Kloosterman, J. L., and Rugama, Y. (2005). Feynman-α measurements on the fast critical zero-power reactor MASURCA. Progress in Nuclear Energy, 46(2), 111-125.

Kostić, L. (2002). Reactivity determination in accelerator driven reactors using reactor noise analysis. Nuclear Technology and Radiation Protection, 17(1-2), 19-26.

Kuang, Z. F., and Pazsit, I. (2000). A quantitative analysis of the Feynman-and Rossi-Alpha formulas with multiple emission sources. Nuclear science and engineering, 136(2), 305-319.

Kulik, V. V., & Lee, J. C. (2006). Space-time correction for reactivity determination in source-driven subcritical systems. Nuclear science and engineering, 153(1), 69-89.

Kumar, R., Ali, M. Y., Degweker, S. B., Vishwasrao, S. C., and Jadhav, R. T. (2015). Development and testing of neutron pulse time stamping data acquisition system for neutron noise experiment. Nuclear Instruments and Methods in Physics Research Section A: Accelerators, Spectrometers, Detectors and Associated Equipment, 770, 8-13.

Kumar, R., Degweker, S. B., Roy, T., Singh, K. P., Samanta, S., Bajpai, S., ... and Sinha, A. (2017). Measurement of reactivity in a source driven deep sub-critical system using neutron noise methods. Annals of Nuclear Energy, 103, 315-325.

Kumawat, H. and Barashenkov, V. S. (2005). Development of the Monte Carlo model CASCADE-2004 of high-energy nuclear interactions. *Euro. Phys. J., A 26, 61.*

Lebrat, J.F., Aliberti, G., D'Angelo, A., Billebaud, A., Brissot, R., Brockmann, H., Carta, M., Destouches, C., Gabrielli, F., Gonzalez, E., Hogenbirk, A., Klein-Meulenkamp, R., Le Brun, C., Liatard, E., Mellier, F., Messaoudi, N., Peluso, V., Plaschy, M., Thomas, M., Villamaran, D., Vollaire, J. (2008). Global results from deterministic and stochastic analysis of the MUSE-4 experiments on the neutronics of accelerator-driven systems. Nucl. Sci. Eng. 158 (1), 49–67.

Marie, N., Lecouey, J. L., Lehaut, G., Chevret, T., Billebaud, A., Chabod, S., ... & Mellier, F. (2019). Reactivity monitoring of the accelerator driven VENUS-F subcritical reactor with the "current-to-flux" method. *Annals of Nuclear Energy*, *128*, 12-23.

Masters, C. F., & Cady, K. B. (1967). A procedure for evaluating modified pulsed-neutron-source experiments in subcritical nuclear reactors. Nuclear Science and Engineering, 29(2), 272-282.

Mercatali, L., Serikov, A., Baeten, P., Uyttenhove, W., Lafuente, A., Teles, P. (2010). Design study of a fast spectrum zero-power reactor dedicated to source driven sub-critical experiments. Energy Convers. Manage. 51, 1818–1825.

Mesytek. MRS-2000. Retrieved from: https://www.mesytec.com/products/neutron-scattering/MRS-2000.html

Misawa, T., Shiroya, S., & Kanda, K. (1990). Measurement of prompt neutron decay constant and large subcriticality by the Feynman-α method. Nuclear Science and Engineering, 104(1), 53-65.

Möller, E., & Sjöstrand, N. G. (1963). Measurement of the slowing-down and thermalization time of neutrons in water (No. AE--125). AB Atomenergi.

Muñoz-Cobo, J. L., Berglöf, C., Peña, J., Villamarín, D., and Bournos, V. (2011). Feynman-α and Rossi-α formulas with spatial and modal effects. Annals of Nuclear Energy, 38(2-3), 590-600.

Muñoz-Cobo, J. L., Peña, J., and González, E. (2008). Rossi-α and Feynmann Y functions for non-Poissonian pulsed sources of neutrons in the stochastic pulsing method: Application to subcriticality monitoring in ADS and comparison with the results of Poissonian pulsed neutron sources. Annals of Nuclear Energy, 35(12), 2375-2386.

Muñoz-Cobo, J. L., Rugama, Y., Valentine, T. E., Mihalczo, J. T., and Perez, R. B. (2001). Subcritical reactivity monitoring in accelerator driven systems. Annals of Nuclear Energy, 28(15), 1519-1547.

NationalInstruments.(2019).Retrieved from: http://www.ni.com/gate/gb/GB_ACADEVALLVDL/US.

Nellis, W. J. (1977). Slowing-down distances and times of 0.1-to 14-MeV neutrons in hydrogenous materials. American Journal of Physics, 45(5), 443-446.

Nuclear Energy Outlook 2008. (2008). ISBN 978-92-64-05410-3, OECD/NEA.

Nuclear Power Corporation of India Limited (NPCIL). Nuclear Power Generation. (2010-11 to 2019-20). Retrieved from: https://www.npcil.nic.in/content/302_1_AllPlants.aspx.

Pázsit, I., and Yamane, Y. (1998a). Theory of neutron fluctuations in source-driven subcritical systems. Nuclear Instruments and Methods in Physics Research Section A: Accelerators, Spectrometers, Detectors and Associated Equipment, 403(2-3), 431-441.

Pázsit, I., and Yamane, Y. (1998b). The variance-to-mean ratio in subcritical systems driven by a spallation source. Annals of Nuclear Energy, 25(9), 667-676.

Pázsit, I., Kitamura, Y., Wright, J., and Misawa, T. (2005). Calculation of the pulsed Feynman-alpha formulae and their experimental verification. Annals of Nuclear Energy, 32(9), 986-1007.

Perdu, F., Loiseaux, J. M., Billebaud, A., Brissot, R., Heuer, D., Lebrun, C., ... & Vollaire, J. (2003). Prompt reactivity determination in a subcritical assembly through the response to a Dirac pulse. Progress in Nuclear Energy, 42(1), 107-120.

Persson, C. M., Fokau, A., Serafimovich, I., Bournos, V., Fokov, Y., Routkovskaia, C., ... & Gudowski, W. (2008). Pulsed neutron source measurements in the subcritical ADS experiment YALINA-Booster. Annals of Nuclear Energy, 35(12), 2357-2364.

Persson, C. M., Seltborg, P., Åhlander, A., Gudowski, W., Stummer, T., Kiyavitskaya, H., ... & Chigrinov, S. (2005). Analysis of reactivity determination methods in the subcritical experiment Yalina. Nuclear Instruments and Methods in Physics Research Section A: Accelerators, Spectrometers, Detectors and Associated Equipment, 554(1-3), 374-383.

Plaschy, M., Destouches, C., Rimpault, G., Chawla, R. (2005). Investigation of ADS Type heterogeneities in the MUSE-4 critical configuration. J. Nucl. Sci. Technol. 42 (9), 779–787.

Prael, R. E. and Madland, D. G. (2000). The LAHET code system with LAHET2.8. *Report, LA-UR-00-2140.*

Preskitt, C. A., Nephew, E. A., Brown, J. R., & Howe, K. V. (1967). Interpretation of Pulsed-Source Experiments in the Peach Bottom HTGR. Nuclear Science and Engineering, 29(2), 283-295.

Pyeon, C. H., Yamanaka, M., Endo, T., van Rooijen, W. F. G., and Chiba, G. (2017). Experimental benchmarks on kinetic parameters in accelerator-driven system with 100 MeV protons at Kyoto University Critical Assembly. Annals of Nuclear Energy, 105, 346-354.

Pyeon, C.H., Hervault, M., Misawa, T., Unesaki, H., Iwasaki, T., Shiroya, S. (2008). Static and kinetic experiments on accelerator driven system with 14 MeV neutrons in Kyoto University Critical Assembly. J. Nucl. Sci. Technol. 45 (11), 1171–1182.

Pyeon, C.H., Hirano, Y., Misawa, T., Unesaki, H., Ichihara, C., Iwasaki, T., Shiroya, S. (2007). Preliminary experiments on accelerator-driven subcritical reactor with pulsed neutron generator in Kyoto university critical assembly. J. Nucl. Sci. Technol. 44 (11), 368–1378.

Rana, Y. S., Singh, A., and Degweker, S. B. (2013). Diffusion Theory-Based Analog Monte Carlo for Simulating Noise Experiments in Subcritical Systems. Nuclear Science and Engineering, 174(3), 245-263.

Rineiski, A., & Maschek, W. (2005). Kinetics models for safety studies of accelerator driven systems. Annals of Nuclear Energy, 32(12), 1348-1365.

Rosselet, M., Williams, T., & Chawla, R. (1998). Subcriticality measurements using an epithermal pulsed-neutron-source technique in pebble-bed HTR configurations. Annals of Nuclear Energy, 25(4-5), 285-294.

Rubbia, C., Buono, S., Gonzalez, E., Kadi, Y., & Rubio, J. A. (1997). A realistic plutonium elimination scheme with fast energy amplifiers and thorium-plutonium fuel.

In *Advanced Nuclear Systems Consuming Excess Plutonium* (pp. 89-134). Springer, Dordrecht.

Rubbia, C., Roche, C., Rubio, J. A., Carminati, F., Kadi, Y., Mandrillon, P., ... & Gelès, C. (1995). Conceptual design of a fast neutron operated high power energy amplifier (No. CERN-AT-95-44-ET).

Rugama, Y., Kloosterman, J. L., and Winkelman, A. (2004). Experimental results from noise measurements in a source driven subcritical fast reactor. Progress in Nuclear Energy, 44(1), 1-12.

Rugama, Y., Muñoz-Cobo, J. L., and Valentine, T. E. (2002). Modal influence of the detector location for the noise calculation of the ADS. Annals of Nuclear Energy, 29(3), 215-234.

Ryves, T. B., & Scott, M. C. (1962). Subcritical reactivity measurement by a source-jerk method. Journal of Nuclear Energy. Parts A/B. Reactor Science and Technology, 16(9), 455-463.

Sakon, A., Hashimoto, K., Sugiyama, W., Taninaka, H., Pyeon, C. H., Sano, T., ... and Ohsawa, T. (2013). Power spectral analysis for a thermal subcritical reactor system driven by a pulsed 14 MeV neutron source. Journal of Nuclear Science and Technology, 50(5), 481-492.

Seidel, M., Adam, S., Adelmann, A., Baumgarten, C., Bi, Y. J., Doelling, R., ... & Kiselev, D. (2010). Production of a 1.3 MW proton beam at PSI. IPAC10, 1309.

Seltborg, P., Wallenius, J., Tucek, K., & Gudowski, W. (2003). Definition and application of proton source efficiency in accelerator-driven systems. Nuclear science and engineering, 145(3), 390-399.

Shahbunder, H., Pyeon, C. H., Misawa, T., Lim, J. Y., & Shiroya, S. (2010). Effects of neutron spectrum and external neutron source on neutron multiplication parameters in accelerator-driven system. Annals of Nuclear Energy, 37(12), 1785-1791.

Shahbunder, H., Pyeon, C. H., Misawa, T., Lim, J. Y., & Shiroya, S. (2010). Subcritical multiplication factor and source efficiency in accelerator-driven system. Annals of Nuclear Energy, 37(9), 1214-1222.

Shukla, M., Desai, S. S., Roy, T., Kashyap, Y., Ray, N., Bajpai, S., ... and Sinha, A. (2015). Neutron spatial flux profile measurement in compact subcritical system using miniature neutron detectors. Nuclear Instruments and Methods in Physics Research Section A: Accelerators, Spectrometers, Detectors and Associated Equipment, 772, 118-123.

Simmons, B. E., & King, J. S. (1958). A pulsed neutron technique for reactivity determination. Nuclear science and engineering, 3(5), 595-608.

Singh, K. P., Degweker, S. B., Modak, R. S., and Singh, K. (2011). Iterative method for obtaining the prompt and delayed alpha-modes of the diffusion equation. Annals of Nuclear Energy, 38(9), 1996-2004.

Singh, K. P., Modak, R. S., Degweker, S. B., and Singh, K. (2009). Iterative schemes for obtaining dominant alpha-modes of the neutron diffusion equation. Annals of Nuclear Energy, 36(8), 1086-1092.

Sinha, A., Roy, T., Kashyap, Y., Ray, N., Shukla, M., Patel, T., ... and Adhikari, P. S. (2015). BRAHMMA: a compact experimental accelerator driven subcritical facility using DT/DD neutron source. *Annals of Nuclear Energy*, *75*, 590-594.

Sjostrand, N. G. (1956). Measurements on a subcritical reactor using a pulsed neutron source. Arkivfysik, 11.

Soule, R., Assal, W., Chaussonnet, P., Destouches, C., Domergue, C., Jammes, C., Laurens, J.M., Lebrat, J.F., Mellier, F., Perret, G., Rimpault, G., Servière, H. (2004). Neutronic studies in support of accelerator-driven systems: the MUSE experiments in the MASURCA facility. Nucl. Sci. Eng. 148 (1), 124–152.

Srinivasan, M. (1985). Feasibility of the application of statistical correlation techniques for the experimental study of the multiplication of 14 MeV neutrons in Be assemblies. Annals of Nuclear Energy, 12(3), 125-135.

Status of Minor Actinides Fuel Development. (2009). IAEA Nuclear Energy Series, No. NF-T-4.6.

Suzaki, T. (1991). Subcriticality Determination of Low-Enriched UO2Lattices in Water by Exponential Experiment. Journal of Nuclear Science and Technology, 28(12), 1067-1077.

Szieberth, M., Klujber, G., Kloosterman, J. L., & de Haas, D. (2015). Measurement of multiple α-modes at the Delphi subcritical assembly by neutron noise techniques. Annals of Nuclear Energy, 75, 146-157.

Talamo, A., Gohar, Y., Cao, Y., Zhong, Z., Kiyavitskaya, H., Bournos, V., ... & Routkovskaya, C. (2012a). Impact of the neutron detector choice on Bell and Glasstone spatial correction factor for subcriticality measurement. Nuclear Instruments and Methods in Physics Research Section A: Accelerators, Spectrometers, Detectors and Associated Equipment, 668, 71-82.

Talamo, A., Gohar, Y., Gabrielli, F., Rineiski, A., & Pyeon, C. H. (2017). Advances in the computation of the Sjöstrand, Rossi, and Feynman distributions. Progress in Nuclear Energy, 101, 299-311.

Talamo, A., Gohar, Y., Rabiti, C., Aliberti, G., Kondev, F., Smith, D., ... & Routkovskaya, C. (2009). Pulse superimposition calculational methodology for estimating the subcriticality level of nuclear fuel assemblies. Nuclear Instruments and Methods in

Physics Research Section A: Accelerators, Spectrometers, Detectors and Associated Equipment, 606(3), 661-668.

Talamo, A., Zhong, Z., & Gohar, Y. (2012b). Monte Carlo and deterministic calculation of the Bell and Glasstone spatial correction factor. Computer Physics Communications, 183(9), 1904-1910.

Taninaka, H., Hashimoto, K., Pyeon, C. H., Sano, T., Misawa, T., Unesaki, H., ... & Ohsawa, T. (2011). Determination of subcritical reactivity of a thermal accelerator-driven system from beam trip and restart experiment. Journal of nuclear science and technology, 48(6), 873-879.

Tesinsky, M., Berglof, C., Back, T., Martsynkevich, B., Serafimovich, I., Bournos, V., Khilmanovich, A., Fokov, Y., Korneev, S., Kiyavitskaya, H., Gudowski, W. (2011). Comparison of calculated and measured reaction rates obtained through foil activation in the subcritical dual spectrum facility YALINA Booster. Ann. Nucl. Energy 38 (6), 1412–1417.

Trieste, Italy.

United Nations Climate Change. The Paris Agreement. Retrieved from: https://unfccc.int/process-and-meetings/the-paris-agreement/the-paris-agreement

Unser, K., 1969. Beam Current Transformer with DC to 200 MHz Range (No. ISR-CO-69- 6).

Unser, K., 1981. A toroidal DC beam current transformer with high resolution. IEEE Trans. Nucl. Sci. 28, 2344–2346. CERN-ISR-OP-81-14.

Uyttenhove, W., Baeten, P., Van den Eynde, G., Kochetkov, A., Lathouwers, D., Carta, M. (2011). The neutronic design of a critical lead reflected zero-power reference core for on-line subcriticality measurements in Accelerator Driven Systems. Ann. Nucl. Energy 38, 1519–1526.

Uyttenhove, W., Lathouwers, D., Kloosterman, J. L., Van der Hagen, T. H. J. J., Van den Eynde, G., & Baeten, P. (2014). Methodology for modal analysis at pulsed neutron source experiments in accelerator-driven systems. Annals of Nuclear Energy, 72, 286-297.

Williams, M. M. R. (1974). Random processes in nuclear reactors. Pergamon Press, New York.

World Thorium Occurrences Deposits and Resources. (2019). IAEA-TECDOC-1877.

Wright, J., & Pázsit, I. (2006). Neutron kinetics in subcritical cores with application to the source modulation method. Annals of Nuclear Energy, 33(2), 149-158.

Yamamoto, T. (2013). Energy-higher order mode analyses in Feynman-α method. Annals of Nuclear Energy, 57, 84-91.

Yamamoto, T. (2014). Higher order mode analyses of power spectral density and Feynman-α method in accelerator driven system with periodically pulsed spallation neutron source. Annals of Nuclear Energy, 66, 63-73.

Zucker, M. S., Tsoupas, N., Vanier, P. E., Von Wimmersperg, U., Mughabghab, S. F., & Schmidt, E. (1998). Spallation neutron production measurements. Nuclear science and engineering, 129(2), 180-186.

Appendix I

Abstract of oral presentation at 19th International conference on Emerging Nuclear Energy Systems, 2019, Indonesia

Noise Experiments in BRAHMMA Subcritical System using Isotopic Poisson Source and Accelerator based Neutron Source

Nirmal Kumar Ray[a,b*], Rajeev Kumar[c], Tarun Patel[a], P.S. Sarkar[a,b], L. M. Pant[b,d]

[a]Technical Physics Division, Bhabha Atomic Research Centre, Mumbai 400085, India
[b]Homi Bhabha National Institute, Mumbai 400094, India
[c]Reactor Physics Design Division, Bhabha Atomic Research Centre, Mumbai 400085, India
[d]Nuclear Physics Division, Bhabha Atomic Research Centre, Mumbai 400085, India

[*]**Corresponding author address:** Technical Physics Division, Bhabha Atomic Research Centre, Mumbai 400085, India.
E-mail: nirmal@barc.gov.in

Abstract

The energy production and transmutation rate in Accelerator Driven Subcritical (ADS) system depends on the subcriticality of the core. In this perspective, it is essential to develop suitable and robust reactivity measurement methods. Noise methods (Williams, 1974) based on neutron correlation are suitable for reactivity measurement in case of continuous operation without any perturbation. In this context, reactivity measurement using noise methods have been carried out using isotopic Poisson neutron source (Am-Be) and accelerator based non-Poisson neutron source (D-T neutron generator) in zero power subcritical system BRAHMMA, installed in BARC, India for physics studies of ADS (Sinha et al., 2015).

In deep subcritical system, reactivity measurement is challenging due to the presence of higher order modes which can be eliminated by placing detectors at locations based on modal analysis (Rana et al., 2013). During noise experiments using mode cancellation method, an Am-Be neutron source (1Ci) has been placed at the centre of the subcritical system (Kumar et al., 2017). However, the proposed external neutron source in ADS is based on particle accelerator is different from isotopic neutron source and the inherent fluctuation in beam current and accelerating voltage makes the former source non-Poisson. Also, periodically chopped beam cannot be considered as Poisson character. In this perspective, Degweker and Rana (2007) had postulated a noise theory based on exponentially correlated Gaussian source characteristics for ADS. In noise experiments based on this postulate, a D-T neutron generator has been used in pulsed mode and source characterisation has been carried out to determine the distribution function, source correlation factor and D^+ beam pulse shape. It has been observed that the source is Gaussian in nature, the source correlation factor ($50.44 ms^{-1}$) is very large compared to the prompt neutron decay constant ($\alpha=2.31 ms^{-1}$) and the pulsed D^+ beam is rectangular in shape. Furthermore, the time stamped data has been analysed using various noise descriptors, namely variance to mean ratio (v/m), Rossi-alpha and Auto Power Spectral Density (*APSD*) method (Ray et al., 2019). The measured prompt neutron decay constant using Poisson source and correlated Gaussian source are in good agreement with theoretical value and amongst them.

Reference

1. Degweker, S. B., and Rana, Y. S. (2007). Reactor noise in accelerator driven systems–II. *Annals of Nuclear Energy*, *34*(6), 463-482.
2. Kumar, R., Degweker, S. B., Roy, T., Singh, K. P., Samanta, S., Bajpai, S., ...and Sinha, A. (2017). Measurement of reactivity in a source driven deep sub-critical system using neutron noise methods. *Annals of Nuclear Energy*, *103*, 315-325.
3. Rana, Y. S., Singh, A., and Degweker, S. B. (2013). Diffusion Theory-Based Analog Monte Carlo for Simulating Noise Experiments in Subcritical Systems. *Nuclear Science and Engineering*, *174*(3), 245-263.
4. Ray, N. K., Pant, L. M., Patel, T., Kumar, R., Roy, T., Sarkar, P. S., ... & Gadkari, S. C. (2019). Experimental validation of noise theory developed by considering the source as an exponentially correlated process in DT neutron generator driven subcritical system. Progress in Nuclear Energy, 117, 103087.
5. Sinha, A., Roy, T., Kashyap, Y., Ray, N., Shukla, M., Patel, T., ...and Adhikari, P. S. (2015). BRAHMMA: a compact experimental accelerator driven subcritical facility using DT/DD neutron source. *Annals of Nuclear Energy*, *75*, 590-594.
6. Williams, M. M. R. (1974). *Random processes in nuclear reactors*. Pergamon Press, New York.

Appendix II

Proceeding of the DAE symposium on Nuclear Physics (2018)

Source correlation factor measurement using D-T neutron generator

Nirmal Kumar Ray[1,2,*] Tarun Patel[1], Rajeev Kumar[3], P. S. Sarkar[1,2], L. M. Pant[2,4]

[1] *Technical Physics Division, Bhabha Atomic Research Centre, Mumbai 400085, India*
[2] *Homi Bhabha National Institute, Mumbai 400094, India*
[3] *Reactor Physics Design Division, Bhabha Atomic Research Centre, Mumbai 400085, India*
[4] *Nuclear Physics Division, Bhabha Atomic Research Centre, Mumbai 400085, India*
[*] *email: nirmal@barc.gov.in*

Introduction

Accelerator Driven Subcritical (ADS) systems are being studied worldwide for their potential of burning minor actinides and reducing long term radiotoxicity. Various zero power subcritical systems (KUCA, MUSE, YALINA and BRAHMMA) have been developed to study the physics aspect of ADS using D-D or D-T fusion based neutron source. One of the important physics issue in ADS is to maintain the subcriticality throughout its operation by measuring the reactivity.

During 1960, on the basis of neutron correlation technique, noise methods such as variance to mean ratio (*v/m*) or Feynman-alpha and Auto Co-variance (*ACV*) were developed to measure the reactor kinetic parameters and reactivity [1]. Later, noise methods resumed interest with the proposal of ADS by Carlo Rubbia [2]. Theoretical and experimental work has advanced in continuous and pulsed mode using synchronous and asynchronous detection techniques [3,4]. These works have been carried out considering the external neutron source as Poisson character. But, this assumption is inappropriate for an accelerator based neutron source [5] and this can be explained with a simple example. Let us consider a D-T neutron source having yield 10^{10}n/s. Under the consideration of Poisson distribution, the variance will be its mean (M), the standard deviation (SD) will be 10^5n/s and the fluctuation (SD/M) considering Poisson distribution must be 0.001%. But, it is practically impossible to achieve such stability because of inherent fluctuation in beam current and accelerating voltage. Therefore, it is interesting to study the source characteristic which is relevant for noise studies in ADS system.

Methodology

The experimental setup consists of a D-T neutron generator, ^{3}He detector with electronics and time stamp data acquisition system. The neutron counts were registered with the incident time for duration (τ). The time stamp data has been analysed using *v/m* and *ACV* methods. For *v/m*, entire dataset has been divided into equal time segments (say T). The number of counts in each segment ($Z(T)$) was used to calculate the variance to mean ratio using eqn.1.

$$\frac{v(T)}{m(T)}=\frac{\langle Z(T)^2\rangle-\langle Z(T)\rangle^2}{\langle Z(T)\rangle}=\frac{\frac{1}{N}\sum_{i=1}^{N}Z_i^2(T)-\left(\frac{1}{N}\sum_{i=1}^{N}Z_i(T)\right)^2}{\frac{1}{N}\sum_{i=1}^{N}Z_i(T)} \quad (1)$$

The ACV of the neutron counts is given by:

$$ACV(T)=\frac{1}{M}\sum_{i=1}^{M}(N(i\Delta t)-\bar{N})(N(i\Delta t+T)-\bar{N}) \quad (2)$$

where $\bar{N}$ is the DC part of the counts for time segment Δt.

Results and discussion

During source characterization, a ^{3}He detector (active length: 10cm and diameter: 2.54cm) has been placed at a distance of 10cm from the beam target. The detector was encapsulated by a Perspex cylinder followed by 2mm cadmium sheet. The Perspex was used to thermalize the fast neutrons and the cadmium to stop the scattered thermal neutrons from surroundings entering the detector.

The neutron generator was used with pulse repetition frequency of 10kHz having 10% duty cycle. The time stamp data have been divided into time segments of one second to study the source fluctuation. In Fig.1, the normalise counts per second (CPS) can be seen. The source fluctuation (Std/Mean) as shown in inset of Fig.1 is 2.0%. Data have been analysed using *v/m* method and the *v/m-1* is shown in Fig.2. In case of, Poisson source characteristics the *v/m-1* should be zero, whereas the measured v/m-1 is close to 0.1. Therefore, the neutron source having fluctuation of 2% and non-zero *v/m-1* cannot be assumed as Poisson character.

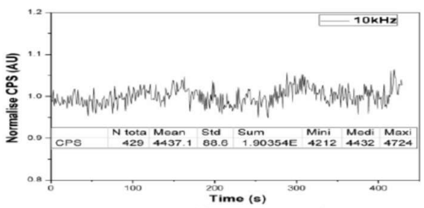

Fig. 1 Normalise CPS at 10kHz

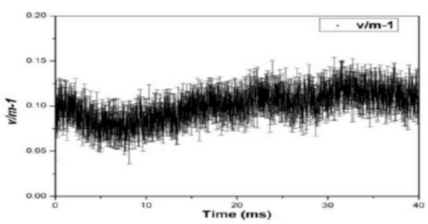

Fig. 2 *v/m-1* plot at 10kHz

In the next step, data have been analyzed using *ACV* method and the measured *ACV* has been shown in Fig.3. The *ACV* has periodicity corresponding to the source frequency and has exponential decay following the neutron pulse. Therefore, the source correlation factor and correlation time can be estimate from the exponential decay of the measured *ACV* and the values are 50.44±10.76ms^{-1} and 19.8±4.2μs respectively.

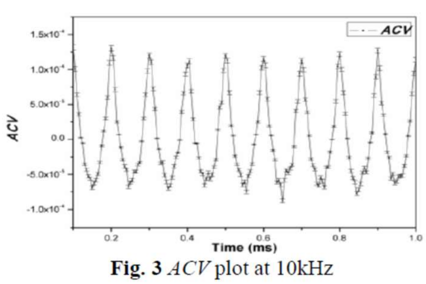

Fig. 3 *ACV* plot at 10kHz

The error in the measured correction factor is high. This can be attributed to the decay of *ACV* in high frequency, which is sharp and the number of data points is also less as shown in Fig.4. The measured source correlation factor is very high and the D-T neutrons have very short term correlation.

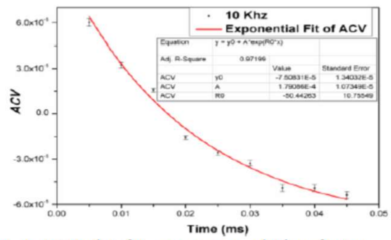

Fig. 4 *ACV* plot for source correlation factor measurement

Conclusion

An investigation of the source correlation factor has been carried out using D-T neutron generator and results have been presented for accelerator frequency 10kHz. The source correlation factor which appears due to inherent source fluctuation is very large. This new approach has been implemented to understand the source characteristics for noise studies in accelerator driven subcritical system.

Reference

[1] Williams, M. M. R. (1974). *Random processes in nuclear reactors*. Pergamon Press, New York.

[2] Rubbia, C., ... and Gelès, C. (1995). *Conceptual design of a fast neutron operated high power energy amplifier* (No. CERN-AT-95-44-ET).

[3] Pazsit, I., and Yamane, Y. (1998). Theory of neutron fluctuations in source-driven subcritical systems. *Nuclear Instruments and Methods in Physics Research Section A*, *403*(2-3), 431-441.

[4] Kitamura, Y., ... and Oigawa, H. (2006). Application of variance-to-mean technique to subcriticality monitoring for accelerator-driven subcritical reactor. *IJNEST*, *2*(3), 266-284.

[5] Degweker, S. B., and Rana, Y. S. (2007). Reactor noise in accelerator driven systems–II. *Annals of Nuclear Energy*, *34*(6), 463-482.